UNIVERSIDAD AUTÓNOMA DEL ESTADO DE MÉXICO

FACULTAD DE QUÍMICA

"ELECTRO-OXIDACIÓN DE FENOL EN UNA COLUMNA DE BURBUJEO DE FLUJO PARALELO DESCENDENTE"

TESIS

QUE PARA OBTENER EL GRADO DE

DOCTOR EN CIENCIAS QUÍMICAS

PRESENTA:

M en C.Q GERMÁN SANTANA MARTÍNEZ

DIRIGIDO POR:

Dra. REYNA NATIVIDAD RANGEL

Dra. GABRIELA ROA MORALES

Toluca, Estado de México, Enero 2019

AGRADECIMIENTOS

A la Dra.Reyna Natividad Rangel y Dra.Gabriela Roa Morales, por aceptarme en su grupo de investigación llevando a cabo el presente proyecto, para obtener el grado de Doctor en Ciencias Químicas.

Al apoyo económico de la beca CONACYT para estudios de Doctorado con número 295553. De igual manera, por el apoyo recibido a través de los proyectos CONACYT 168305 y 269093, para el desarrollo del proyecto.

Por el soporte técnico computacional, a L.I.A María Citlalit Martínez Soto.

Al sínodo evaluador, por sus comentarios y revisiones, que contribuyeron a mejorar la presentación del formato final de la presente tesis.

Por las facilidades otorgadas y equipos analíticos para realizar la investigación en los laboratorios de Ingeniería Química (CCIQS), Análisis Químico (CCIQS), Análisis Instrumental (Facultad de Química UAEM) y Toxicología Ambiental (Facultad de Química UAEM).

ÍNDICE

Contenido

RESUMEN

Para reducir el efecto contaminante de las moléculas orgánicas presentes en agua, los procesos de oxidación avanzada (POA) son una solución eficaz. No obstante, los sistemas de reacción en la mayor parte de los casos suelen ser altamente costosos, por la adición de sustancias químicas o bien por el consumo energético, esto limita su aplicación a escala industrial. Esto ha motivado el desarrollo de tecnologías que no solamente intensifiquen los POA, sino que aumenten su sustentabilidad reduciendo tanto el consumo energético como de sustancias químicas. En este contexto, el objetivo principal de esta investigación fue establecer la factibilidad y eficiencia del proceso de electro-oxidación en una columna de burbujeo de flujo descendente para mineralizar soluciones fenólicas

Las variables de estudio fueron: densidad de corriente, concentración de electrolito, concentración inicial de fenol, recirculación de la fase líquida y pH. Como variables de respuesta del proceso se realizaron determinaciones de carbono orgánico total (COT) en la medición del porcentaje de mineralización y de manera conjunta el análisis de los subproductos de degradación del contaminante inicial mediante cromatografía de líquidos de alta resolución. Al mismo tiempo, fueron cuantificadas las concentraciones electro-generadas in situ de H_2O_2 y O_3 mediante técnicas espectrofotométricas. La generación electrolítica de O_2 fue cuantificada mediante un sensor HACH 400. También fueron determinados algunos parámetros hidrodinámicos, como el diámetro de burbuja y fracción volumétrica de gas. También se calcularon coeficientes volumétricos de transferencia de masa.

En términos de mineralización, los mejores resultados (75 %) se encontraron con una densidad de corriente de 60 mA/cm^2, pH 3, flujo de 4.7 L/min y una concentración de electrolito de 0.05 M. Se determinó que a este pH la oxidación del compuesto aromático ocurre principalmente por un ataque directo del ozono y el principal compuesto remanente es ácido oxálico. A pH 7, el grado de mineralización fue menor (65%), sin embargo, con un estudio de toxicidad realizado sobre *Cyprinus carpio*, se concluyó que a pesar de no estar completamente mineralizado, la toxicidad del efluente original se redujo significativamente.

Con los resultados obtenidos, se demuestra que la columna de burbujeo de flujo paralelo descendente se puede aplicar a escala pre-piloto, en el proceso de electro-oxidación, en el cual a su vez se lleva a cabo la generación *in situ* de O_2, H_2O_2 y O_3, obteniendo con ello el proceso de electro-peroxonación, lo cual es el principal aporte al conocimiento, debido a que la generación *in-situ* de estas dos especies y su aprovechamiento para llevar a cabo la mineralización del efluente sintético se considera una contribución importante a la sustentabilidad de este proceso.

Esta tecnología se está tratando de proteger intelectualmente mediante una patente y la solicitud correspondiente se realizó en 2017 ante el IMPI con el número Mx/a/2017/012722.

ABSTRACT

In the context of water remediation, advanced oxidation processes have been proven to be an effective solution. In most of the cases, however, the reaction systems are usually highly expensive, because of the addition of chemical substances or energy consumption. This usually constrains their application at an industrial scale. This has motivated several researchers to develop technologies able not only to intensify the processes but able also to increase the sustainability of the whole process. In this sense, this work aimed to assess a relatively novel technology, a Downflow Bubble Column Electrochemical Reactor (DBCER), in the mineralization of a rather typical organic pollutant, phenol.

The studied variables were: current density (20-60 mA/cm^2), electrolyte concentration (0-0.01 M), recirculation of the liquid phase (4.7 and 6 L/min) and pH (3 and 7). The response variables were total organic carbon (TOC), phenol and by-products concentration, oxidant species concentration (O_2, H_2O_2 and O_3). Some hydrodynamic parameters and volumetric mass transfer coefficient were also determined, such as the bubble diameter and volume fraction of gas.

The highest mineralization degree was around 75 % under pH 3, 60 mA/cm^2, 4.7 L/min and an electrolyte concentration of 0.05 M. Under these conditions, it was figured out that the phenol oxidation occurs mainly by ozone attack and the main remaining compound was oxalic acid. Although at pH 7 the mineralization degree was lower than at pH 3, it was demonstrated by a biotoxicity study on *Cyprinus carpio* that the original toxicity was significantly decreased.

Thus, it was demonstrated that the DBCER can be applied at a pre-pilot scale, in the electro-oxidation process, in which *in-situ* generation of O_2, H_2O_2 and O_3. Because of the unique design of this reactor, the electrogenerated gases can be better utilized than in other reactors.

An application to intellectually protect the developed technology was submitted to IMPI and the number of the application is Mx/a/2017/012722.

INTRODUCCIÓN

La nueva generación de reactores electroquímicos, proponen tendencias orientadas principalmente a la reducción de costos operativos y la no generación de residuos peligrosos, los cuales son factores clave para poder escalar los procesos a volúmenes de reacción mayores. Partiendo de esto, es conocido que otros procesos de oxidación avanzada se ha implementado la tecnología conocida como columna de burbujeo de flujo paralelo descendente, la cual ofrece varias ventajas con respecto a las columnas de burbujeo tradicionales, en las cuales se inyecta la fase gas por el fondo de la columna. Esta mejora se logra adicionando la fase gas por el domo de la columna y suministrando el gas a través de un inyector tipo Venturi. Con este modo de operación el gas queda atrapado y se dispersa en forma de burbujas, las cuales facilitan el transporte de masa en una zona con régimen turbulento. Partiendo de esta ventaja que ofrece este sistema de reacción novedoso en el área electroquímica, el objetivo principal de la investigación fue implementar el proceso de Electro-Oxidación en una Columna de burbujeo de flujo paralelo descendente, con ello electro-generar *in situ* dos especies altamente oxidantes: O_3 y H_2O_2. Una vez generados estos agentes oxidantes, se logra llevar a cabo un proceso electroquímico, denominado Electro-peroxonación, el cual tiene varias ventajas con respecto a una electro-oxidación normal y en el sistema de reacción propuesto, no requiere adición de gases y otros reactivos, únicamente la aplicación de corriente eléctrica y de un electrolito soporte.

En el capítulo 1, se presentan los antecedentes que sustentan el fundamento teórico de la investigación, así como una breve descripción de los sistemas de reacción más empleados en los procesos de oxidación avanzada y hacia donde se direccionan las mejoras aplicadas a los mismos. Con respecto a los capítulos 2, 3 y 4, se describe la justificación, objetivos y metodología del proyecto, respectivamente.

Los resultados son presentados en el capítulo 5, donde se incluyen los productos de la presente investigación los cuales fueron evaluados por revisores de reconocidas editoriales, indexadas al Journal Citation Reports. El primer producto de ellos es un capítulo de libro publicado en la editorial Springer, el cual está enfocado a los fundamentos teóricos de la ozonación y algunas de sus variantes, como la electro-peroxonación, así como su aplicación a la remoción de compuestos farmacéuticos. En segundo se encuentra un artículo, el cual se

envió a revisión, para aprobarlo o sugerir correcciones al mismo. El contenido incluye todos los experimentos para el cumplimiento de los objetivos del presente proyecto.

Finalmente, para complementar y resaltar los resultados mencionados en el capítulo 5, se presenta un breve apartado con una discusión general y conclusiones. La información de soporte se encuentra en las referencias y anexos.

Antecedentes

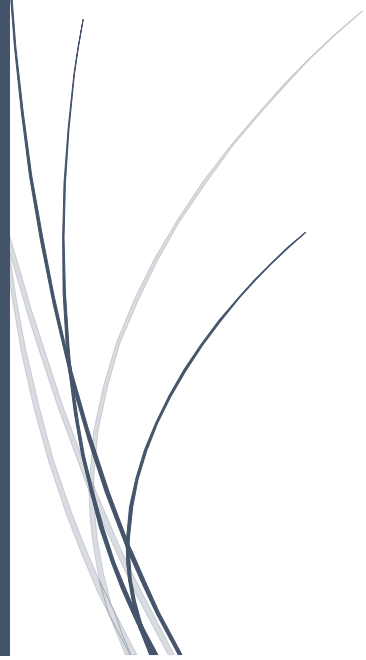

1. ANTECEDENTES

1.1 Contaminación del Agua

La disponibilidad de agua libre de contaminantes se ha convertido en una constante preocupación del ser humano. Esto no sólo porque una gran parte de la población del mundo no goza del vital líquido sino también por los efectos negativos observados en el ecosistema acuático. La contaminación del agua ocurre fundamentalmente debido a las descargas industriales, agrícolas y domésticas, las cuales deberían ser tratadas para poder obtener una mejor calidad del agua. Del total del agua dulce (2.5% del agua total), más de dos tercios se encuentra acumulada en los polos. Así pues, solo una pequeña fracción, del orden del 1% del total del agua en la Tierra se encuentra accesible en los ríos o en los acuíferos (Carrera, 2008).

Ante la problemática de la conservación del agua, han cobrado relevancia en los últimos años las investigaciones sobre la remediación del agua. Dentro de estos contaminantes sobresalen los que se conocen como persistentes y a continuación se aborda este tema con mayor detalle por ser importante para justificar el presente proyecto de investigación.

1.2 Contaminantes Orgánicos Persistentes (COP´s)

Una clase de sustancias en particular, denominadas contaminantes orgánicos persistentes (COPs), son motivo de inquietud. Muchos de estos contaminantes ocasionan importantes daños a la salud y al medio ambiente. Ante esta problemática, los gobiernos del mundo se reunieron en Suecia en el año 2001, para adoptar un tratado internacional destinado a restringir y a su vez eliminar de forma definitiva la producción de COPs (PNUMA, 2006).

Los primeros 12 contaminantes que encabezan la lista de los COPs, son la aldrina, bifenilos policlorados, clordano, DDT, dieldrina, dioxinas, endrina, furanos, heptacloro, hexaclorobenceno, mirex y toxafeno.

Los productos químicos conocidos como COPs, además de ser poderosos plaguicidas, sirven para varias aplicaciones industriales. Algunos de estos contaminantes se emiten

como subproductos no deliberados de la combustión y de procesos industriales. Algunas características que tienen en común los COPs, son las siguientes:

a) Son altamente tóxicos
b) Son persistentes y tienen una duración de años, incluso décadas, antes de degradarse en formas menos peligrosas.
c) Se evaporan y se desplazan a través del aire y del agua.
d) Se acumulan en el tejido adiposo

Este tratado, llamado el Convenio de Estocolmo sobre Contaminantes Orgánicos Persistentes, es un logro capital y lo más importante es que es un sistema que toma medidas frente a otros productos químicos identificados como peligrosos. El convenio entró en vigor en el año 2004 y para el año 2005 más de 90 países se habían incorporado a dicho tratado (PNUMA 2006).

Si bien los contaminantes mencionados en este apartado son los prioritarios, la lista completa abarca otro tipo de compuestos como clorofluorocarbonados, herbicidas, fenoles y clorofenoles, por mencionar algunos.

Por lo tanto, debido a la importancia que tiene la degradación de compuestos fenólicos, en este proyecto de investigación se adoptó al fenol como molécula modelo para demostrar la eficiencia de la tecnología desarrollada. A continuación, se describen generalidades de esta molécula que resaltan la importancia tanto de su uso como de su imperante degradación y/o disposición en el medio ambiente.

1.3 Fenol

En los Estados Unidos de Norte-América, la Agencia para sustancias tóxicas y el registro de enfermedades, (ATSDR) por sus siglas en inglés, describe al fenol como un sólido incoloro a blanco cuando se encuentra en forma pura. A temperatura ambiente, tiene una presión de vapor baja y es una masa cristalina clara o ligeramente rosada, polvo blanco o líquido espeso, además de ser muy soluble en alcohol y ligeramente soluble en agua.

El fenol, en su preparación comercial, es un líquido que se evapora más lentamente que el agua. Su olor es alquitranado y dulce (ATSDR, 2008). La fórmula química del fenol es

C_6H_5OH y su estructura química se muestra en la Figura 1 y en la tabla 1 se presentan sus propiedades físicas.

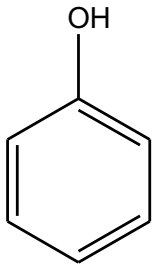

Figura 1. Estructura molecular del fenol

Tabla 1. Propiedades físicas del fenol (ATSDR, 2008)

Propiedad	Valor
Peso Molecular	94.11
Estado Físico	Sólido
Color	Sin color a un rosado bajo
Olor	Aromas definidos, algo repugnante, dulce y picante
Punto de Ebullición	181.75 °C
Punto de Fusión	43 °C y 40.9 °C (material ultrapuro)
Solubilidad	Agua: $8.28x10^4$ $mg{\cdot}L^{-1}$ a 25 °C Solventes Orgánicos: Soluble en agua y etanol, muy soluble en éter, miscible con acetona y benceno.
pH	4.8-6.0 al 5% en agua

La presencia del anillo bencénico permite que el fenol tenga la capacidad de estabilizarse y esto puede producir que pierda con relativa facilidad el hidrógeno de su grupo hidroxilo, permitiendo que se comporte como un ácido débil. El fenol es sensible a agentes oxidantes. Puede sufrir múltiples reacciones de sustitución electrofílica como, por ejemplo, halogenación y sulfonación. Además, reacciona con compuestos carbonílicos, en medio ácido y básico. La formación de resinas fenólicas son producto de la hidroximetilación con la subsecuente condensación del fenol en presencia de formaldehído. Así mismo, el fenol puede quemarse en presencia de oxígeno y producir monóxido de carbono (CO) como producto de combustión incompleta, siendo éste último un gas tóxico (Wade Jr, 2012).

La producción de Fenol alrededor del mundo se encuentra en una tasa de 6 millones de toneladas por año. La síntesis de cumeno y los procesos de oxidación consisten en una síntesis simultánea de fenol y acetona, produciendo alrededor del 95% de Fenol en el mundo (Busca *et al.*, 2008). El uso principal del Fenol es para la producción de colorantes y resinas sintéticas.

Los Fenoles son tóxicos a concentraciones menores de 1µg/L, pues inactivan las proteínas celulares vitales, incluidas las enzimas (Wen *et al*., 2013). Los fenoles son corrosivos cutáneos y se absorben con facilidad por la piel y las mucosas. Su toxicidad está directamente relacionada con una gran variedad de órganos y tejidos, (pulmones, hígado, riñones, sistema genito-urinario). Sus efectos provocan un cuadro general caracterizado por fallo hepático y renal, así como edema pulmonar y cerebral. La Agencia de Protección al Medio Ambiente de E.U. (EPA), en el 2003, señaló en su informe anual que los compuestos fenólicos afectan al hombre por vía de la ingestión y por el contacto con la piel. La dosis mínima que puede provocar la muerte es de 140 mg/kg peso corporal. Reporta además efectos como irritación, necrosis, afecciones cardiovasculares, acidosis metabólica, efectos neurológicos y cianosis (USEPA, 2002). De acuerdo a la legislación de la Unión Europea, la concentración permisible de fenoles y clorofenoles en el agua potable debe ser menor a 5 µg/L (Montiel, 2013).

Debido a su elevada toxicidad y su potencial carácter mutagénico, el fenol es un compuesto de especial relevancia en el campo de la investigación del tratamiento de aguas contaminadas y es ampliamente utilizado como contaminante modelo, existen numerosos trabajos sobre su tratamiento y destrucción (Pimentel *et al.*, 2008; Babuponnusami and Muthukumar, 2012; Prince *et al.*, 2015; Zhang *et al.*, 2015; Amado-Piña *et al.*, 2017).

1.4 Métodos de remoción del fenol.

En la última década, el tratamiento de los efluentes contaminados con fenol ha llamado mucho la atención debido a su alta toxicidad y baja biodegradabilidad. A nivel industrial,

los compuestos fenólicos son muy difíciles de degradar mediante métodos de tratamiento convencionales.

Para la remediación de los efluentes contaminados, se han desarrollado diversos métodos principalmente fisicoquímicos y biológicos. De manera general los métodos más aplicados, tanto a escala laboratorio como a nivel industrial, se presentan en la Figura 2.

Sin embargo, no todos los tratamientos mencionados en la figura anterior son aplicables a la remoción de contaminantes orgánicos persistentes, dado que los tratamientos biológicos son ineficaces ante las sustancias orgánicas de alta toxicidad. Por ello, los procesos de oxidación avanzada (POA´s), métodos electroquímicos, fotoquímicos y algunas combinaciones de esta, han tenido alta aplicabilidad en este contexto.

Retomando lo anterior, en la Tabla 2 se presentan algunos métodos de tratamientos de agua, en los cuales se empleó como molécula modelo al fenol. En todos los casos se presentan, porcentajes de remoción mayores al 50% e inclusive una mineralización total del contaminante. Con respecto a las investigaciones donde se presenta una mineralización parcial, se reportan subproductos de degradación, con menor toxicidad respecto al fenol, como lo son los compuestos alifáticos (ácidos carboxílicos, principalmente), por otro lado, en los primeros minutos de tratamiento se reporta la formación de compuestos de mayor toxicidad (hidroquinona, benzoquinona y p-benzoquinona).

Al ser objeto de estudio los procesos de Electro-Oxidación y Ozonación de la presente investigación, se abordan con mayor énfasis sus respectivos fundamentos en las secciones subsecuentes, así como los sistemas de reacción más empleados en cada uno de los casos

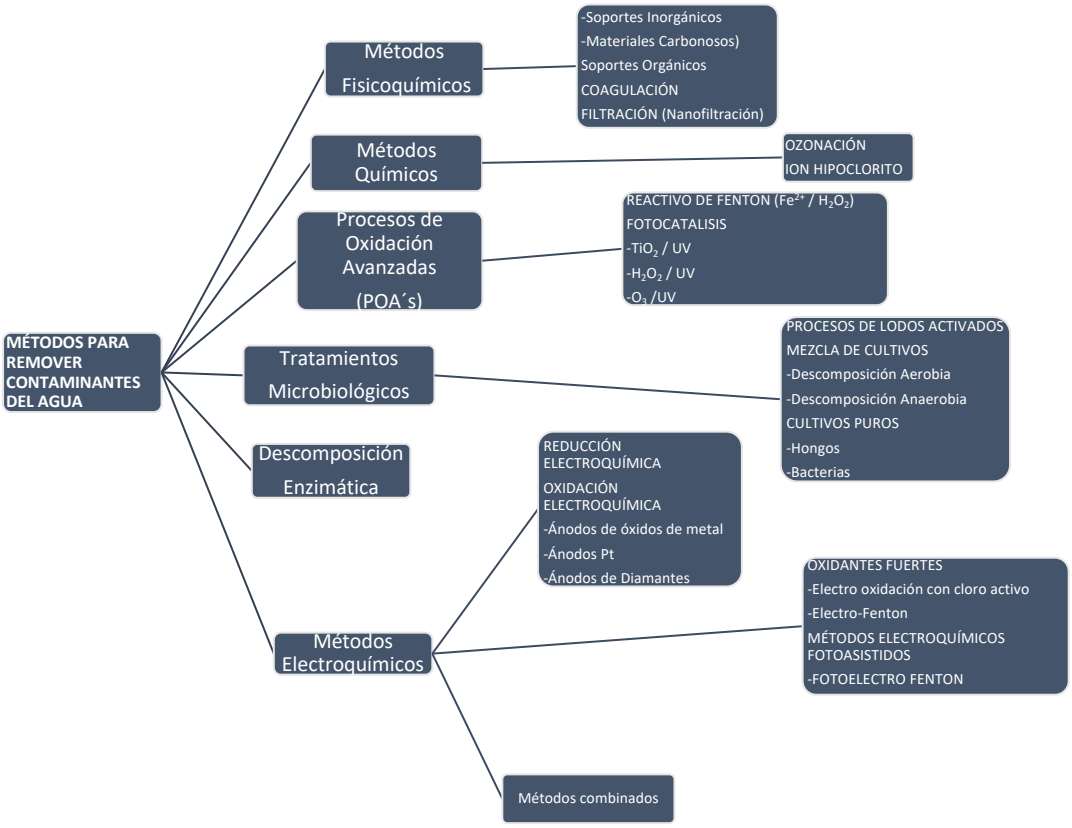

Figura 2. Métodos de remoción de contaminantes del agua (Brillas y Martínez-Huitle, 2015)

Tabla 2. Métodos de remoción del fenol

Método	Concentración inicial [ppm]	Porcentaje de remoción [%]	Monitoreo de la concentración	Volumen de reacción [L]	Tiempo de tratamiento [h]	Catalizador y / o electrodos	Subproductos	Referencias
Ozonación	26	60	TOC	1.8	6	O_3	No reportados	(Hurwitz *et al.*, 2014)
	1100	70	DQO	0.2	2.1	O_3, MgO	No reportados	(Moussavi, khavanin and Alizadeh, 2010)
Electro - Fenton	100	75	TOC	0.35	12	WO_3 / Cátodo difusor de oxígeno, Fe	Hidroquinona, benzoquinona, ácido maleico, ácido tartárico, ácido malónico y ácido oxálico.	(Assumpção *et al.*, 2013)
	200	67.93	DQO	1.0	0.6	Acero inoxidable - Acero inoxidable, Fe	No reportados	(Babuponnusami and Muthukumar, 2012)
	24	100	TOC	0.4	4	Platino - Fieltro de carbono, Fe y Cu	Catecol, hidroquinona, p-benzoquinona, ácido succínico, ácido maleico, ácido fumárico y ácido oxálico.	(Pimentel *et al.*, 2008)
Foto - catalítico	40, 80	60, 80	UV-VIS	0.2	6	ZnGaAl	No reportados	(Prince *et al.*, 2015)
	30	82	TOC	0.2	5	$ZnTiO_2$	No reportados	(Sanchez-Dominguez *et al.*, no date)
	20	97	TOC	0.1	1	Bi_2WO_6	No reportados	(H. Sun *et al.*, 2011)
	25	79	UV-VIS	0.2	3	ZnO(10%)/MCM-22/UV/PDS	No reportados	(S. Sun *et al.*, 2011)
Electro - Oxidación	26	96	TOC	1.8	6	DSA-Cl_2 -- DDB	No reportados	(Hurwitz *et al.*, 2014)
	50	85	TOC	0.2	3	PbO_2 / Acero inoxidable	Catecol, hidroquinona, benzoquinona, ácido maleico, ácido fumárico, resorcinol y ácido oxálico.	(Duan *et al.*, 2013)
Electro - peroxonación	100	98.5	TOC	0.9	2.0	BDD / BDD	Catecol, hidroquinona, benzoquinona, ácido maleico,ácido fórmico, ácido fumárico y ácido oxálico.	(Amado-Piña *et al.*, 2017)

1.4.1 Electro-oxidación

La electro-oxidación de contaminantes orgánicos, efectuada en una celda electrolítica, se basa principalmente en los siguientes fundamentos (Martínez-Huitle & Brillas, 2009):

i. **Oxidación directa.** En la superficie del ánodo (M) o por la transferencia de electrones al ánodo.

ii. **Reacción química con radicales hidroxilo electro-generados.** Los radicales libres son generados por la descarga de agua en la superficie del electrodo, como a continuación se presenta.

$$H_2O + M \rightarrow M(\cdot OH) + H^+ + e^- \qquad (1)$$

Una explicación más amplia del mecanismo de electro-oxidación, fue dada por Comninellis, 1994 y años más tarde Marselli *et al.* (2003); Michaud *et al.* (2003), complementaron este modelo que a continuación se presenta:

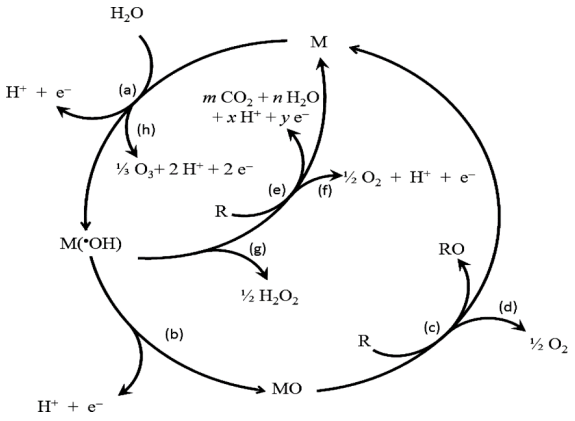

Figura 3. Mecanismo de oxidación anódica de compuestos orgánicos (Comninellis, 1994; Marselli et al., 2003; Michaud et al., 2003)

En la Figura 3 se explica que existen varias rutas para la mineralización de contaminantes orgánicos, así mismo también se presentan algunas reacciones que afectan la eficiencia del

proceso de electro-oxidación. A continuación, se presenta una breve explicación del mecanismo de oxidación anódica:

- **Oxidación indirecta:** La oxidación de materia orgánica se favorece por la formación de radicales hidroxilos los cuales están fisisorbidos M (•OH) en la superficie del metal. Adicionalmente hay formación de H_2O_2 y O_3, los cuales son oxidantes indirectos.
- **Oxidación directa:** Las moléculas orgánicas también se oxidan en la superficie del ánodo, sin estar presente un radical hidroxilo. La quimisorción del radical hidroxilo (MOH), favorece este mecanismo.
- **Reacciones parásitas:** La formación de Hidrógeno y la evolución del oxígeno, son reacciones que disminuyen la generación de radicales hidroxilo, por consecuencia afectan de manera global la eficiencia de la electro-oxidación (Comninellis & Chen, 2010).

Tal vez el aspecto más importante en el proceso de electro-oxidación de compuestos orgánicos, es la selección del material del ánodo, debido a que en este electrodo se lleva a cabo la oxidación del contaminante. Comninellis & Chen (2010) clasificaron a los ánodos en base a su poder oxidante, el cual está principalmente determinado por la fuerza de las interacciones de los radicales hidroxilo en la superficie de los electrodos.

Tabla 3 .Potencial de oxidación de diferentes materiales utilizados como ánodos (Comninellis & Chen, 2010; Martínez-Huitle *et al.*, 2015).

Electrodos	Potencial de Oxidación (Volts)	Sobre-potencial de evolución de O_2 (Volts)	Entalpía de absorción	Poder oxidante del ánodo
RuO - TiO (DSA - Cl_2)	1.4 - 1.7	0.18	Quimisorción	
IrO_2 - Ta_2O_5 (DSA - O_2)	1.5 - 1.8	0.25		
Ti / Pt	1.7 - 1.9	0.3		
Ti / PbO_2	1.8 - 2.0	0.5		
Ti / SnO_2 - Sb_2O_5	1.9 - 2.2	0.7		
p-Si / DDB	2.2 - 2.6	1.3	Fisisorción	

Un parámetro importante en la selección de un par de electrodos, es el sobrepotencial de evolución de oxígeno, debido a que limita la formación de radicales hidroxilo a partir de la

reacción de la descarga del agua sobre la superficie de los electrodos, para contrarrestar este efecto es preferible emplear un par de electrodos con un sobre-potencial de evolución de oxígeno alto (Comninellis & Chen, 2010). En la presente investigación se propone el uso de electrodos DDB y por lo tanto a continuación se abordan con más detalle.

1.4.1.1 Electrodos de DDB (Diamante Dopado con Boro)

El material sintético DDB, es aplicado a diversos sustratos como lo son el Nb, Ti y Si, para posteriormente ser utilizado como electrodo. Desde 2008 se han empleado de manera significativa los electrodos de DDB en la mineralización de colorantes sintéticos (Brillas & Martínez-Huitle, 2015). En los electrodos de DDB, la formación de radicales hidroxilo proviene de la reacción de la descarga de agua sobre la superficie de los electrodos, por ello los radicales hidroxilo se encuentran fisisorbidos en la superficie del ánodo DDB ($^{\bullet}OH$). En varias investigaciones, la aplicación de los electrodos de DDB en celdas de electrólisis han reportado porcentajes de mineralización cercanos al 100% en diferentes tipos de contaminantes (Brillas & Martínez-Huitle, 2015b; Martínez-Huitle *et al.*, 2015; Moreira *et al.*, 2017). En las celdas electroquímicas que utilizan un par de electrodos de DDB-DDB, la oxidación de materia orgánica no se logra únicamente por la reactividad del radical hidroxilo, sino también por la formación de H_2O_2 y O_3, compuestos que oxidan de manera indirecta a la materia contaminante, así mismo durante la electrólisis se generan otras especies muy oxidantes, tales como las especies de cloro activo, per-oxidisulfatos, per-oxidicarbonatos, per-oxidifosfatos, entre otros (Brillas & Huitle, 2011; Brillas & Martínez-Huitle, 2015b; Moreira *et al.*, 2017) .

La Figura 4 describe el mecanismo de la oxidación del agua sobre la superficie de los electrodos de DDB, la formación de especies oxidantes como el peróxido de hidrógeno y radical hidroxilo, sin olvidar la evolución del oxígeno (Michaud *et al.*, 2003).

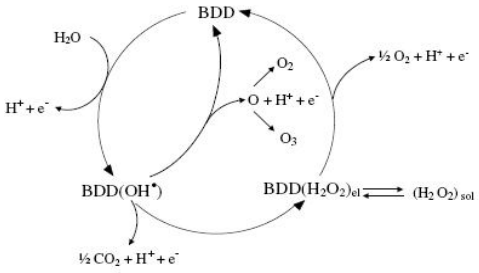

Figura 4. Mecanismo de oxidación del agua sobre la superficie de un ánodo de DDB(Michaud *et al.*, 2003; Brillas and Huitle, 2011; dos Santos *et al.*, 2018)

1.4.1.2 Reactores empleados en Electro-Oxidación

La evaluación a escala laboratorio de un proceso de Electro-Oxidación, primeramente, se efectúa en volúmenes pequeños, iniciando desde 100 mL, por mencionar un volumen. La celda electroquímica sin división consiste básicamente en un recipiente de geometría cilíndrica, un par de electrodos, un sistema de agitación y una fuente de poder. A partir de volúmenes de reacción pequeños se pueden establecer diferentes condiciones de reacción fijando una concentración inicial del contaminante problema, como lo son la densidad de corriente, concentración de electrolito soporte, velocidad de agitación y temperatura (Martínez-Huitle *et al.*, 2015). En la Figura 5, se presenta una celda sin división para llevar a cabo el proceso de Electro-Oxidación.

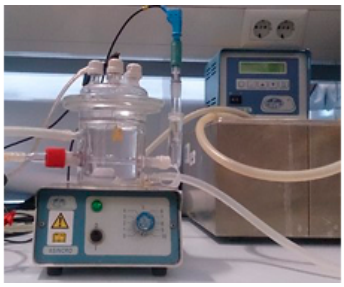

Figura 5. Celda de Electro-Oxidación (Martínez-Huitle *et al.*, 2015)

El aumento en el tamaño de volumen tratado ha obligado a los diferentes grupos de

investigación a desarrollar y/o modificar sus sistemas de reacción, para efectuar el tratamiento de volúmenes a escala pre-piloto y piloto. Tal es el caso del grupo de investigación de Enric Brillas (Olvera-Vargas *et al.*, 2015; Pérez *et al.*, 2015; Garcia-Segura and Brillas, 2016), en el cual se han enfocado en realizar estudios en volúmenes de 2.5 L y 10 L. Su sistema de reacción es un reactor tipo filtro prensa sin división en el cual se colocan los electrodos (ánodo y cátodo). Si bien este compartimento no es muy grande, el aumento de volumen se logra mediante el almacenamiento de la solución contaminante en un tanque, posteriormente este volumen es recirculado hacia los electrodos, adicionalmente se tiene un sistema de bombeo, un sistema de intercambio de calor para mantener la temperatura y un panel solar, de tal manera que es un sistema más sustentable y mayor ahorro energético (ver Figura 6). Este sistema de reacción es empleado en procesos de Electro-Oxidación, pero también en procesos de Electro-Fenton y cuando es efectuado este proceso se emplea un cátodo difusor de oxígeno el cual de manera simultánea suministra oxígeno para la formación de peróxido de hidrógeno.

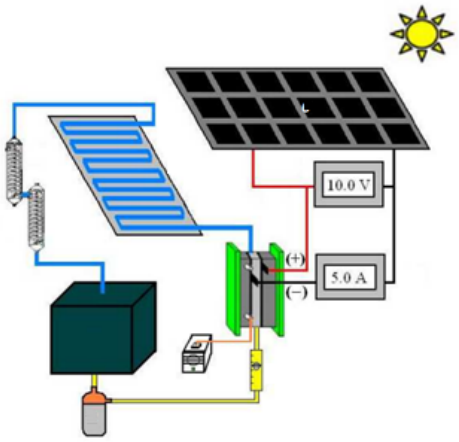

Figura 6. Sistema de reacción tipo filtro prensa(Garcia-Segura and Brillas, 2014)

Una variante del sistema descrito anteriormente es la celda Diaclean o Diacell (Figura 7), en este tipo de sistema de reacción es prácticamente igual, la diferencia más significativa es que la celda Diacell es comercial y pueden acoplarse otros módulos de electrodos, tal como se muestra en la Figura 8, por tanto, se puede estar trabajando con más de un par de electrodos a la vez, por consecuencia el tiempo de tratamiento es menor.

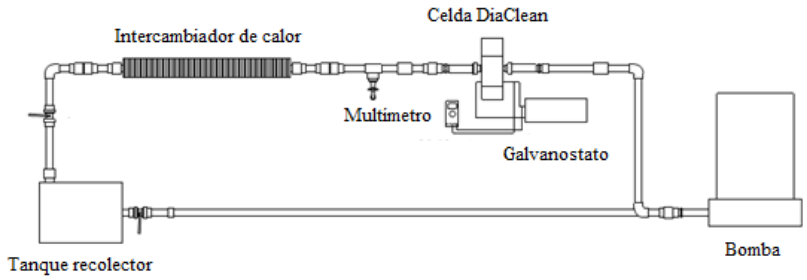

Figura 7. Celda Diaclean o Diacell (Barrera-Díaz *et al.*, 2014; Armijos-Alcocer *et al.*, 2017)

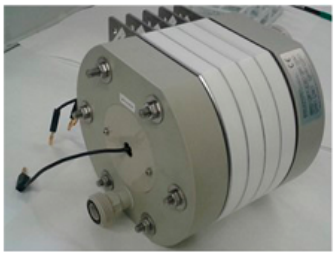

Figura 8. Celda Diacell con 4 módulos (Martínez-Huitle *et al.*, 2015)

Otra modificación del reactor tipo filtro prensa, es la estudiada por el grupo de investigación de Pablo Cañizares y Manuel Rodrigo, quienes propusieron incrementar la taza de producción *in situ* de peróxido de hidrógeno, mediante una inyección tipo venturi (ver Figura 10), el sistema también es conocido como jet aerator presurizado. Con este acoplamiento y utilizando un cátodo de carbono PTFE y ánodo de IrO_2, han logrado producir alrededor de 500 mg/dm^3 de peróxido de hidrógeno en un tiempo de 2 horas (Pérez *et al.*, 2017). Recientemente en el mismo grupo de investigación, comprobaron que al presurizar el sistema a una presión de 6 bar, se triplica la concentración de oxígeno en la celda electroquímica y puede producirse peróxido de hidrógeno de manera instantánea, desde el inicio de la reacción (Pérez *et al.*, 2018).

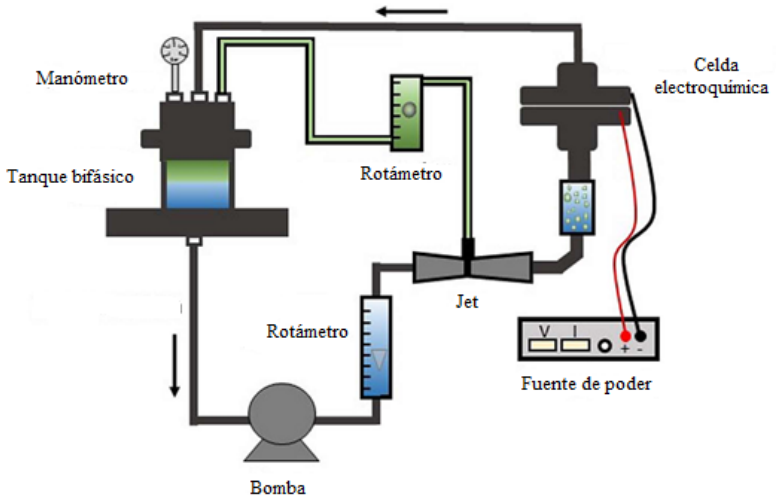

Figura 9. Celda tipo jet aerator presurizado (Pérez et al., 2018)

Deleted: (

1.4.2 Ozonación

La ozonación es una tecnología avanzada de oxidación que no es exclusiva para la potabilización de agua, ya que también se aplica en la degradación de compuestos orgánicos, debido a su alto poder oxidante (E^o: 2.07 V), por otro lado, también mejora la biodegradabilidad del efluente.

A través de los numerosos trabajos publicados que se ocupan de la ozonación, las ventajas de este proceso para el tratamiento de agua residual han sido evidenciadas:

- Es efectivo en un amplio rango de temperatura y pH.
- Reacciona rápidamente con bacterias, virus y protozoos.
- Es un potente oxidante que requiere períodos cortos de contacto.
- Reduce la demanda química de oxígeno, turbiedad, color.
- No requiere de la adición de reactivos químicos en el tratamiento

Así mismo la ozonación también tiene desventajas entre las cuales destacan las siguientes (Mohammadi *et al.*, 2014):

I. La solubilidad en agua es baja.
II. La velocidad de remoción es baja, en contaminantes orgánicos estables, por lo cual requiere un alto consumo de ozono.
III. El ozono es tóxico, por lo cual se requiere de una etapa de destrucción en el proceso.

El ozono puede actuar mediante dos vías: directa (molecular) e indirecta (producción de radicales hidroxilo). En la práctica ambos mecanismos actúan de manera simultánea, por lo cual es necesario especificar las diferencias entre ambas rutas.

1.4.2.1 Oxidación directa.

También es conocida como el mecanismo de Criegee y consiste principalmente en reacciones selectivas entre la molécula de ozono y moléculas orgánicas no saturadas. En este mecanismo, la naturaleza nucleofílica del contaminante orgánico es determinante. La reactividad aumenta cuando hay presencia de compuestos alifáticos saturados o hay presencia de compuestos aromáticos. En consecuencia, la oxidación es más lenta en compuestos orgánicos de cadena corta o que se encuentran disociados.

Por otra parte, con respecto a los compuestos inorgánicos, el mecanismo directo actúa con mayor rapidez con respecto a las sustancias orgánicas y se ve favorecido en condiciones ácidas. Lo mismo ocurre con respecto a los compuestos inorgánicos ionizados y disociados (Gottschalk, Libra & Saupe, 2009).

1.4.2.2 Oxidación Indirecta

La principal diferencia con respecto al mecanismo de oxidación directa es que el ozono no es el agente oxidante principal, pero contribuye a la generación de especies oxidantes y electrones desapareados. Para una mejor explicación del mecanismo, se contemplan tres etapas: iniciación, propagación y terminación. Las reacciones más representativas de dichas etapas se presentan en la Tabla 4.

En la primera etapa el ozono reacciona con iones hidróxido para generar aniones superóxido ($O_2^{\bullet-}$) y radicales hidroperoxilo ($HO_2^{\bullet}$). Algunas especies de la primera etapa reaccionan una vez más para obtener el radical hidroxilo ($OH^{\bullet}$), el oxidante más poderoso. La segunda etapa del mecanismo (propagación), promueve una regeneración de radicales hidroperoxilo en la reacción (1.8), los cuales son nuevamente utilizados en la reacción (1.3) de iniciación.

Los radicales hidroxilo reaccionan también con moléculas orgánicas (R), por consecuencia se forman radicales orgánicos y en presencia de oxígeno también hay formación de peroxi-radicales. Desafortunadamente, no todas las reacciones forman radicales con alto poder oxidante, el mecanismo indirecto se ve afecto por la presencia del CO_2 disuelto en el agua, el cual tiende a formar los iones carbonato / bicarbonato, los cuales fungen como secuestrantes del radical hidroxilo, es por ello que a esta última etapa se denomina terminación. La reacción global del ozono es una combinación de las reacciones (1.2 – 1.8).

Tabla 4. Reacciones del mecanismo indirecto de ozonación (Santana-Martínez, et., al 2018)

Etapa	Reacción	
Iniciación		
	$O_3 + OH^- \rightarrow O_2^{\bullet -} + HO_2^{\bullet}$	(1.2)
	$HO_2^{\bullet} \leftrightarrow O_2^{\bullet -} + H^+$	(1.3)
Propagación	$O_3 + O_2^{\bullet -} \rightarrow O_3^{\bullet -} + O_2$	(1.4)
	$HO_3^{\bullet} \leftrightarrow O_3^{\bullet -} + H^+$	(1.5)
	$HO_3^{\bullet} \rightarrow OH^{\bullet} + O_2$	(1.6)
	$OH^{\bullet} + O_3 \rightarrow HO_4^{\bullet}$	(1.7)
	$HO_4^{\bullet} \rightarrow O_2 + HO_2^{\bullet}$	(1.8)
	En presencia de moléculas orgánicas (R):	
	$H_2R + OH^{\bullet} \rightarrow HR^{\bullet} + H_2O$	(1.9)
	$HR^{\bullet} + O_2 \rightarrow HRO_2^{\bullet}$	(1.10)
	$HRO_2^{\bullet} \rightarrow R + HO_2^{\bullet}$	(1.11)
	$HRO_2^{\bullet} \rightarrow RO + OH^{\bullet}$	(1.12)
Terminación	$OH^{\bullet} + CO_3^{2-} \rightarrow OH^- + CO_3^{\bullet -}$	(1.13)
	$OH^{\bullet} + HCO_3^- \rightarrow OH^- + HCO_3^{\bullet}$	(1.14)
	$OH^{\bullet} + HO_2^{\bullet} \rightarrow O_2 + H_2O$	(1.15)
Reacción global	$3O_3 + OH^- + H^+ \rightarrow 2OH^{\bullet} + 4O_2$	(1.16)

1.4.2.3 Reactores de ozonación.

Las reacciones del proceso de ozonación, se llevan a cabo en sistemas de reacción multifásicos líquido-gas, partiendo de que el ozono tiene una baja solubilidad en agua el objetivo principal es incrementar la transferencia de masa del ozono y la destrucción de la materia orgánica en solución.

El sistema de reacción más empleado en los procesos de ozonación, es una columna de burbujeo de flujo ascendente de geometría cilíndrica, la cual opera en modo semi-batch ya que se inyecta de manera constante la fase gas constituida por aire y ozono. Esta mezcla se deriva de un ozonador al cual se inyecta primeramente aire para posteriormente ser inyectado por el fondo de la columna. El exceso de fase gas, es eliminado hacia una trampa de KI, para destruir la cantidad remanente de ozono la cual no se consumió en la oxidación de materia orgánica disuelta.

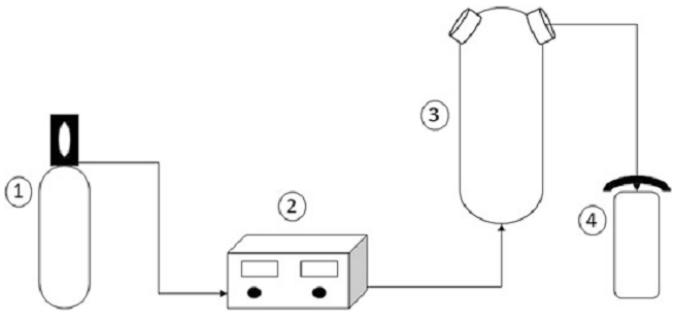

Figura 10. Sistema de ozonación semi-batch en Columna de burbujeo (Santana-Martínez, et., al 2018)

Si bien, la eficiencia en los sistemas de reacción de tipo columna de burbujeo en modo semi-batch es baja con respecto en el consumo de ozono, la degradación de los contaminantes es parcial y los tiempos de tratamiento largos, han surgido diversas investigaciones acoplando la ozonación a tratamientos foto-catalíticos y electroquímicos (Beltrán *et al.*, 2012; Quiñones *et al.*, 2015; Amado-Piña *et al.*, 2017). Por otra parte, el incremento en la eficiencia de los sistemas de tratamiento basados en el ozono, no solo se encuentra en el acoplamiento de dos tecnologías de oxidación avanzada, otra opción que ha

resultado favorable es implementar mejoras en el suministro y menor desperdicio del ozono, como en los sistemas de reacción que a continuación se describen.

Una variante al sistema de reacción presentado en la Figura 11, es la adaptación con recirculación y con dos columnas, en una inyectando ozono y en una segunda columna se empaca catalizador, esta modificación fue denominada como proceso TOCCATA (Crousier *et al.*, 2016). Este arreglo, ha permitido llevar a cabo reacciones empleando volúmenes a escala piloto, sin embargo, en las columnas de burbujeo de flujo ascendente se debe tener cuidado con el tamaño de partícula y densidad del catalizador e igualmente con el flujo de gas, al no tomar en cuenta estas variables la transferencia de masa puede convertirse en la etapa limitante del proceso.

A pesar del incremento de la eficiencia en el uso del ozono en el sistema del proceso TOCCATA, el uso del ozono en este sistema sigue sin utilizarse en su totalidad, debido a que no se ha prescindido de la trampa de KI para destruir el ozono remanente. Este desperdicio de ozono resulta costoso y perjudicial al medio ambiente, esto ha motivado a diferentes investigadores del área de reactores a optimizar el uso del ozono. Dada esta problemática, el grupo de investigación de Gian Luca Li Puma, desarrolló un sistema de ozonación denominado Columna con bafle de multi orificio oscilatorio (CBMO), el cual se representa en la Figura 12. Este sistema de reacción consiste en una columna de acoplada con bafles multi-orificio los cuales son impulsados mediante la acción de un pistón, el contar con multi-orificio favorece la transferencia de masa, lo cual permite un consumo del 100% del ozono suministrado a la columna. Los autores emplearon 50mg/L de ácido p-hidroxibenzoico, en un volumen de 9.6 L, en recirculación de 4L/min, pH 10, flujo de gas 2.1 - 4.7 L/min con una concentración de 23 gO_3 /m^3 (Lucas *et al.*, 2009). Comparando los resultados con los experimentos llevados a cabo en una columna de burbujeo convencional, los autores encontraron se incrementó en un 20% la degradación del contaminante principal y en un 75% la mineralización por mol de ozono consumido, así mismo se incrementó en seis veces la concentración de oxígeno disuelto.

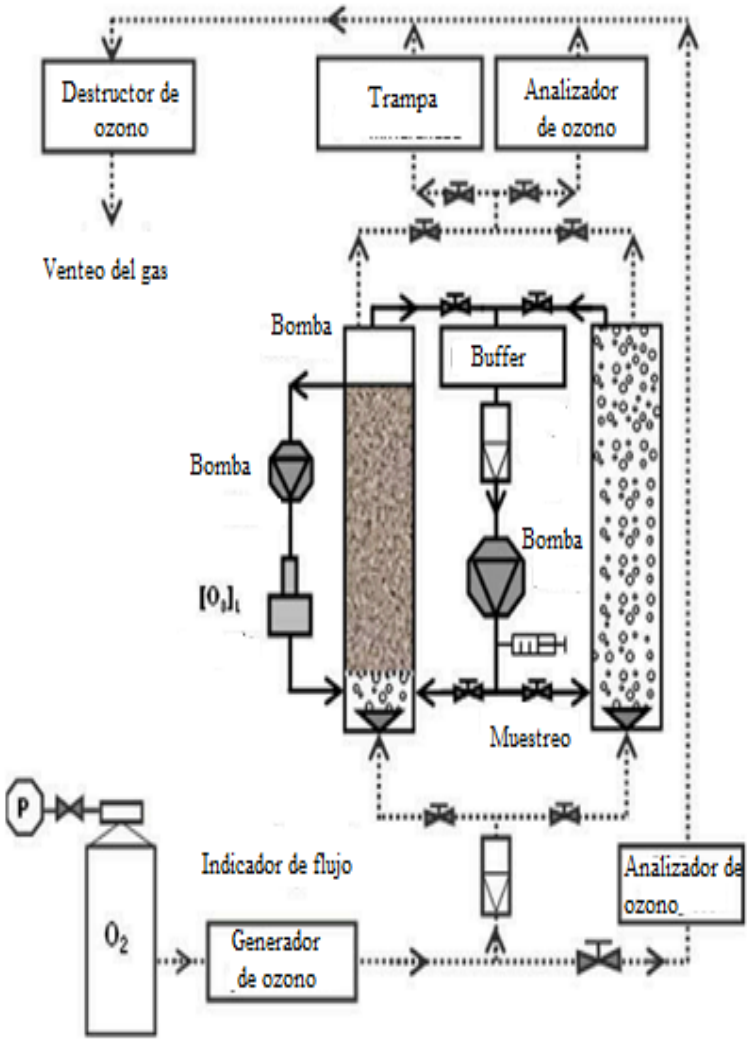

Figura 11. Proceso TOCCATA (Crousier et al.*, 2016)*

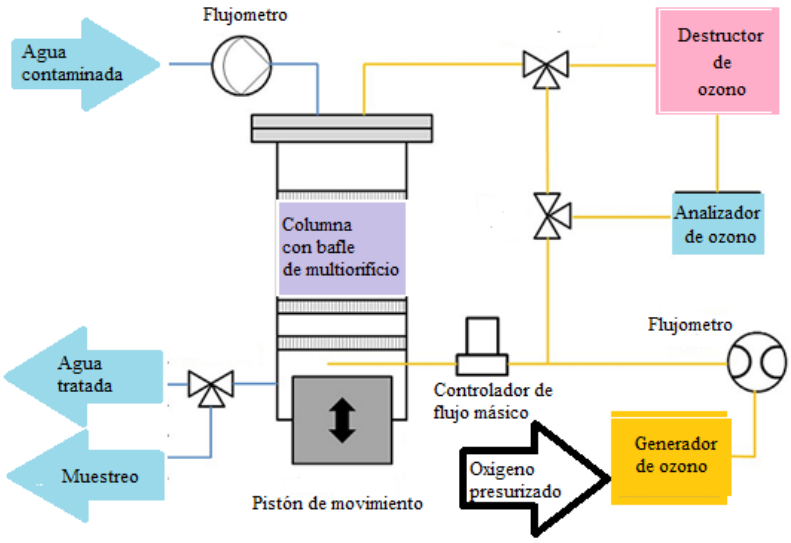

Figura 12.. Columna con bafle de multi orificio oscilatorio (Lucas et al.*, 2009)*

1.4.3 Electro-Peroxonación

Cuando se suministra O_2 en un sistema de reacción electroquímico, en el cátodo se lleva a cabo una reducción catódica del oxígeno y como producto se obtiene peróxido de hidrógeno *in situ,*

$$O_2 + 2e^- + 2H^+ \rightarrow H_2O_2 \qquad (1.17)$$

La interacción entre la molécula de ozono con la molécula de peróxido de hidrógeno se conoce como peroxonación (reacción (1.18)), en este proceso hay formación de radicales hidroxilo (reacción 1.20). En algunas reacciones este proceso se ve afectado por la presencia de agua, tal como se observa en la reacción (1.19), en la cual hay una disociación hacia iones hidronio y anión hidróxido, sin embargo, este último reacciona de nueva cuenta con el ozono y forma iones hidroxilo (Santana-Martínez *et al*., 2018).

$$H_2O_2 + 2O_3 \rightarrow 2OH^{\bullet} + 3O_2 \qquad (1.18)$$

$$H_2O_2 + H_2O \rightarrow HO_2^- + H_3O^+ \qquad (1.19)$$

$$O_3 + HO_2^- \rightarrow OH^{\bullet} + 2O_2 \qquad (1.20)$$

Un exceso en la formación peróxido de hidrógeno (>10mM), trae como consecuencia radicales hidroxilo, esto es explicado en las siguientes dos reacciones (Gomes *et al.*, 2017):

$$OH^{\bullet} + H_2O_2 \rightarrow HO_2^{\bullet} + H_2O \qquad (1.21)$$

$$OH^{\bullet} + O_3 \rightarrow HO_2^{\bullet} + O_2 \qquad (1.22)$$

En la Figura 13, se presenta el sistema de reacción comúnmente empleado en electro-peroxonación, en el cual podemos observar que la diferencia principal con respecto a un reactor de electro-oxidación es la presencia de un generador de ozono.

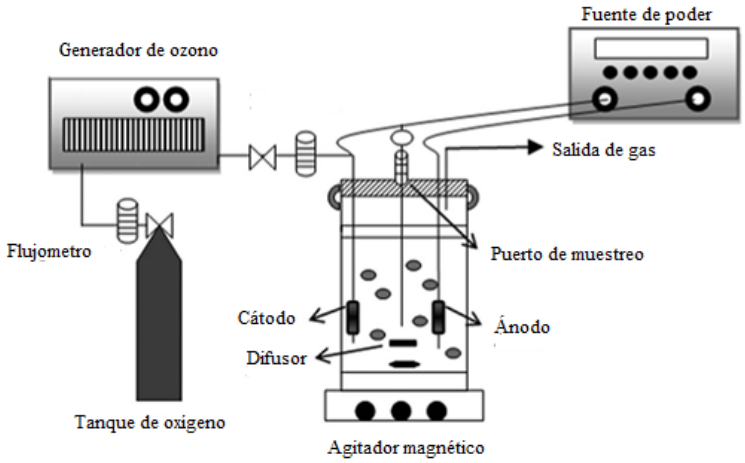

Figura 13. Reactor de Electro-Peroxonación (Turkay, Ersoy & Barışçı, 2017)

Con respecto a los contaminantes fenólicos, hay un trabajo realizado por Amado *et al*., (2015), quien trabajó con una solución sintética de Fenol a una concentración de 100 mg/L, obteniendo sus mejores resultados aplicando una densidad de corriente de 60 mA/cm^2 (Electrodos de DDB), pH: 7.0, con un flujo de fase gas continuo con una concentración de 5 ±0.5 mg/L de ozono a un volumen de 1.0 L de solución de contaminante. Después de 60 minutos de tratamiento, se obtuvo un 100% de degradación y un 98.5% de mineralización cuantificada mediante el análisis de Carbono Orgánico Total (COT).
En los arreglos experimentales de los trabajos mencionados en la sección anterior, una constante es el uso del generador de ozono al cual se alimenta oxígeno.

Sin embargo, en esta propuesta de investigación, se desarrolló un sistema que no solamente generó el peróxido de hidrógeno *in situ* sino también al ozono. Esto bajo la premisa de que la producción electroquímica de ozono y oxígeno es viable mediante reacciones electroquímicas (Christensen, Yonar & Zakaria, 2013; Yang *et al.*, 2018).

La electro-generación de peróxido de hidrógeno *in situ*, ha sido llevada con éxito mediante la reducción catódica del oxígeno en materiales carbonosos como: fieltro de carbono (Mousset *et al.*, 2014), cátodo difusor de oxígeno (Garcia-Segura *et al.*, 2016), esponja de

carbono (Özcan *et al.*, 2008) y grafito (Santana-Martínez *et al.*, 2016). En el mismo tenor, también se ha reportado la electro-generación de H_2O_2 *in situ* en cátodos de DDB (Isarain-Chávez *et al.*, 2013; Peralta *et al.*, 2013).

Por otra parte, con respecto a la generación *in situ* de ozono, se reportan investigaciones empleando materiales como DDB, PbO_2 y Sn_2Sb. En estos trabajos, no se reportó la generación simultanea de ozono y peróxido de hidrógeno, debido al empleo de condiciones de reacción son extremadamente ácidas (pH<1). Teniendo en cuenta esta problemática, el propósito de las nuevas investigaciones es reducir los costos energéticos y de materia prima, esencialmente, para hacer más factible la implementación de la tecnología a mayores escalas. El efecto sinérgico de la electro-peroxonación tiene ventajas, entre las cuales destacan las siguientes:

- Acelera la transformación de O_3 a $^{\bullet}OH$ (Fischbacher *et al.*, 2013).
- La adición de H_2O_2 y O_3, no genera subproductos tóxicos, ya que tiene como subproducto al O_2 y H_2O (Martínez-Huitle & Brillas, 2009; Bakheet *et al.*, 2013)..
- Reduce la formación de bromatos y bromidos, sustancias potencialmente cancerígenas (X. Li *et al.*, 2015; Y. Li *et al.*, 2015).
- Incrementa la eficiencia del proceso y disminuye la demanda de energía, esto es debido a que el tratamiento requiere de menor tiempo con respecto a los procesos separados. También es una opción segura y bajo costo, por ello representa una de las mejores alternativas en los procesos electroquímicos (Wang *et al.*, 2018).
- Mejora la velocidad de degradación de contaminantes persistentes (Wang *et al.*, 2015) .

Tomando en cuenta las ventajas que tiene el proceso de electro-peroxonación sobre los procesos separados (electro-generación in situ de peróxido y ozonación), se ha vuelto un tema de interés, entre la comunidad científica que estudia los procesos electroquímicos de oxidación avanzada. Recientemente, se publicó una investigación en la cual se generan ambas especies oxidantes, con lo cual se prescinde del uso de un generador de ozono(Yang *et al.*, 2018). Los autores de esta investigación emplearon un electrodo de membrana en el cual se genera ozono mediante las siguientes reacciones (1.23y 1.24).

$$Cátodo \quad 1.5O_2 + 6H^+ + 6e^- \rightarrow 3H_2O \qquad (1.23)$$

$$Ánodo \quad 3H_2O \rightarrow 6H^+ + 6e^- + O_3 \qquad (1.24)$$

Por otra parte, ocuparon un cátodo de material carbonoso para reducir catódicamente el oxígeno formado en la reacción. Al reportarse este tipo de investigaciones en el tema de electro-peroxonación, la nueva tendencia es eliminar el generador de oxígeno para hacer más sustentable y económico el proceso, ya que anteriormente solo el peróxido de hidrógeno se podía *generar in situ*. Dada esta problemática, en el presente proyecto, se utiliza un sistema de reacción en el cual también se propone electro-generar de manera simultánea el ozono y oxígeno.

1.4.4 Columnas de Burbujeo

Una Columna de Burbujeo es un equipo que fue diseñado originalmente para poner en contacto de manera eficiente líquidos y gases. El uso de las Columnas de Burbujeo en Procesos de la Industria Química y Bioquímica ha cobrado relevancia, de manera que este tipo de columnas pueden ser utilizadas en procesos de absorción, fermentación y como reactores multifásicos, por mencionar algunas aplicaciones.

Las Columnas de Burbujeo son clasificadas como de flujo ascendente, flujo descendente, concurrente y contracorriente, dependiendo de la dirección de flujo de las fases participantes (gas y líquido). Entre estas, la Columna de Burbujeo de Flujo Paralelo Descendente, fue desarrollada en Birmingham (Inglaterra), hace aproximadamente 3 décadas. En este tipo de columna, la inyección de la fase gas y el líquido, se realiza por la parte superior del equipo, tal que el gas se dispersa en el líquido y forma una matriz de burbujas. Las propiedades físicas del fluido con el que se trabaja, determinan el diámetro de la burbuja y este fluctúa en el intervalo de 1-5 mm (Natividad, 2004). Debido al tamaño de burbuja, densidad de burbujas y turbulencia, se consigue la saturación de un líquido con un gas en un tiempo promedio de 4 s (Lu, Boyes & Winterbottom, 1994). Las variables a modificar para controlar el área de transferencia de masa gas-líquido son: tensión superficial del líquido, velocidad del líquido, velocidad del gas y presión.

Entre las ventajas que presentan las Columnas de Burbujeo de Flujo Paralelo Descendente, se pueden mencionar las siguientes (Lu, Boyes & Winterbottom, 1994):

- Utilización del 100% del gas alimentado
- Alta fracción volumétrica de gas (0.5-0.6)
- Alta eficiencia en la transferencia de masa
- Diseño y escalamiento relativamente simple
- Mantenimiento sencillo debido a que no hay partes movibles

Años más tarde, la Columna de Burbujeo de Flujo Descendente, fue identificada como CDCR (Co-current Downflow Contactor Reactor). En las últimas dos décadas, el CDCR, ha sido aplicado específicamente en procesos catalíticos multifásicos como la hidrogenación selectiva de 2-butin-1,4-diol (Natividad, 2004). Por otra parte, se ha empleado en procesos de oxidación avanzada como reactor fotocatalítico y celda electroquímica (ver Tabla 5).

Con respecto al uso como reactor fotocatalítico encontramos dos aplicaciones a volúmenes de escala piloto, en los cuales se realizó el tratamiento de contaminantes fenólicos. En ambos casos se emplean catalizadores heterogéneos, al emplear el catalizador de TiO_2 se alcanza una remoción del 100% del contaminante 2,4,6 triclorofenol, por otro lado, en la investigación donde se empleó la hidrotalcita doble laminar se obtuvo un 94% de remoción del contaminante 4-Clorofenol. La eficiencia de este reactor en procesos multifásicos se basa en la excelente transferencia de masa que provee. Esto ha motivado el intentar extrapolar la aplicación de dicho reactor a otros procesos, como los electroquímicos, donde la transferencia de masa entre fases requiere ser intensificada.

Tabla 5. Aplicaciones del CDCR

Contaminante	Catalizador y/o electrodos	Condiciones de reacción	Porcentaje de remoción	Referencia
2, 4, 6-triclorofenol	TiO_2	V: 15L C_0: 120mg/L P: 1 bar	100% UV-VIS	(Ochuma *et al.*, 2007)

		T: 50°C Lámpara 2kW T:180 minutos		
4-Clorofenol	HDLMgAlZn	V: 14L C_0: 100mg/L T= 298 K Q: 2.3 x 10^{-4} m^3/s (líquido) Q: 8.3 X 10^{-7} m^3/s (gas) T:180 minutos Lámpara 400W, λ:254nm	94 % UV-Vis 100 % TOC	(del Campo *et al.*, 2011)
4-Clorofenol	Grafito-Grafito	V: 14L C_0: 50mg/L j: 4 mA/cm^2 T= 298 K T:180 minutos Lámpara 400W, λ:254nm	44 % UV-Vis 39.74 % TOC	(Peralta, 2013)

A la fecha únicamente existe un trabajo reportado del acoplamiento de un CDCR como celda electroquímica (Peralta, 2013). Este trabajo consistió en llevar a cabo la electro-generación de peróxido de hidrógeno (H_2O_2) por medio de la reducción catódica del oxígeno disuelto en una solución acuosa de Na_2SO_4 en una Columna de Burbujeo de Flujo Descendente (Peralta, 2013), la celda se presenta en la Figura 14. La cantidad máxima de peróxido de hidrógeno fue de 3 mg/L, con electrodos de grafito (ánodo y cátodo), empleando las condiciones de reacción presentadas en la Tabla 5, para poder degradar el contaminante se acopló al sistema una lámpara de radiación ultravioleta de 400 W. Como se puede apreciar el porcentaje de remoción es parcial y es una investigación novedosa en el área de los procesos electroquímicos, lo cual ha incentivado a evaluar otros procesos electroquímicos y/o acoplados en este sistema de reacción.

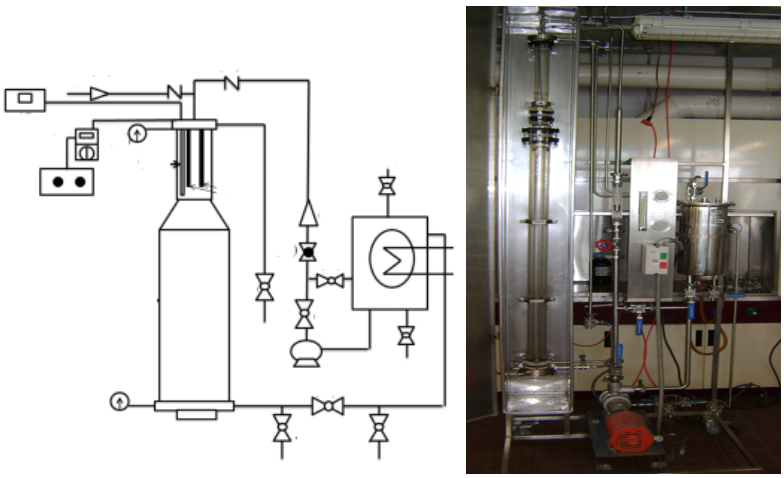

Figura 14. Reactor CDCR acoplado como celda electroquímica (Peralta, 2013)

Justificación.

2.JUSTIFICACIÓN

La disponibilidad de agua libre de contaminantes se ha convertido en una constante preocupación del ser humano. Esto no sólo por una gran parte de la población del mundo que no goza del vital líquido sino también por los efectos negativos observados en el ecosistema acuático. En este sentido, en el 2004 México asumió el compromiso de reducir la emisión de contaminantes orgánicos persistentes (COP's) identificados en la convención de Estocolmo como prioritarios. Dentro de los compromisos adquiridos por México está el de minimizar la generación de COP's a través de la adopción de las mejores técnicas disponibles o mejores prácticas ambientales. En este contexto, el fenol es un contaminante orgánico persistente y su eliminación es de interés mundial. Para tal efecto, se han ensayado varios procesos de oxidación avanzada. En este sentido, el acoplamiento del proceso de ozonación con el proceso electroquímico es altamente eficiente. Sin embargo, en dicho proceso, aún existen áreas de oportunidad de mejora como lo es un mayor aprovechamiento del ozono y que esto conlleve a que se requiera menor alimentación y menor descarga del mismo. En consecuencia, en el presente trabajo se pretende evaluar la viabilidad y eficiencia de llevar a cabo el proceso de electro-oxidación en una tecnología (columna de burbujeo) que permite el uso del gas al 100%, esto es, no se descarga de manera continua el ozono al ambiente. No es del conocimiento del autor que esta tecnología haya sido empleada para dicho proceso con anterioridad y por lo tanto ésta es la contribución al área de conocimiento correspondiente.

Hipótesis y objetivos.

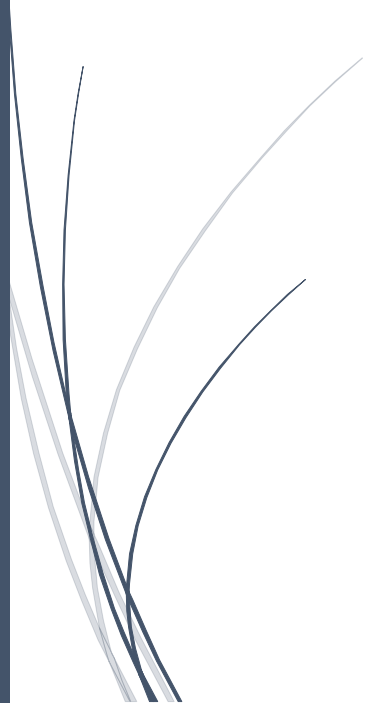

3.1HIPÓTESIS

El empleo de una Columna de Burbujeo de Flujo Descendente permitirá la remoción total de un compuesto fenólico y disminuirá hasta en un 90% el desperdicio de ozono comparado con una celda electroquímica convencional, en el proceso de electro-oxidación.

3.2OBJETIVO GENERAL

Establecer la factibilidad y eficiencia del proceso de electro-oxidación en una columna de burbujeo de flujo descendente para mineralizar soluciones fenólicas.

3.2.1OBJETIVOS ESPECÍFICOS

- Adaptar una columna de burbujeo convencional como reactor para llevar a cabo el proceso de electro-oxidación.
- Determinar la eficiencia de mineralización de Fenol mediante electro-oxidación, considerando los efectos de la concentración de electrolito, pH, flujo volumétrico de la fase líquida y densidad de corriente, con electrodos de DDB en la columna de burbujeo.
- Establecer el mecanismo de degradación del Fenol y de sus subproductos de degradación más representativos en la tecnología propuesta.
- Caracterizar hidrodinámicamente el reactor electroquímico.

Metodología

4.METODOLOGÍA

En la presente sección, se explica de manera general la metodología del proyecto. En la siguiente figura se presentan las cinco etapas más importantes, las cuales van en secuencia de orden cronológico.

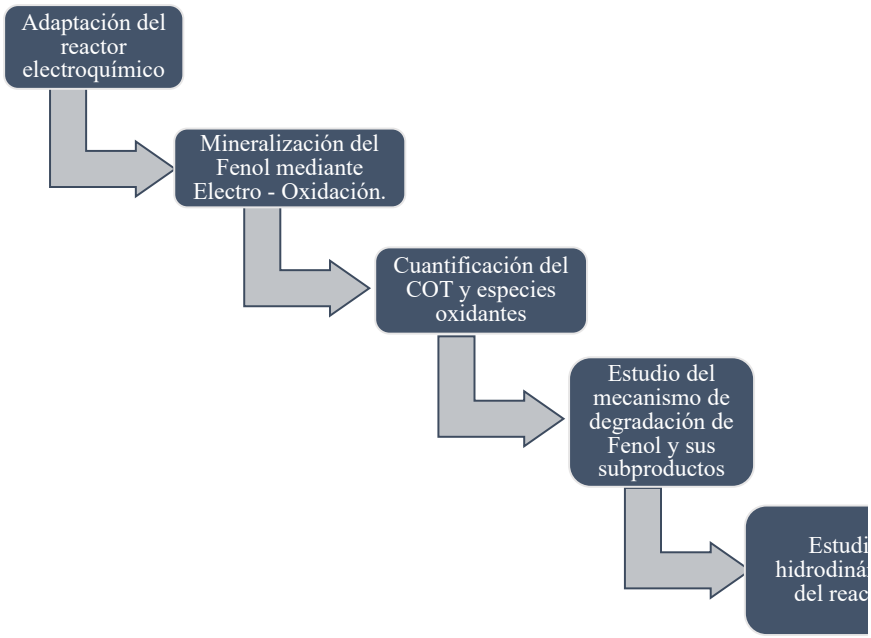

Figura 15. Metodología global del proyecto

En los siguientes apartados se aborda de manera más específica cada uno de los puntos mencionados en la figura anterior.

4.1 Adaptación del reactor electroquímico

El primer paso fue la adaptación de una columna de burbujeo de flujo descendente como reactor electroquímico a emplear en este proyecto de investigación de acuerdo con el diagrama que se muestra en la Figura 15. Esta actividad incluye desde la elección de los componentes hasta el ensamble de los mismos. En la Tabla 6 se presentan los componentes principales del reactor electroquímico.

Tabla 6. Componentes de la Columna de Burbujeo de flujo paralelo descendente adaptada como reactor electroquímico.

Elemento	Descripción de los elementos del reactor electroquímico multifásico de flujo concurrente.
1	Fuente de poder.
2	Electrodos de Diamante Dopado con Boro (DDB).
3	Columna de burbujeo de flujo paralelo descendente (3.5 L).
4	Medidor de flujo de recirculación de la fase líquida. (4.7 – 6 L/min)
5	Destructor de ozono.
6	Tanque de recirculación.
7	Bomba de recirculación (1 HP).
8	Sensor de oxígeno disuelto HACH.
9	Serpentín de enfriamiento.
10	Tanque de enfriamiento y bomba de recirculación (0.5 HP)
IP	Manómetro de presión.
IT	Sensor de temperatura.

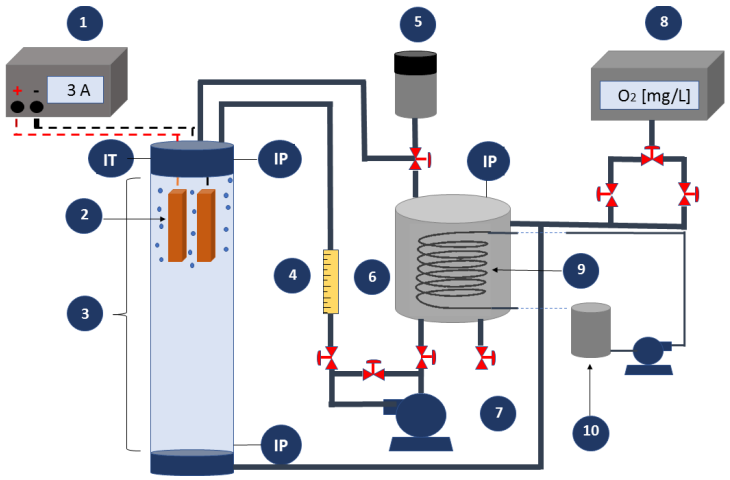

Figura 15. Columna de Burbujeo de flujo paralelo descendente adaptada como reactor electroquímico

4.2Reactivos.

A continuación, en la Tabla 7, se enlistan los reactivos empleados en las reacciones de electro-oxidación y en los análisis químicos realizados a las muestras tratadas electroquímicamente. Con respecto a los solventes son grado HPLC y así mismo los estándares. El resto de las sustancias químicas empleadas, son grado reactivo.

Las soluciones empleadas en las técnicas analíticas se prepararon con agua deionizada. Hycel (<18 mΩ). Únicamente se utilizó agua del suministro municipal en la preparación de la solución sintética de fenol.

Tabla 7. Reactivos utilizados en el proyecto.

Reactivo	Proveedor
Fenol (99.5%)	Merck
Na_2SO_4	Reasol
NaOH	Fermont
H_2SO_4	Fermont
TiO_2	Degussa
H_3PO_4 (85%)	Merck
K_2HPO_4	J.T Baker
Metanol HPLC	Fermont
Trisulfonato potásico de indigo	Sigma Aldrich
Estándar de benzoquinona	Sigma Aldrich
Estándar de catecol	Sigma Aldrich
Estándar de hidroquinona	Merck
Estándar de ácido fumárico	Merck
Estándar de ácido maleico	Merck
Estándar de ácido malónico	Merck
Estándar de ácido succínico	Merck
Estándar de ácido acético	Merck
Estándar de ácido oxálico	Sigma Aldrich
Agua deionizada	Hycel (<18mΩ)

4.3Variables de reacción a evaluar en la experimentación.

La evaluación de cada una de las variables del proceso en el reactor electroquímico presentado en la figura 15, se realizó empleando un volumen de reacción de 3.5 L, considerando un tiempo de tratamiento de 6 horas en cada experimento. El proceso se trabajó en dos etapas, la primera consistió en realizar el estudio de la electro-generación de especies oxidantes *in situ*, en esta etapa no hubo adición de fenol, pero se cuantificó el

oxígeno disuelto se determinó mediante un sensor ECO 400 de HACH. De igual manera se cuantificó la cantidad de ozono disuelto y la de peróxido de hidrógeno.

En la segunda etapa, los experimentos se efectuaron primeramente a una concentración inicial de 100mg/L de fenol y posteriormente las mejores condiciones de reacción fueron evaluadas a 50 y 200mg/L. Al igual que en la primera etapa, se cuantificaron el O_2, O_3 y H_2O_2.

Tabla 8. Variables de reacción.

Variable	Electrogeneración de O_2, O_3 y H_2O_2	Electro – oxidación de fenol
Densidad de corriente [mA/cm^2]	20, 40 y 60	20, 40 y 60
Recirculación de la fase líquida [L/min]	4.7 y 6	4.7 y 6
pH	3, 7	3, 7
Concentración de Na_2SO_4 [M]	0.05	0.025, 0.05 y 0.1

En las siguientes secciones, se abordan con más detalle las determinaciones y análisis realizados a las muestras tomadas durante el tratamiento electroquímico.

4.4 Determinación del carbono orgánico total (COT).

La cuantificación del carbono orgánico total (COT), es una medición indirecta, la cual está dada por la diferencia entre la cantidad de carbono total (CT) y el carbono inorgánico (CI). Esta técnica analítica tiene su fundamento en la combustión de la materia orgánica que se analiza, la cual se efectúa a 680°C en un horno que contiene catalizador de platino soportado en alúmina. Como productos de la combustión se obtienen H_2O y CO_2, con respecto al agua, esta se evapora y el CO_2 es arrastrado por una corriente de aire de ultra pureza (Infra 32020), hacia un analizador de infrarrojo no dispersivo. Con ello se obtienen el CT y CI.

El análisis de COT se realizó para cada una de las condiciones de reacción presentadas en la sección anterior, de esta manera se obtuvo un perfil de concentración para evaluar la mineralización del contaminante. La cuantificación del COT se realizó en un equipo Shimadzu TOC-L_{CSN}. Los resultados de COT, nos indican el porcentaje de mineralización de una molécula orgánica, al compararlo con el valor inicial de COT. Esto nos indica si hay un valor de COT igual a cero, que es una mineralización completa.

4.5Determinación de la eficiencia de corriente basada en las mediciones de COT.

En el apartado anterior, se describió de manera breve la importancia de las mediciones de COT. Con estas determinaciones, también se puede realizar un cálculo de la eficiencia de corriente, lo cual nos da información del porcentaje aproximado de la corriente eléctrica que se emplea para llevar a cabo la mineralización de la molécula orgánica. A continuación, se presenta la expresión matemática para realizar el cálculo de la eficiencia de corriente:

$$M.C.E = \frac{nFV_s\Delta(TOC)_{EXP}}{4.32x10^7 mIt} x100 \qquad (1.25)$$

Las iniciales M.C.E, vienen de su nombre en inglés (Mineralization current efficiency). Describiendo cada uno de los términos, **n** corresponde al número de electrones consumidos en la mineralización del fenol (reacción 1.26), **F** es la constante de Faraday (96487 C*mol^{-1}), $\mathbf{V_S}$ es el volumen de la solución en L, $\mathbf{\Delta(TOC)_{EXP}}$ es la diferencia de COT a cierto intervalo de tiempo, **m** es el número de átomos de carbono de la molécula de fenol, **I** corresponde a la intensidad de corriente en Amperes y finalmente t, el tiempo de tratamiento en segundos.

$$C_6H_5OH + 11H_2O \rightarrow 6CO_2 + 28H^+ + 28e^- \qquad (1.26)$$

4.6Determinación espectroscópica del H_2O_2.

En los procesos electrolíticos, la generación de oxígeno es una reacción secundaria, la cual siempre ocurre. Cuando el sistema de reacción no está adecuado para captar o absorber el oxígeno, este se libera hacia la atmósfera. Para el caso del presente proyecto de

investigación, la columna de burbujeo puede absorber el oxígeno generado en la electrólisis y por consecuencia puede ser reducido catódicamente, lo cual trae producto la generación *in situ* de H_2O_2. La concentración de este compuesto oxidante es cuantificada, mediante una técnica espectroscópica, en la cual se toma una muestra de la reacción para combinarse con sulfato de titanio, como se muestra en la siguiente reacción:

$$Ti^{4+} + H_2O_2 + 2H_2O \rightarrow TiO_2 \cdot H_2O_2 + 4H^+ \qquad (1.27)$$

El sulfato de titanio es obtenido a partir de una reacción de digestión durante 15-16 horas, en la cual se emplean como reactivos 1g de dióxido de titanio y 100 mL de H_2SO_4. El producto de esta reacción es filtrado a través de fibra de vidrio y posteriormente se puede utilizar para la cuantificación de peróxido de hidrógeno, en la cual se utiliza 1 mL del sulfato de titanio obtenido con 9 mL de muestra de reacciones en las cuales se conoce la generación de peróxido de hidrógeno. Como producto de la reacción entre la muestra con contenido de peróxido de hidrógeno y el sulfato de titanio, se obtiene ácido per-titánico, el cual tiene una coloración amarilla. Esto se analiza en un equipo Perkin Elmer Lambda 25 UV/VIS a λ: 408 nm, con esta medición se cuantificó el peróxido de hidrógeno electro-generado *in situ* (Eisenberg, 1943).

4.7Determinación espectroscópica del O_3.

Al igual que en la generación del peróxido de hidrógeno, el ozono también puede ser generado mediante reacciones electroquímicas. Por ello, se puede hacer la cuantificación del ozono en solución, en este caso se empleó el método de trisulfonato potásico de índigo, en el cual se prepara una solución de este reactivo (Ver anexo 2), para mezclarse con un volumen conocido de muestra en el cual se sabe que hay presencia de ozono (Bader & Hoigné, 1981). La relación volumétrica entre el volumen de la muestra y el de la solución de trisulfonato potásico de índigo, es de 9/1 v/v.

Se basa en el principio de que, al aumentar la concentración de ozono disuelto, hay una disminución lineal de la absorbancia inicial del trisulfonato potásico de índigo. Algunas sustancias como el peróxido de hidrógeno suelen interferir en esta determinación, sin embargo, se ha comprobado que es únicamente a tiempos prolongados, mayores a 6 horas (Hoigné, 1998).

La expresión matemática empleada para la cuantificación de ozono disuelto es la siguiente:

$$[O_3]_R = \frac{(A_b - A_m)100}{0.42 V_m C} \qquad (1.28)$$

Donde A_b, es el valor de la absorbancia inicial del trisulfonato potásico de índigo, A_m corresponde a la absorbancia de la muestra, ambas determinaciones se realizaron en un espectrofotómetro Perkin Elmer Lambda 25 UV/VIS a λ: 600 nm. Por otra parte, el valor de 0.42, es un factor de sensibilidad para el cambio de absorbancia. Finalmente, V_m es el volumen de la muestra y C la longitud de paso en la celda, en este caso 1 cm.

4.8Mecanismo de degradación del fenol.

En la sección 1.4 se mencionan algunos subproductos de degradación del fenol, los cuales pueden ser identificados por una técnica de cromatografía de líquidos, con ello conocer la ruta que sigue el mecanismo de degradación de la molécula principal. A continuación, se describen brevemente las técnicas cromatográficas para la cuantificación del fenol y sus principales subproductos generados durante el tratamiento electroquímico.

4.8.1Determinación de subproductos aromáticos en la degradación del Fenol, mediante UHPLC.

La cuantificación del Fenol y la determinación de los subproductos aromáticos producidos durante la electro-oxidación del Fenol se llevó a cabo por cromatografía líquida de alta resolución, utilizando un equipo UHPLC Vanquish,Thermo Scientific, el cual está equipado con una bomba cuaternaria, auto muestreador, detectores UV y DAD. El volumen de inyección empleado fue de 5 µL con una tasa de flujo de fase móvil de 1 $mL \cdot min^{-1}$ (metanol-agua 80:20 (v:v)) acidificada con 5 mM de H_2SO_4. La separación de los compuestos se efectuó en una columna Ascentis® Express C-18 (Supelco), longitud de 3 cm, diámetro interno de 4.6 mm y con longitudes de onda de 280, 270 y 246 nm. El software, para el procesamiento e integración de los cromatogramas obtenidos para cada uno de los compuestos separados, se utilizó el software Chromeleon 7.

4.8.2Determinación de subproductos alifáticos en la degradación del Fenol, mediante UHPLC.

Con el empleo del mismo equipo mencionado en la técnica cromatográfica anterior y con diferentes condiciones de separación, se procedió a determinar los subproductos de degradación alifáticos producidos durante la electro-oxidación del fenol. El volumen de inyección empleado fue de 5 µL con una tasa de flujo de fase móvil de 0.5 $mL{\cdot}min^{-1}$. La fase móvil es una solución buffer de agua-metanol en 90:10 (v:v) y 30mM de K_2HPO_4, acidificada con H_3PO_4 a pH 2.5. La separación de los compuestos se efectuó en una columna Eclipse ZORBAX XDB C-18 (Agilent), tamaño de partícula 5 µm, diámetro interno de 4.6 mm y 150 mm de longitud, en esta técnica únicamente se empleó λ 210 nm, en el detector UV.

4.9Estudio hidrodinámico del reactor

Algunos parámetros hidrodinámicos importantes para el buen funcionamiento de una columna de burbujeo son: el diámetro de burbuja y la fracción volumétrica de gas, por lo tanto, son contemplados en el estudio de la hidrodinámica del reactor. El tamaño de las burbujas de gas es de suma importancia, ya que afecta directamente al área de transferencia de masa. En base a los estudios de (Lu *et al*., 1994) y (Prince & Blanch 1990), se determinó el tamaño de burbuja mediante la toma de una fotografía a escala milimétrica, en el lecho empacado de burbujas formadas en el volumen ocupado por los electrodos de DDB. A continuación, se presentan las expresiones matemáticas para la determinación de algunos parámetros hidrodinámicos.

a) Diámetro medio de Sauter

$$\boldsymbol{d_{ms}} = \frac{\sum_{i=1}^{N} \boldsymbol{d_i^3}}{\sum_{i=1}^{N} \boldsymbol{d_i^2}} \qquad (1.29)$$

b) Fracción volumétrica de gas

$$\varepsilon_G = \frac{V_G}{V_{DB}} \qquad (1.30)$$

c) Área interfacial gas-líquido

$$a_b = \frac{6\varepsilon_G}{d_{ms}} \qquad (1.31)$$

A las diferentes densidades de corriente y tasa de recirculación, se estudiaron los parámetros citados en las expresiones matemáticas anteriores, en el sistema bifásico oxígeno-ozono-agua en la concentración de 0.05 M de Na_2SO_4.

Resultados

5.Resultados

5.1Capítulo de libro publicado.

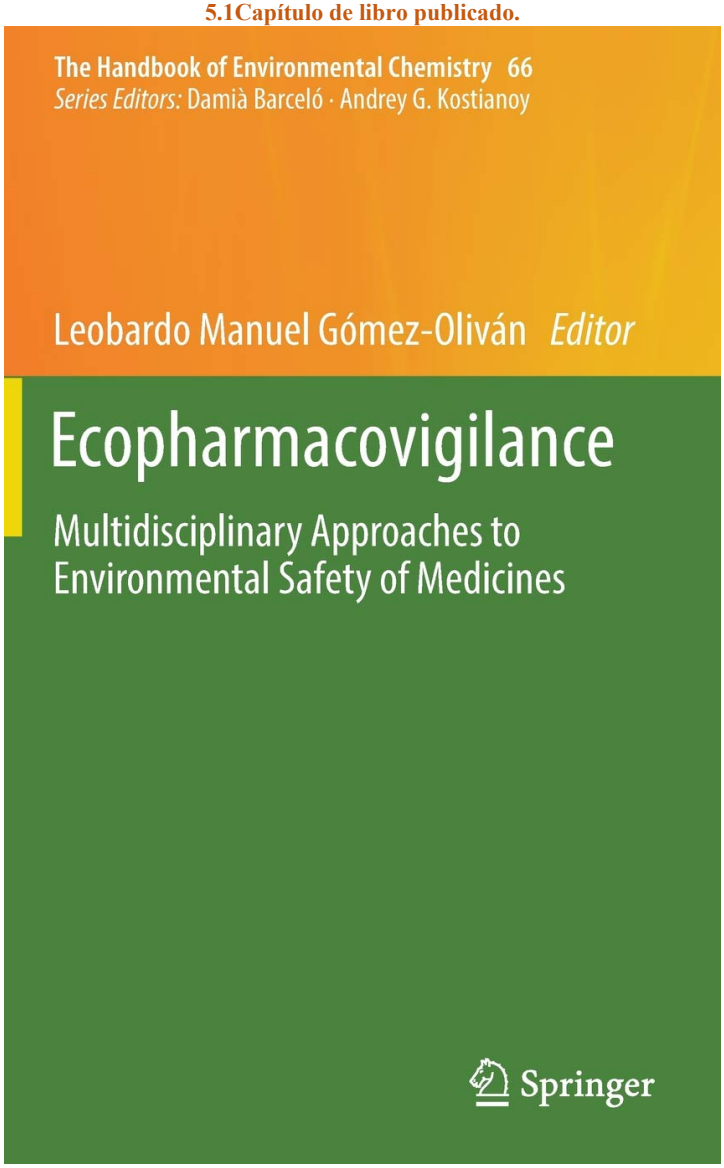

Advanced Oxidation Processes: Ozonation and Fenton Processes Applied to the Removal of Pharmaceuticals

Santana-Martínez Germán, Roa-Morales Gabriela, Solís-Casados Dora, Romero Rubí, and Natividad Reyna

Contents

Abstract This chapter aims to present the fundamentals, important variables, and pharmaceuticals removed by ozonation and Fenton, which are only two of the current existing advanced oxidation processes. Some toxicological information regarding pharmaceuticals oxidized by ozonation is also included. Some strategies to improve such processes, like adding a catalyst, light, or electrical current, are also analyzed. Thus, this chapter intends to present general but fundamental aspects of the aforementioned processes.

S.-M. Germán, R.-M. Gabriela, S.-C. Dora, R. Rubí, and N. Reyna (✉)
Centro Conjunto de Investigación en Química Sustentable UAEM-UNAM, Facultad de Química, Universidad Autónoma del Estado de México, Toluca, Estado de México, Mexico
e-mail: reynanr@gmail.com

L.M. Gómez-Oliván (ed.), *Ecopharmacovigilance: Multidisciplinary Approaches to Environmental Safety of Medicines*, Hdb Env Chem, DOI 10.1007/698_2017_166,

Keywords Hydrogen peroxide, Hydroxyl radicals, Mineralization, Oxidation, Water remediation

1 Introduction

For centuries, the scientific and technological efforts of human being were mainly dedicated to provide comfort and make life "easier." In the last decades, however, it has been demonstrated that such a good intention while benefiting many has also had a detrimental effect on global environment, thus affecting the whole planet. This awareness of unsustainability has urged the development of processes not only for cleaner good production but also to clean the already contaminated industrial effluents and water bodies. In this context, pharmaceutical compounds have been identified as an important group of water pollutants, and therefore their removal by any means is imperative. To achieve so, advanced oxidation processes (AOPs) have emerged as an important alternative to eliminate them. Therefore, herein the fundamentals, advantages, and drawbacks of two important AOPs, ozonation and Fenton, are summarized. General aspects of variants of ozonation, like catalyzed ozonation and peroxonation, are revised too. The results of applying such processes to some pharmaceutical removal can also be found. The included pharmaceuticals were the most referenced ones in the last 5 years.

2 Ozonation

2.1 Fundamentals

The ozone molecule (O_3) possesses a high oxidant power ($E^\circ = 2.07$ V); it is highly reactive and finds a diversity of applications, mainly in the oxidation of organic/inorganic compounds, disinfection, wastewater, and potable water treatment. Due to its reactivity, ozone tends to form oxygen. However, at some atmospheric conditions (like pressure, temperature, humidity, velocity) and pH, the ozone half-life can be increased from seconds until days.

A limitation of ozonation is its inherent high cost to produce ozone at the point of use. Ozone production is mainly conducted by electrical discharge or electrolysis at industrial or laboratory scale [1].

Compound oxidation by ozone can be either through direct or indirect mechanisms. Although in practice both ways may take place simultaneously, it is necessary to specify the difference between the two routes as follows.

2.1.1 Indirect Reaction

In this mechanism ozone is not the oxidant specie but helps to the generation of species that have an unpaired electron. This is possible under alkaline conditions, and under this condition is when ozonation can be considered an advanced oxidation process since it is based on the production of hydroxyl radicals. For a better explanation of this reaction path, it is necessary to consider three steps: initiation, chain propagation, and termination. The main reactions involved in these steps are summarized in Table 1. In summary, the main oxidant specie is the hydroxyl radical and not the ozone molecule.

In the first step, ozone reacts with hydroxide ions to generate superoxide anion ($O_2^{\bullet -}$) and hydroperoxyl radical ($HO_2^{\bullet}$). Some species from the first stage react once more with ozone to obtain new anions and radicals like the following: ozonide anion ($O_3^{\bullet -}$), hydrogen trioxide ($HO_3^{\bullet}$), and hydroxyl radical ($OH^{\bullet}$) which is the most powerful oxidant. The second stage is denominated chain reaction because of the regeneration of hydroperoxyl radicals on reaction (7), which also participates in reaction (2), so this promotes the chain reaction.

Moreover, hydroxyl radical can also react with some organic molecules (R), and this is exemplified in reactions (8)–(11). In this route new species are formed like organic radicals ($R^{\bullet}$), and when there is the presence of oxygen, peroxy radicals $ROO^{\bullet}$ can also be formed.

Unfortunately not all reactions allow to increase the amount of strong oxidants like in the stage of chain reaction. As a consequence of the reactivity of hydroxyl radicals with some organic/inorganic compounds, other anions that act as scavengers are generated. In this case, in reactions (12) and (13), carbonate/bicarbonate

Table 1 Ozone decomposition reactions [2]

Step	Reaction	
Initiation	$O_3 + OH^- \rightarrow O_2^{\bullet -} + HO_2^{\bullet}$	(1)
	$HO_2^{\bullet} \leftrightarrow O_2^{\bullet -} + H^+$	(2)
Chain propagation	$O_3 + O_2^{\bullet -} \rightarrow O_3^{\bullet -} + O_2$	(3)
	$HO_3^{\bullet} \leftrightarrow O_3^{\bullet -} + H^+$	(4)
	$HO_3^{\bullet} \rightarrow OH^{\bullet} + O_2$	(5)
	$OH^{\bullet} + O_3 \rightarrow HO_4^{\bullet}$	(6)
	$HO_4^{\bullet} \rightarrow O_2 + HO_2^{\bullet}$	(7)
	In presence of organic molecules (R):	
	$H_2R + OH^{\bullet} \rightarrow HR^{\bullet} + H_2O$	(8)
	$HR^{\bullet} + O_2 \rightarrow HRO_2^{\bullet}$	(9)
	$HRO_2^{\bullet} \rightarrow R + HO_2^{\bullet}$	(10)
	$HRO_2^{\bullet} \rightarrow RO + OH^{\bullet}$	(11)
Termination	$OH^{\bullet} + CO_3^{2-} \rightarrow OH^- + CO_3^{\bullet -}$	(12)
	$OH^{\bullet} + HCO_3^- \rightarrow OH^- + HCO_3^{\bullet}$	(13)
	$OH^{\bullet} + HO_2^{\bullet} \rightarrow O_2 + H_2O$	(14)
Overall reaction	$3O_3 + OH^- + H^+ \rightarrow 2OH^{\bullet} + 4O_2$	(15)

appears to quench the chain reaction; these ions are produced initially from CO_2 dissolved into the water, which tends to form carbonic acid; as a consequence this acid is partially dissociated to carbonate, and a second dissociation forms ion bicarbonate. Reaction (15) is the result of combining the first reactions (1)–(7).

2.1.2 Direct Oxidation Reaction

Another path for the ozone decomposition is the direct reaction or also so-called Criegee mechanism, which consists of selective reactions between the ozone molecules with an unsaturated bond. In this mechanism the degree of nucleophilicity is determinant; for that reason, the reactivity of ozone molecule increases when there is the presence of saturate aliphatic or aromatic compounds. The oxidation is slower in the presence of unsaturated aliphatic, non-dissociated, and dissociated organic compounds.

On the other hand, with respect to the inorganic compounds, sometimes these can react much faster than organic compounds. More or less in the same way this happens with its degree of nucleophilicity. On the contrary, ionized or dissociated inorganic compounds can react faster with ozone [2]. This type of oxidation is favored under acidic reaction conditions.

2.2 Technologies for Ozonation Applied to the Removal of Pharmaceutical Compounds and Other Organic Molecules

The removal of pollutants in solution by ozonation implies the use of multiphase reactors in order to efficiently contact gas and liquid and even solid if the use of a heterogeneous catalyst is on demand. Thus, at this point, it is worth highlighting the importance of the reactors in ozonation process and also pointing out the most significant factors to be taken into account in their operation and design.

According to existing literature [3–5], semi-batch upflow bubble column is the preferred reactor to carry out the ozonation of pharmaceutical compounds. This reactor mainly consists of a cylindrical bubble column with a gas diffusor at the bottom where the ozone stream is fed. Ozone is produced from the decomposition of oxygen or air by an ozone generator; thus, the reactor feed stream is usually a mixture of ozone and air or oxygen since the effectiveness of ozone generation is not 100%. This reactor is batch regarding the liquid phase and semi-batch regarding the gas phase, and this is to be considered in the transport balances used for design. Since O_3 can be highly toxic, a common characteristic among ozonation reactors is that the outlet gas line of the reactor is connected to a trap with KI solution, in order to destroy the unconsumed ozone. To enhance the gas-liquid mass transfer, the

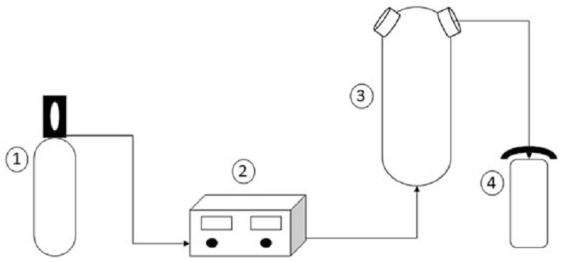

Fig. 1 Semi-batch ozonation system. Description: (1) oxygen, (2) ozonator, (3) upflow bubble column reactor, (4) KI trap

reactor is coupled to a magnetic stirring apparatus [6]. Figure 1 depicts a typical setup of an upflow bubble column reactor [7].

A variant of the reactor depicted in Fig. 1 is the semicontinuous reactor that has also been utilized to conduct the catalyzed ozonation of industrial effluents [8–10]. The main difference with a typical semi-batch reactor is the recirculation of liquid phase by a pump; the other elements are basically the same. An advantage of this kind of systems is the increase of volume, which allows working at pilot scale. In this context, a rather novel proposal was made by Crousier et al., who tested the TOCCATA® catalyst in the treatment on urban wastewater [9]. In this work the reactor consisted of two bubble columns, one column was packed with the catalyst (TOCCATA®) and the other remained empty. This arrangement allowed the wastewater to be treated in both columns.

In any type of upflow bubble columns, special care should be taken with the particle size and density of the catalyst and gas flow rate. If the adequate values of these variables are not used, the catalyst will not be properly fluidized, and thus mass transfer would be the limiting step, and catalyst would be subdued.

Although the destruction of ozone is carried out in the trap of KI of the semi-batch and semicontinuous reactors, it still has the disadvantage of wasting ozone, because this gas is continuously supplied to the reactor and its generation can be costly. Furthermore, in the aforementioned systems, the ozone destruction is not complete, and this is another disadvantage because of ozone undesirable effects [11]. This has motivated the design of new ozonation reactors like the one proposed by Lucas et al. [12]. Such a reaction system was called multi-orifice oscillatory baffled column (MOBC). Its design of several orifices in each baffle allows a reduction in the volume reactor and intensifies the ozonation process. To test the efficiency of this reactor, the degradation of p-hydroxybenzoic (p-HBA) acid was carried out [12] and was also benchmarked against a conventional bubble column. The reaction conditions were a total volume reaction of 9.6 L, liquid flow rate of 4 L/min, pH 10 $\pm$ 0.1, gas flow rate of 2.1–4.7 L/min with ozone concentration of 23 gO_3/m^3, and 50 mg/L of p-HBA. Main results reported of this investigation were an increase of 20% of p-HBA degradation, 75% in the rate of mineralization per

mole of ozone consumed, and the increase from 4.5 to 5 times of rate of mineralization per mole of ozone supplied. All these results are compared with those obtained in a conventional bubble column. It is well known that one baffle may increase dissolved oxygen concentration in water up to six times [13]. Additionally, the use of several baffles along the column allows a better distribution of the bubbles and the complete ozone consumption.

In this sense, another promising technology is the cocurrent downflow bubble column (CDBC) that has been successfully applied to conduct heterogeneous catalyzed hydrogenation and UV photo-catalyzed processes [14–16]. The main difference with the aforementioned reactors is that both phases, gas and liquid, are fed at the column top.

2.3 *Pharmaceutical Compound Removal by Ozonation*

O_3 molecule high oxidant power and also the oxidant radicals produced during its decomposition have been applied for the removal of several compounds. Although there are many other pharmaceutical compounds that have been attempted to be degraded by ozone, Table 2 summarizes the ones that have been mostly reported.

It is worth noticing that the initial concentrations of the pharmaceutical compounds are rather low and this is because many of them have been shown [18, 20–25] to represent a biological hazard even at very low concentrations. It can also be observed that a complete mineralization is not reached in some cases. This may be due to the low ozone dosage, but also one should not forget the effect of the alkalinity produced by carbonated and bicarbonates, which tend to be scavengers of the hydroxyl radical. On the other hand, despite that mineralization is not

Table 2 Ozonation applied to removal of pharmaceutical compound

Pharmaceutical	Reaction conditions	Removal (%)	References
Carbamazepine (CBZ) Diclofenac (DCF) Sulfamethoxazole (SMX) Trimethoprim (TMP)	Ozone dosage: 1.6 mg/L 2.3 mg/L 2.8 mg/L 4.5 mg/L $C_0 = 5$ mg/L, for each compound	LC-MS: 100 LC-MS: 100 LC-MS: 100 LC-MS: 100	[17]
Indomethacin (IM)	[O_3]: 35 mg/L Flow rate: 250 mL/min pH: 7 C_0: 25 μM Time: 30 min	TOC ~50	[18]
Mixture: Atenolol (ATL) Hydrochlorothiazide (HCT) Ofloxacin (OFX) Trimethoprim (TMP)	[O_3]: 2.5 mg/L Flow rate: 36 L/h pH: 7 C_0: 2.5 mg/L Time: 120 min	TOC ~35	[19]

complete, in several cases like mentioned earlier, by-products are less harmful, with respect to parent compounds. Thus, in those cases where mineralization is not complete, it is desirable to establish the toxicology of the treated solution in order to elucidate weather or not the ozone treatment is effective in oxidizing the organic compounds into less toxic ones. Ozone concentration can be low either because of inherent limitations of the system or mainly because ozonation may become rather expensive due to the high consumption of energy and type of technology to generate it. Thus, to reduce the cost of treatment, the most of ozone applications tend to employ low concentrations of this oxidant.

Regarding pH, during ozonation this parameter is usually adjusted to a neutral value in order to promote the two mechanisms of ozone attack.

In order to increase removal efficiency and reduce the amount of ozone usage, there are reported some successfully assessed approaches. One is the addition of catalysts and the other one is the addition of hydrogen peroxide (peroxonation). The following two sections deal with such processes.

2.4 Pharmaceutical Compound Removal by Catalyzed Ozonation

The ozonation process can be enhanced by the addition of a catalyst, which can be homogeneous or heterogeneous. In the former case, this material must be a transition metal that can be oxidized and reduced back to initial state, but this kind of catalyst is not used in several applications because its recovery is rather difficult. For that reason, the most employed catalyst is the heterogeneous [26, 27]. Considering this, it is easy to identify when the ozonation is heterogeneously catalyzed, because chemisorption reactions between ozone – catalytic surface – organic molecule occur simultaneously [28].

In this process, there are several variables that affect the efficiency of the process. These are pH, ozone dosage, stirring, temperature, type, concentration, and size of the catalyst. Stirring and particle size are particularly important when the efficiency of two catalysts are to be compared since in order to have a reflection of the catalytic surface, the whole process should be free of transport phenomena resistances. These variables are also important in order to avoid catalyst subutilization. Stirring is the first variable to be assessed since will not affect only the mass transfer from the solution to the catalyst but also from the ozone to the bulk solution and therefore to the catalyst. Particle size effect should also be discriminated since the very beginning. A particle size lower than 60 μm usually guarantees the elimination of intra-particle transport resistances. Regarding pH, when its value increases, the ozone is decomposed into hydroxyl radicals which are more reactive than ozone and less selective [7]; it also affects the surface of catalyst and the dissociation of organic pollutants in water [29]. If the pH value is low, ozone exists in water in a molecular state [30]. In acid medium, the oxidation of

contaminants is by molecular ozone oxidation and not by hydroxyl radicals. Optimal values of pH have been obtained in neutral or alkaline medium [27, 31]. Based on reactions (12) and (13), it is clear that carbonate ions are scavengers much stronger than bicarbonate ions. The increase of these ions is by addition of Na_2CO_3; this is common in dyes containing effluents [32]. If the $HO^{\bullet}$ scavengers are present in the process, the molecular ozonation might prevail. Other $HO^{\bullet}$ scavengers are phosphate and tert-butanol, the former blocks the Lewis site of catalyst [27], the latter reacts in bulk solution with $HO^{\bullet}$ [33]. The presence of tert-butanol reduces the percentage of mineralization even more than 20%.

The addition of catalyst increases the number of active sites, but not always higher dosages of catalysts increase the removal of pollutant. This is why this process is not always an alternative to not catalyzed ozonation, despite reducing ozone flow rate and its concentration.

Table 3 shows typical assessed variables and their values applied to the pharmaceutical removal by catalyzed ozonation. The shown pharmaceuticals were selected because they represent an important portion of the existing literature.

Table 3 Catalyzed ozonation applied to the removal of pharmaceutical compounds

Pharmaceutical	Reaction conditions	Removal (%)	References
Sulfamethoxazole (SMX)	Catalyst: Fe_3O_4 Catalyst dosage: 0.3 g/L [O_3]: 2 g/h pH: 7 C_0: 50 mg/L Time: 5 min	100	[34]
Phenacetin (PNT)	Catalyst: $CuFe_2O_4$ Catalyst dosage: 2.0 g/L [O_3]: 0.36 mg/min pH: 7.72 C_0: 0.2 mM Time: 5 min Time: 3 h (mineralization)	100 TOC: 90	[35]
Sulfamethazine	Catalyst: $Cu_{0.1}Fe_{0.9}OOH$ Catalyst dosage: 0.2 g/L [O_3]: 15 mg/min pH: 7 C_0: 20 mg/L Time: 10 min Time: 120 min (mineralization)	100 TOC: 44	[36]
Ibuprofen	Catalyst: Fe_2O_3/Al_2O_3@SBA-15 Catalyst dosage: 1.5 g/L [O_3]: 30 mg/L Flow rate: 0.2 L/min pH: 7 C_0: 10 mg/L Time: 60 min	90 TOC: 26	[37]

2.5 Pharmaceutical Compound Removal by Peroxonation

In order to enhance ozonation action, H_2O_2 instead of a catalyst can be added to the reacting system, and this process is known as peroxonation. The added reactions of this process are presented below. In summary, these reactions imply that the interaction H_2O_2/O_3 can be affected by other species like water, as can be seen in reaction (16) where water is partially dissociated into hydroxide anions. This ion can also react with ozone (reaction 18), obtaining a hydroxyl radical, which is also produced by reaction (17).

$$H_2O_2 + H_2O \rightarrow HO_2^- + H_3O^+ \quad (16)$$
$$H_2O_2 + 2O_3 \rightarrow 2OH^\bullet + 3O_2 \quad (17)$$
$$O_3 + HO_2^- \rightarrow OH^\bullet + 2O_2 \quad (18)$$

Some pharmaceutical compounds that have been removed by peroxonation are in Table 4. Reaction conditions and removal efficiency are also included.

Gomes and collaborators [18, 21, 39] have reported that when more than 10 mM of hydrogen peroxide is used, this reagent and ozone can act as radical scavengers, and their addition may be detrimental rather than helpful. This phenomenon occurs by the following reactions (19) and (20):

$$OH^\bullet + H_2O_2 \rightarrow HO_2^\bullet + H_2O \quad (19)$$
$$OH^\bullet + O_3 \rightarrow HO_2^\bullet + O_2 \quad (20)$$

The products of these reactions are radicals with lower oxidant power than hydroxyl radicals. Thus H_2O_2 concentration must be kept at low values to prevent its action as scavenger. Regarding pH values, these are preferred neutral.

Table 4 Peroxonation applied to removal of pharmaceutical compounds

Pharmaceutical	Reaction conditions	Removal (%)	References
Fluoxetine	[O_3]: 30 mg/L [H_2O_2]: 0.02 mM C_0: 50 mg/L Time: 20 min	86.14	[38]
Sulfamethoxazole (SMX) and Diclofenac (DCF)	[O_3]: 20 mg/L [H_2O_2]: 5 mM pH: 7 C_0: 88.5 mg/L Time: 120 min	100 COD: 91	[21]

2.6 Kinetics of Pharmaceuticals Removed by Ozonation

Based on bench-scale studies, in general it is necessary to consider the kinetic study with the purpose of understanding the behavior of reactors at full scale [40]. All cases presented in this chapter used the following method to establish the reaction rate and kinetic constant, considering the data obtained from the profile degradation of the main pollutant and is known as integral method. The following equation can be integrated, assuming an *n*th pseudo-order reaction,

$$r_1 = -\frac{dC}{dt} = k_{\text{obs}} C^n \tag{21}$$

In most of the cases, this order has been found to be 1 or 2 for most of pharmaceuticals [21, 41]. When Eq. (21) is integrated assuming either order 1 or order 2, the resulting equations are (22) and (23), respectively.

$$\frac{\ln C_0}{\ln C_t} = k_{\text{obs}} t \tag{22}$$

$$\frac{1}{C_t} - \frac{1}{C_0} = k_{\text{obs}} t \tag{23}$$

Sometimes in the aforementioned equations, mineralization data from analysis of COD or TOC can also be employed. In the ozonation process, the kinetic study is focused on the determination of reactivity of ozone in direct and indirect form. To achieve so, the kinetic constants respect to ozone (k_{O3}) and hydroxyl radical ($k_{HO\bullet}$) are calculated. Generally speaking, in the degradation of pharmaceuticals like trimethoprim, valsartan, furosemide, lidocaine, tramadol, and fluconazole between others, the reported kinetic constants are in the order of 1–10^7 M^{-1} s^{-1} with respect to the ozone and for hydroxyl radical in the order of 1×10^8–10^{10} M^{-1} s^{-1} [18, 21, 31]. Despite several studies employing distillated water, this behavior can be extrapolated to other water matrix. The nature of nonselective oxidant of hydroxyl radical allows that their kinetic constants are higher than ozone. The study of [42] determined that pharmaceutical compounds with aromatic ring show high reactivity (~10^4–10^7 M^{-1} s^{-1}), while saturated aliphatic compounds present a very low reactivity (<5 M^{-1} s^{-1}).

2.7 Toxicity of Effluents Treated by Ozonation

In all water treatments, the aim is to remove contaminants either by chemical reduction or oxidation. In the latter, near complete mineralization is usually taken as an indicative of the treated effluent that can be safely discharged. This, however, is not always a guarantee [43]. This is due to the generation of species more harmful than the parent compound and to the addition of chemicals for changing pH, for example. In this section a variety of tests that have been applied to the effluents treated by ozonation is presented.

Within literature, it can be observed that toxicity removal directly depends on ozone dosage. For instance, working at high ozone dosages, toxicity can be eliminated at 100%, this was demonstrated with the indomethacin ozonation where several ozone concentrations were assessed and toxicity was estimated by means of essays with a luminescent bacterium called *Photobacterium phosphoreum*. Authors report that 35 mg/L of ozone concentration is enough to eliminate the toxicity after 60 min [18]. According to this investigation, it is not necessary to mineralize all organic matter; in fact the TOC removal is almost 50%. Some by-products that remain are essentially chloride and organic acids (acetic, formic, and oxalic). Oxalic acid, however, has been demonstrated to be highly toxic when biological hazard is established by means of other essays, with *Lactuca sativa*, for example.

Ecotoxicity tests can also be simultaneously conducted by some microbiological tests and can be corroborated with a software. In fact ECOSAR program (version 1.11), developed by USEPA, has been applied in the study of ofloxacin (OFX) ozonation, specifically on the determination of its hazard indices on *green algae*, *daphnia*, and fish [5]. Based on the proposed mechanism for the OFX degradation, 14 by-products were identified, which most of them after the treatment are not harmful, but when is exposed until 96 h, some by-products like OFX 336A and OFX 364 present a high chronic toxicity. In such study, ozone concentration was 15 mg/L in the flow rate.

As can be seen from the results presented above, the increase of ozone concentration increases the efficiency of toxicity removal. Such concentration, however, may be so high than the process cost that significantly increases too. In this case, adding a catalyst might be practical. Specifically, the group of Fei Qi and Zhonglin Chen, has tested the molecule of bezafibrate (BZF) with two different catalysts [39, 44]. In one study, these investigators employed 50 mg/L of a catalyst-denominated cobalt-doped red mud (Co/RM), with 0.5 mg/L of ozone concentration to remove 2.76 μM of BZF. Toxicity assessment was evaluated by *Chlorella vulgaris*, which presented a 96h-EC_{50} of 63%. In a second study, the reaction conditions, toxicity tests, and pollutant of the first study were kept constant; the only difference was the catalyst, where instead of cobalt cerium (IV), (Ce (IV)/RM-p) was employed and more than 50% of detoxification in 96h-EC_{50} test was attained. Still, toxicity was not fully eliminated when using the catalyst. A similar problem is observed during the peroxonation process. This can be ascribed to the addition of hydrogen peroxide whose excess must be quenched with catalase solution.

Sulfamethoxazole and diclofenac were studied by Rui Martins' group [21]; from this investigation, they assessed the removal of both pollutants in a synthetic solution and also from a secondary effluent by peroxonation. The toxicity was evaluated by a procedure described in ISO/DIS11348/3, which employs marine bacteria called *Vibrio fischeri* and measures the percentage on inhibition of light emission. Using this method, the samples of these water matrices (synthetic and secondary effluent) were analyzed; after 2 h of peroxonation, results are the following: the inhibition was 29% and 38%, for secondary effluent and synthetic solution, respectively.

3 Fenton Process Applied to the Removal of Pharmaceutical Compounds

3.1 Fenton Process Fundamentals

Fenton reaction (24) is named after H.J.H. Fenton who added Fe^{2+} ions to catalyze the decomposition of H_2O_2 into hydroxyl radicals, hydroxyl ions, and Fe^{3+} ions and to intensify, in this way, tartaric acid oxidation.

$$Fe^{2+} + H_2O_2 \rightarrow Fe^{3+} + OH^{\bullet} + OH^{-} \quad (24)$$

This reaction depends strongly on pH values, specifically on the ratio Fe^{2+}/Fe^{3+} ($E^{\circ} = 0.77$ V/SHE). The best results to dissociate hydrogen peroxide toward hydroxyl radicals have been reported in the range of 2.8–3 of pH [45, 46]. Taking into account that in acidic media Fenton's reaction presents better results, similar reactions occur simultaneously (25). When Fe^{3+}, decompose hydrogen peroxide is so-called Fenton reaction (26) and tends to form hydroperoxyl radicals, and by means of this reaction, the catalytic ion Fe^{2+} (27) is regenerated.

$$Fe^{2+} + H_2O_2 + H^{+} \rightarrow Fe^{3+} + OH^{\bullet} + H_2O \quad (25)$$
$$Fe^{3+} + H_2O_2 \rightarrow Fe^{2+} + HO_2^{\bullet} + H^{+} \quad (26)$$
$$Fe^{3+} + HO_2^{\bullet} \rightarrow Fe^{2+} + O_2 + H^{+} \quad (27)$$

The excess of Fenton's reagent (Fe^{2+}/H_2O_2) has been reported to inhibit the oxidant power of hydroxyl radical generating undesirable reactions (28)–(31) [47], through which scavenging species or oxidants with lower oxidant power are obtained. Additionally, working under neutral media, the reaction (30) takes place at this condition, and selective oxidants like high-valent ferryl-oxo species $Fe^{(IV)}$ might be produced [48].

$$Fe^{2+} + OH^{\bullet} \rightarrow Fe^{3+} + OH^{-} \quad (28)$$
$$H_2O_2 + OH^{\bullet} \rightarrow HO_2^{\bullet} + H_2O \quad (29)$$
$$OH^{\bullet} + OH^{\bullet} \rightarrow H_2O_2 \quad (30)$$
$$Fe^{2+} + H_2O_2 \rightarrow Fe^{(IV)}O^{2+} + H_2O \quad (31)$$

The main disadvantages of Fenton reaction are the storage and the risks of hydrogen peroxide; also the catalytic ion Fe^{2+} tends to oxidize toward Fe^{3+}, which forms sludge or metal hydroxides (reactions 32 and 33) and Fe(III) carboxylic acids complexes [46, 49] and the acid pH [50]. Nevertheless, some variants of this process are focused on generating hydrogen peroxide in situ, to minimize the process costs, disadvantages, and undesirable reactions abovementioned. Also, other than Fe salts have been used as source of catalyst. In this sense, iron-pillared clays have been successfully used and have considerably reduced the difficulty of recovering the catalyst [51]. Also, other metals, like cupper, have been successfully

applied as catalysts of H_2O_2 dissociation [52]. In such a case, the process is called Fenton-like.

$$Fe^{3+} + H_2O_2 \leftrightarrow Fe^{III}(HO_2)^{2+} + H^+ \quad (32)$$

$$FeOH^{2-} + H_2O_2 \leftrightarrow Fe^{III}(OH)(HO_2)^- + H^- \quad (33)$$

3.2 *Hydrogen Peroxide In Situ Production (Electrochemical and Photochemical Methods)*

The oxidant power of hydrogen peroxide not only finds application in wastewater treatment; it can also be applied to organic synthesis and paper industry, like disinfectant [53]; in addition it is used as rocket fuel [54]. One of the main advantages that make of H_2O_2 an environmentally safe oxidant is the by-products (oxygen and water). To diminish the risk in the handling of this oxidant, some methods, like anthraquinone process [53], electrochemical process [55], and photocatalytic process [56], have been developed in the generation of hydrogen peroxide. Specifically the last two mentioned processes are preferred because of the low energetic costs and because it allows the H_2O_2 production at mild conditions and most of them are green technologies.

According to the electrochemical process, the hydrogen peroxide is produced mainly by oxygen reduction at the cathode in acidic/neutral media by the following reaction [55]:

$$O_{2(g)} + 2H^+ + 2e^- \rightarrow H_2O_2 \quad (34)$$

Table 5 summarizes the results of some investigations about this topic in which it can be observed that the carbonaceous materials are the most studied ones with respect to this process by the low cost and high concentrations electro-generated in electrochemical cells; it also requires an acidic media (pH 2–4) and an electrolyte-like sodium sulfate. On the other hand, in this kind of carbonaceous materials is not possible to employ high current intensities ($i > 300$ mA), due to the material structure. However a variant of carbonaceous materials called gas diffusion [63] electrode (GDE) is also applied with success at undivided cells, even at pilot-scale (reactors type filter press) applications [64, 65] in the pharmaceutical removal (ranitidine and metronidazole). In such investigations the amount of H_2O_2 is not reported, but the mineralization is almost complete in volumes of 2.5 L and 10 L, respectively. The main advantage of GDE is that it can simultaneously be applied to current intensity and flow rate of air/oxygen. GDE also is doped with other materials like CeO_2 with the purpose of increasing the production of H_2O_2 [61]. Another material reported with a high concentration of hydrogen peroxide is the boron-doped diamond [57, 63], which has the advantage of support high current densities and overpotential oxygen.

Table 5 H_2O_2 generated by electrolysis

Electro-generated H_2O_2 (mg/L)	Reaction conditions	Observations	References
82	Anode: boron-doped diamond Cathode: boron-doped diamond *j*: 31 mA/cm^2 *V* = 3 L Recirculation: 12 L/min Electrolyte: 0.05 M Na_2SO_4 pH 3 Time: 180 min	Reactor type filter press	[57]
116	Cathode: graphite felt Anode: Pt Rotating speed: 10 rpm *j*: 50 mA/cm^2 *V* = 0.1 L Electrolyte: 0.05 M Na_2SO_4 pH 3 Time: 60 min	Rotating reactor with rotating disk anodes Without oxygen aeration	[58]
472.9	Cathode: carbon black/PTFE Anode: Pt *j*: 5 mA/cm^2 *V* = 0.1 L Electrolyte: 0.05 M Na_2SO_4 pH 3 Time: 60 min	Without oxygen aeration	[59]
960	Cathode: modified carbon felt *j*: 50 mA/cm^3 *V* = 1 L Electrolyte: 0.05 M Na_2SO_4 Time: 180 min	Jet aerator Does not require oxygen supply	[60]
871	Working electrode: gas diffusion electrode (GDE) with 4% of CeO_2/C Counter electrode: Pt Reference electrode: Ag/AgCl (KCl sat) *E*: −2.3 V *V* = 250 mL Electrolyte: NaOH 1M Time: 120 min	Divided cell	[61]
240	Working electrode: modified (with iron (II) phthalocyanine) GDE (gas diffusion electrode) Counter electrode: Pt Reference electrode: Ag/AgCl *E*: −1.0 (vs Ag/AgCl *V* = 400 mL Electrolyte: 0.1 M H_2SO_4 and 0.1 M K_2SO_4 Time: 90 min	Divided cell The presence of a modifier induces an increase in ring current	[62]

(continued)

Table 5 (continued)

Electro-generated H_2O_2 (mg/L)	Reaction conditions	Observations	References
9,371	Cathode: carbon black/PTFE *j*: 60 mA/cm^2 $V = 20$ mL (cathodic cell) and 40 mL (anodic cell) Flow rate (air): 40 mL/min Electrolyte: 0.2 M Na_2SO_4 pH 4 Time: 120 min	Divided cell (nafion 117) Phenol (C_0: 100 mg/L), remotion 100% (40 min) TOC removal 85% (120 min)	[20]
180.27	Anode: stainless steel Cathode: reticulated vitreous carbon (RVC) *i*: 170 mA $V = 1$ L each compartment Catholyte: 0.05 M Na_2SO_4, 0.01 M H_2SO_4 Anolyte: 0.8 M H_2SO_4 $\Delta E_{Cell:}$ 2–3 V pH ~2 Time: 180 min	Divided cell 0.001 M $FeSO_4{\cdot}7H_2O$ in the catholyte, for electro-Fenton process 90% of discoloration for blue basic 9 (C_0: 0.08 mM) at 14 min Reactive black 5 (C_0: 0.063 mM) at 90 min Acid orange 7 (C_0: 0.14 mM) at 70 min	[21]

More recently the investigation of undivided cells has focused on not feeding oxygen to the cell. This can be functional by the modification of the reaction system, at this respect a reactor with rotating disk anodes [58] and other possibility is with a jet aerator system [60] which can be produced until 960 mg/L.

In order to increase by ten times the concentration of hydrogen peroxide by an electrochemical method, the cell can be improved coupling three electrodes separated by a membrane [66, 67], each compartment is called catholyte (or cathodic cell) and anolyte (or anodic cell). It is noted that in this variant, the hydrogen peroxide concentration is almost 10,000 mg/L (see Table 5).

H_2O_2 can also be produced in situ by photocatalysis. Considering this, essentially there are two ways to generate hydrogen peroxide by photocatalysis. Both are based on the use of a semiconductor photocatalyst to generate hydrogen peroxide by two-electron reduction of O_2 [68]. The most employed method is using an organic reducer like ethanol, methanol, oxalate, or other similar organic compounds, which is required as a sacrificial electron source; in contrast there are undesirable reactions [68–70]. In this case, alcohols are employed to reduce the probability of electron-hole recombination [71]. In order to decrease the concentration of by-products and eliminate the use of organic reducers, recently some studies report the use of catalysts that can produce hydrogen peroxide only by water oxidation [56, 71]. Table 6 shows the concentrations obtained by several catalysts, taking into account the two methods mentioned above. It can be observed that the employed volume is rather low when comparing with the electrochemical method.

Table 6 H_2O_2 generated by photochemical methods

H_2O_2 photo-catalyzed (mg/L)	Reaction conditions	Observations	References
115.64	Photoirradation: $\lambda > 280$ nm Catalyst: $Au_{0.1}Ag_{0.4}/TiO_2$ Catalyst dosage: 5 mg System: ethanol/water [4/96] v/v $V = 5$ mL Time: 12 h	266 µmol of CH_3CHO 13.8 nm, metal particle size	[22]
2.14	Photoirradation: 100 mW/cm^2 Catalyst: composite MMO@C_3N_4 Catalyst dosage: 1 g/L pH 3 Time: 90 min	Production only from water and oxygen	[71]
3,741	Photoirradation: $\lambda < 420$ nm, Xe lamp 300 W Catalyst: $Cd_3(C_3N_3S_3)_2$ Catalyst dosage: 80 mg/L $V = 20$ mL System: methanol/water [1/19] v/v pH 2.8 Time: 4 h	Visible light illumination	[70]
204	Photoirradiation: $\lambda > 420$ nm Xe lamp 2 kW Catalyst: graphite carbon nitride g-C_3N_4 Catalyst dosage: 20 mg $V = 5$ mL System: methanol/water [9/1] v/v Time: 12 h	The catalyst can also be activated by sunlight. Inexpensive metal-free photocatalyst	[72]
54.42	Photoirradation: 0.56 W/cm^2 λ: 420 nm Xe lamp 300 W Catalyst: graphite carbon nitride g-C_3N_4 Catalyst dosage: 50 mg $V = 50$ mL Time: 120 min	Production only from water and oxygen	[56]

Moreover, the catalyst dosage is too high, so in most of the cases, the catalyst can be activated by sunlight. In fact, working volumes at pilot scale are not reported, and this suggests this method requires further improvement in order to be applied at larger scale.

3.3 Pharmaceuticals Removed by Fenton

Despite the drawbacks implicit in this process, this has been successfully applied to the removal of pharmaceutical compounds. Table 7 summarizes some applications in real and synthetic effluents. In this process the catalyst can be homogeneous or heterogeneous. In the former case, the typical source of Fe^{2+} is the commercial salt $FeSO_4$ or $FeSO_4 \cdot 7H_2O$ [73–76]. One of the major problems related to homogeneous Fenton is the high concentrations of Fe^{n+} ions (in order of 20–80 mg/L) that need the process for an efficient removal of pollutant. The acceptable discharge to the environment is only of 2 mg/L [81]. In homogeneous systems, the separation of the catalyst is rather difficult. Nevertheless, $FeSO_4$ has also been applied at industrial scale (250 L) in the removal of berberine employing real wastewater, obtaining good results and mineralization almost complete at low concentrations and only partial for a high pollutant load [75]. Considering this and meanly the recovery of catalyst, a significant amount of research has focused on the use of heterogeneous catalysts like iron oxides, iron doped with other metals, supported iron, and other approaches. The aim of this method is to facilitate the separation of iron ions after the treatment [82]. In both catalytic systems, the key parameter is the molar ratio H_2O_2/Fe^{2+}. When this ratio is higher than 10, the removal efficiency decays by the scavenging effect of hydroxyl radical [83]. Some catalysts, like nanostructured, provide more surface area and active sites which decompose hydrogen peroxide [84]. Other important parameter in heterogeneous catalysis is the decrease of the catalyst activity after a long time of use. This loss of activity can be mainly due to the catalyst leaching. This, however, promotes homogeneous fenton. Nevertheless, heterogenous fenton allows the re-use of the catalyst. Moreover, unlike homogeneous Fenton, the heterogeneous one can be conducted under near neutral pH [78]. The main limitation for heterogeneous Fenton is the catalyst synthesis, since in the most cases this is only a few grams. In the investigations shown in Table 7, there is only one investigation at pilot scale employing a catalyst-denominated modified polyacrylonitrile obtaining a poor removal of initial concentration.

As can be observed in most of the cases, the pollutant mineralization is only partial, and the treatment time sometimes is rather large. This has motivated the combination of this process with others like photochemical and electrochemical. These so modified processes are called photo-Fenton and electro-Fenton [46].

Table 7 Examples of pharmaceutical compounds removed by Fenton

Pharmaceutical compound	Reaction conditions	Removal (%)	Observations	References
Acetaminophen, atenolol, atrazine, carbamazepine, metoprolol, Dilantin, DEE, diclofenac, pentoxifylline, oxybenzone, caffeine, fluoxetine, gemfibrozil, ibuprofen, iopromide, naproxen, propranolol, sulfamethoxazole, and trimethoprim	Catalyst: Fe^{2+} Catalyst dosage: 20 mg/L $[H_2O_2/Fe^{2+}]$: 2.5 M ratio pH: 3 C_0: 9.6 mg/L [C_0: 1 μg/L for each compound] Time: 30 min	100 HPLC/LC-MS and GC TOC ~30	Not eliminated, atrazine and iopromide	[73]
Sulfamethoxazole/acetaminophen	Catalyst: Fe^{2+} $[H_2O_2]$: 1.3×10^{-4} mol/L *V*: 1 L $[H_2O_2/Fe^{2+}]$: 5 M ratio C_0: 11.88 mg/L Time: 120 min	TOC: 11.3	In situ generation of H_2O_2 by previous ozonation process	[74]
Berberine	Catalyst: $FeSO_4$ *V*: 250 L $[Fe^{2+}/H_2O_2]$: 0.1 M ratio pH: 3 C_0: 4,061 mg/L high concentration C_0: 709 mg/L low concentration Volumetric flow rate: 100 L/h Time: 60 min (hydraulic retention time)	COD: 35.6 for high concentration COD: 91.4% for low concentration	Industrial scale BOD_5/COD: 0.3, increased biodegradability Real wastewater with pH extremely low 0.06–0.09	[75]
Carbamazepine (CBZ)	Catalyst: $FeSO_4.7H_2O$ *V*: 100 mL $[H_2O_2]$: 8.5 g/L $[Fe^{2+}/H_2O_2]$: 1 M ratio pH: 3.5 C_0: 442 mg/L Time ~25 min	HPLC: 49.49	Industrial wastewater Treatment followed by GAC obtaining 99.51% of removal	[76]

(continued)

Table 7 (continued)

Pharmaceutical compound	Reaction conditions	Removal (%)	Observations	References
Steroid hormones, personal care products, and pharmaceuticals	Catalyst: PAN (modified polyacrylonitrile) *V*: 31.34 L [H_2O_2]: 200 mg/L Volumetric flow rate: 10.6 L/h pH natural of wastewater C_0: 6–11.08 mg/L Time ~180 min	LC-MS/MS: >90 (hormones) LC-MS/MS: >40 (pharmaceuticals) TOC: 30–40	Pilot plant. Municipal wastewater The catalyst not needs ranges of pH 2–4 Reported leaching is less than 4% BOD reduce to less than 1 mg/L	[77]
Diclofenac	Catalyst: Fe-doped CeO_2 Catalyst dosage: 0.5 g/L *V*: 150 mL [H_2O_2]: 10 mM pH 5 C_0: 20 mg/L Time: 40 min	HPLC: 85.25	Removal of 2.2% only with H_2O_2 after 40 min	[78]
Paracetamol	Catalyst: MGN1 (Fe_3O_4 powder <50 nm) MGN2 (Fe_3O_4 powder <5 nm) MGM (Fe_3O_4 powder <50 nm) Catalyst dosage: 6 g/L V: 650 mL [H_2O_2]: 153 mM pH 2.6 C_0: 100 mg/L Time: 5 h	TOC: 43 (MGN1) TOC: 34 (MGN2) TOC: 39 (MGM)	With three catalysts, the total removal of paracetamol was obtained Without catalyst there is no removal	[79]
Ofloxacin	Catalyst: alginate iron (4%) Catalyst dosage: 400 mg/L *V*: 100 mL [H_2O_2]: 4.067 mM pH 3 C_0: 30 mg/L Time: 180 min	UV: 98	After three successive runs, activity decreases only around 10%	[80]

4 Conclusions

Ozonation and Fenton are processes that are capable to remove 100% of a wide variety of pharmaceutical compounds from wastewater. These processes fail, however, on achieving full mineralization, and this may lead to worsen the problem from a toxicological point of view. Therefore such processes should be combined with toxicological analysis, either theoretical or experimental, of the treated effluents. The main reaction variables affecting the efficiency of such processes are pH, ozone, and H_2O_2 concentration, reactor design, and the presence of catalysts, light, or electrolysis.

References

1. Brillas E, Huitle CAM (2011) Synthetic diamond films: preparation, electrochemistry, characterization and applications. Wiley, Hoboken
2. Gottschalk C, Libra JA, Saupe A (2009) Ozonation of water and waste water: a practical guide to understanding ozone and its applications. Wiley, Hoboken
3. Alpatova AL, Davies SH, Masten SJ (2013) Hybrid ozonation-ceramic membrane filtration of surface waters: the effect of water characteristics on permeate flux and the removal of DBP precursors, dicloxacillin and ceftazidime. Sep Purif Technol 107:179–186
4. Borowska E, Bourgin M, Hollender J et al (2016) Oxidation of cetirizine, fexofenadine and hydrochlorothiazide during ozonation: kinetics and formation of transformation products. Water Res 94:350–362
5. Tay KS, Madehi N (2015) Ozonation of ofloxacin in water: by-products, degradation pathway and ecotoxicity assessment. Sci Total Environ 520:23–31
6. Huang G, Pan F, Fan G, Liu G (2016) Application of heterogeneous catalytic ozonation as a tertiary treatment of effluent of biologically treated tannery wastewater. J Environ Sci Health Toxicol Hazard Subst Environ Eng 51:626–633
7. Martins RC, Cardoso M, Dantas RF et al (2015) Catalytic studies for the abatement of emerging contaminants by ozonation. J Chem Technol Biotechnol 90:1611–1618
8. Polat D, Balci I, Özbelge TA (2015) Catalytic ozonation of an industrial textile wastewater in a heterogeneous continuous reactor. J Environ Chem Eng 3:1860–1871
9. Crousier C, Pic J-S, Albet J et al (2016) Urban wastewater treatment by catalytic ozonation. Ozone Sci Eng 38:3–13
10. Chen S-Y, Li Y-M, Lei L-R (2015) Tertiary treatment of paper-making tobacco sheet wastewater via catalytic ozonation with Ti(IV) ions. Huanan Ligong Daxue Xuebao J South China Univ Technol Nat Sci 43:131–139
11. Wang T, Xue L, Brimblecombe P et al (2017) Ozone pollution in China: a review of concentrations, meteorological influences, chemical precursors, and effects. Sci Total Environ 575:1582–1596
12. Lucas MS, Reis NM, Li Puma G (2016) Intensification of ozonation processes in a novel, compact, multi-orifice oscillatory baffled column. Chem Eng J 296:335–339
13. Hewgill MR, Mackley MR, Pandit AB, Pannu SS (1993) Enhancement of gas-liquid mass transfer using oscillatory flow in a baffled tube. Chem Eng Sci 48:799–809
14. Martín del Campo E, Valente JS, Pavón T et al (2011) 4-chlorophenol oxidation photocatalyzed by a calcined Mg–Al–Zn layered double hydroxide in a co-current downflow bubble column. Ind Eng Chem Res 50:11544–11552

15. Ochuma IJ, Fishwick RP, Wood J, Winterbottom JM (2007) Optimisation of degradation conditions of 1,8-diazabicyclo 5.4.0 undec-7-ene in water and reaction kinetics analysis using a cocurrent downflow contactor photocatalytic reactor. Appl Catal B Environ 73 (3–4):259–268
16. Ochuma IJ, Fishwick RP, Wood J, Winterbottoom JM (2007) Photocatalytic oxidation of 2,4,6-trichlorophenol in water using a cocurrent downflow contactor reactor (CDCR). J Hazard Mater 144:627–633
17. Alharbi SK, Price WE, Kang J et al (2016) Ozonation of carbamazepine, diclofenac, sulfamethoxazole and trimethoprim and formation of major oxidation products. Desalin Water Treat 57:29340–29351
18. Zhao Y, Kuang J, Zhang S et al (2017) Ozonation of indomethacin: kinetics, mechanisms and toxicity. J Hazard Mater 323:460–470
19. Rodríguez EM, Márquez G, León EA et al (2013) Mechanism considerations for photocatalytic oxidation, ozonation and photocatalytic ozonation of some pharmaceutical compounds in water. J Environ Manag 127:114–124
20. Gimeno O, García-Araya JF, Beltrán FJ et al (2016) Removal of emerging contaminants from a primary effluent of municipal wastewater by means of sequential biological degradation-solar photocatalytic oxidation processes. Chem Eng J 290:12–20
21. Gomes DS, Gando-Ferreira LM, Quinta-Ferreira RM, Martins RC (2017) Removal of sulfamethoxazole and diclofenac from water: strategies involving O_3 and H_2O_2. Environ Technol 1–42. https://doi.org/10.1080/09593330.2017.1335351
22. Kermani M, Farzadkia M, Esrafili A et al (2016) Removal of catechol from aqueous solutions using catalytic ozonation by magnetic nanoparticles of iron oxide doped with silica and titanium dioxide: a kinetic study. J Mazandaran Univ Med Sci 26:139–154
23. Oropesa AL, Novais SC, Lemos MFL et al (2017) Oxidative stress responses of Daphnia magna exposed to effluents spiked with emerging contaminants under ozonation and advanced oxidation processes. Environ Sci Pollut Res 24:1735–1747
24. Prado M, Borea L, Cesaro A et al (2017) Removal of emerging contaminant and fouling control in membrane bioreactors by combined ozonation and sonolysis. Int Biodeterior Biodegrad 119:577–586
25. Salimi M, Esrafili A, Gholami M et al (2017) Contaminants of emerging concern: a review of new approach in AOP technologies. Environ Monit Assess 189(8):414
26. Nawrocki J (2013) Catalytic ozonation in water: controversies and questions. Discussion paper. Appl Catal B Environ 142–143:465–471
27. Nawrocki J, Kasprzyk-Hordern B (2010) The efficiency and mechanisms of catalytic ozonation. Appl Catal B Environ 99:27–42
28. Martínez-Huitle CA, Rodrigo MA, Sirés I, Scialdone O (2015) Single and coupled electrochemical processes and reactors for the abatement of organic water pollutants: a critical review. Chem Rev 115:13362–13407
29. Liu Z-Q, Ma J, Cui Y-H et al (2011) Factors affecting the catalytic activity of multi-walled carbon nanotube for ozonation of oxalic acid. Sep Purif Technol 78:147–153
30. Dai Q, Wang J, Yu J et al (2014) Catalytic ozonation for the degradation of acetylsalicylic acid in aqueous solution by magnetic CeO_2 nanometer catalyst particles. Appl Catal B Environ 144:686–693
31. Qin H, Chen H, Zhang X et al (2014) Efficient degradation of fulvic acids in water by catalytic ozonation with CeO_2/AC. J Chem Technol Biotechnol 89:1402–1409
32. Faria PCC, Órfão JJM, Pereira MFR (2009) Activated carbon and ceria catalysts applied to the catalytic ozonation of dyes and textile effluents. Appl Catal B Environ 88:341–350
33. Buxton GV, Greenstock CL, Helman WP, Ross AB (1988) Critical review of rate constants for reactions of hydrated electrons, hydrogen atoms and hydroxyl radicals ($^{\bullet}OH/^{\bullet}O^{-}$) in aqueous solution. J Phys Chem Ref Data 17:513–886

34. Yin R, Guo W, Zhou X et al (2016) Enhanced sulfamethoxazole ozonation by noble metal-free catalysis based on magnetic Fe_3 O_4 nanoparticles: catalytic performance and degradation mechanism. RSC Adv 6:19265–19270
35. Qi F, Chu W, Xu B (2016) Comparison of phenacetin degradation in aqueous solutions by catalytic ozonation with CuFe2O4 and its precursor: surface properties, intermediates and reaction mechanisms. Chem Eng J 284:28–36
36. Bai Z, Yang Q, Wang J (2016) Catalytic ozonation of sulfamethazine antibiotics using Ce0.1Fe0.9OOH: catalyst preparation and performance. Chemosphere 161:174–180. https://doi.org/10.1016/j.chemosphere.2016.07.012
37. Bing J, Hu C, Nie Y et al (2015) Mechanism of catalytic ozonation in Fe2O3/Al2O3@ SBA-15 aqueous suspension for destruction of ibuprofen. Environ Sci Technol 49:1690–1697
38. Aghaeinejad-Meybodi A, Ebadi A, Shafiei S et al (2015) Degradation of antidepressant drug fluoxetine in aqueous media by ozone/H_2O_2 system: process optimization using central composite design. Environ Technol 36:1477–1488
39. Li H, Xu B, Qi F et al (2014) Degradation of bezafibrate in wastewater by catalytic ozonation with cobalt doped red mud: efficiency, intermediates and toxicity. Appl Catal B Environ 152–153:342–351
40. Hollender J, Zimmermann SG, Koepke S et al (2009) Elimination of organic micropollutants in a municipal wastewater treatment plant upgraded with a full-scale post-ozonation followed by sand filtration. Environ Sci Technol 43:7862–7869
41. Mashayekh-Salehi A, Moussavi G, Yaghmaeian K (2017) Preparation, characterization and catalytic activity of a novel mesoporous nanocrystalline MgO nanoparticle for ozonation of acetaminophen as an emerging water contaminant. Chem Eng J 310:157–169
42. Jin X, Peldszus S, Huck PM (2012) Reaction kinetics of selected micropollutants in ozonation and advanced oxidation processes. Water Res 46:6519–6530
43. Amado-Piña D, Roa-Morales G, Barrera-Díaz C et al (2017) Synergic effect of ozonation and electrochemical methods on oxidation and toxicity reduction: phenol degradation. Int Mex Congr Chem React Eng 198:82–90
44. Xu B, Qi F, Sun D et al (2016) Cerium doped red mud catalytic ozonation for bezafibrate degradation in wastewater: efficiency, intermediates, and toxicity. Chemosphere 146:22–31
45. Brillas E, Sirés I, Oturan MA (2009) Electro-Fenton process and related electrochemical technologies based on Fenton's reaction chemistry. Chem Rev 109:6570–6631
46. Oturan MA, Aaron J-J (2014) Advanced oxidation processes in water/wastewater treatment: principles and applications. A review. Crit Rev Environ Sci Technol 44:2577–2641
47. Bokare AD, Choi W (2014) Review of iron-free Fenton-like systems for activating H_2O_2 in advanced oxidation processes. J Hazard Mater 275:121–135
48. Pang S-Y, Jiang J, Ma J (2011) Oxidation of sulfoxides and arsenic(III) in corrosion of nanoscale zero valent iron by oxygen: evidence against ferryl ions (Fe(IV)) as active intermediates in fenton reaction. Environ Sci Technol 45:3179–3180
49. De Laat HJG (1999) Catalytic decomposition of hydrogen peroxide by Fe(III) in homogeneous aqueous solution: mechanism and kinetic modeling. Environ Sci Technol 33:2726–2732
50. Novoa-Luna KA, Mendoza-Zepeda A, Natividad R et al (2016) Biological hazard evaluation of a pharmaceutical effluent before and after a photo-Fenton treatment. Sci Total Environ 569:830–840
51. Bernal M, Romero R, Roa G et al (2013) Ozonation of indigo carmine catalyzed with Fe-pillared clay. Int J Photoenergy 2013:7
52. Santana-Martínez G, Roa-Morales G, Martin del Campo E et al (2016) Electro-Fenton and electro-Fenton-like with in situ electrogeneration of H_2O_2 and catalyst applied to 4-chlorophenol mineralization. Electrochim Acta 195:246–256
53. Campos-Martin JM, Blanco-Brieva G, Fierro JL (2006) Hydrogen peroxide synthesis: an outlook beyond the anthraquinone process. Angew Chem Int Ed 45:6962–6984
54. Wernimont E, Ventura M, Garboden G, Mullens P (1999) Past and present uses of rocket grade hydrogen peroxide. General Kinetics, LLC Aliso Viejo, CA 92656

55. Moreira FC, Boaventura RAR, Brillas E, Vilar VJP (2017) Electrochemical advanced oxidation processes: a review on their application to synthetic and real wastewaters. Appl Catal B Environ 202:217–261
56. Yang L, Dong G, Jacobs DL et al (2017) Two-channel photocatalytic production of H_2O_2 over g-C_3N_4 nanosheets modified with perylene imides. J Catal 352:274–281
57. Isarain-Chávez E, Martínez-Huitle CA, Peralta-Hernández JM, De la Rosa C (2013) On-site hydrogen peroxide production at pilot flow plant: application to electro-Fenton process. Int J Electrochem Sci 8:3084–3094
58. Yu F, Zhou M, Zhou L, Peng R (2014) A novel electro-Fenton process with H_2O_2 generation in a rotating disk reactor for organic pollutant degradation. Environ Sci Technol Lett 1:320–324
59. Yu F, Zhou M, Yu X (2015) Cost-effective electro-Fenton using modified graphite felt that dramatically enhanced on H_2O_2 electro-generation without external aeration. Electrochim Acta 163:182–189
60. Pérez JF, Llanos J, Sáez C et al (2016) Electrochemical jet-cell for the in-situ generation of hydrogen peroxide. Electrochem Commun 71:65–68
61. Assumpção M, Moraes A, De Souza R et al (2012) Low content cerium oxide nanoparticles on carbon for hydrogen peroxide electrosynthesis. Appl Catal A Gen 411:1–6
62. Silva FL, Reis RM, Barros WRP et al (2014) Electrogeneration of hydrogen peroxide in gas diffusion electrodes: application of iron (II) phthalocyanine as a modifier of carbon black. J Electroanal Chem 722–723:32–37
63. Peralta E, Natividad R, Roa G et al (2013) A comparative study on the electrochemical production of H_2O_2 between BDD and graphite cathodes. Sustain Environ Res 23:259–266
64. Olvera-Vargas H, Oturan N, Oturan MA, Brillas E (2015) Electro-Fenton and solar photoelectro-Fenton treatments of the pharmaceutical ranitidine in pre-pilot flow plant scale. Sep Purif Technol 146:127–135
65. Pérez T, Garcia-Segura S, El-Ghenymy A et al (2015) Solar photoelectro-Fenton degradation of the antibiotic metronidazole using a flow plant with a Pt/air-diffusion cell and a CPC photoreactor. Electrochim Acta 165:173–181
66. Bustos YA, Rangel-Peraza JG, Rojas-Valencia MN et al (2016) Treatment of industrial effluents by electrochemical generation of H_2O_2 using an RVC cathode in a parallel plate reactor. Environ Technol 37:815–827
67. Luo H, Li C, Wu C et al (2015) Electrochemical degradation of phenol by in situ electro-generated and electro-activated hydrogen peroxide using an improved gas diffusion cathode. Electrochim Acta 186:486–493
68. Kato S, Jung J, Suenobu T, Fukuzumi S (2013) Production of hydrogen peroxide as a sustainable solar fuel from water and dioxygen. Energy Environ Sci 6:3756–3764
69. Tsukamoto D, Shiro A, Shiraishi Y et al (2012) Photocatalytic H_2O_2 production from ethanol/O_2 system using TiO_2 loaded with Au-Ag bimetallic alloy nanoparticles. ACS Catal 2:599–603
70. Zhuang H, Yang L, Xu J et al (2015) Robust photocatalytic H_2O_2 production by octahedral $Cd_3(C_3N_3S_3)_2$ coordination polymer under visible light. Sci Rep 5:16947
71. Wang R, Pan K, Han D et al (2016) Solar-driven H_2O_2 generation from H_2O and O_2 using earth-abundant mixed-metal oxide@carbon nitride photocatalysts. ChemSusChem 9:2470–2479
72. Shiraishi Y, Kanazawa S, Sugano Y et al (2014) Highly selective production of hydrogen peroxide on graphitic carbon nitride (g-C3N4) photocatalyst activated by visible light. ACS Catal 4:774–780
73. Li W, Nanaboina V, Zhou Q, Korshin GV (2012) Effects of Fenton treatment on the properties of effluent organic matter and their relationships with the degradation of pharmaceuticals and personal care products. Water Res 46:403–412
74. Aguinaco A, Beltrán FJ, Sagasti JJP, Gimeno O (2014) In situ generation of hydrogen peroxide from pharmaceuticals single ozonation: a comparative study of its application on Fenton like systems. Chem Eng J 235:46–51

75. Cui X, Zeng P, Qiu G et al (2015) Pilot-scale treatment of pharmaceutical berberine wastewater by Fenton oxidation. Environ Earth Sci 73:4967–4977
76. Dwivedi K, Morone A, Chakrabarti T, Pandey RA (2016) Evaluation and optimization of Fenton pretreatment integrated with granulated activated carbon (GAC) filtration for carbamazepine removal from complex wastewater of pharmaceutical industry. J Environ Chem Eng. https://doi.org/10.1016/j.jece.2016.12.054
77. Chi GT, Churchley J, Huddersman KD (2013) Pilot-scale removal of trace steroid hormones and pharmaceuticals and personal care products from municipal wastewater using a heterogeneous fenton's catalytic process. Int J Chem Eng. https://doi.org/10.1155/2013/760915
78. Chong S, Zhang G, Zhang N et al (2016) Preparation of FeCeOx by ultrasonic impregnation method for heterogeneous Fenton degradation of diclofenac. Ultrason Sonochem 32:231–240
79. Velichkova F, Julcour-Lebigue C, Koumanova B, Delmas H (2013) Heterogeneous Fenton oxidation of paracetamol using iron oxide (nano)particles. J Environ Chem Eng 1:1214–1222
80. Titouhi H, Belgaied J-E (2016) Heterogeneous Fenton oxidation of ofloxacin drug by iron alginate support. Environ Technol 37:2003–2015
81. Mirzaei A, Chen Z, Haghighat F, Yerushalmi L (2017) Removal of pharmaceuticals from water by homo/heterogonous Fenton-type processes – a review. Chemosphere 174:665–688
82. Arzate-Salgado S-Y, Morales-Pérez A-A, Solís-López M, Ramírez-Zamora R-M (2016) Evaluation of metallurgical slag as a Fenton-type photocatalyst for the degradation of an emerging pollutant: diclofenac. Catal Today 266:126–135
83. Bautitz IR, Nogueira RFP (2007) Degradation of tetracycline by photo-Fenton process-solar irradiation and matrix effects. J Photochem Photobiol Chem 187:33–39
84. Sun S-P, Lemley AT (2011) P-nitrophenol degradation by a heterogeneous Fenton-like reaction on nano-magnetite: process optimization, kinetics, and degradation pathways. J Mol Catal Chem 349:71–79

5.2Artículo enviado.

Conductive-diamond production of H_2O_2 and O_3 to remove phenol in a Downflow

Elsevier Editorial System(tm) for Applied Catalysis B: Environmental

Manuscript Draft

Manuscript Number:

Title: Conductive-diamond production of H2O2 and O3 to remove phenol in a Downflow Bubble Column Electrochemical Reactor (DBCER)

Article Type: Research Paper

Keywords: Advanced Oxidation Processes; Electro-peroxone; BDD anode/cathode; Mineralization; Phenol toxicity.

Corresponding Author: Dr. Reyna Natividad, Ph.D.

Corresponding Author's Institution: Universidad Autonoma del Estado de Mexico

First Author: Germán Santana-Martínez, M Sc

Order of Authors: Germán Santana-Martínez, M Sc; Gabriela Roa-Morales, Ph.D.; Leobardo Gómez-Olivan, Ph.D.; Ever Peralta-Reyes, Ph.D.; Rubí Romero, Ph.D.; Reyna Natividad, Ph.D.

Bubble Column Electrochemical Reactor (DBCER)

Germán Santana-Martínez[a], Gabriela Roa-Morales[a,*], Leobardo Gómez-Olivan[b], Ever Peralta-Reyes [c], Rubí Romero, Reyna Natividad[a,*]

[a]Centro Conjunto de Investigación en Química Sustentable UAEM-UNAM, Universidad Autónoma del Estado de México, Km. 14.5 carretera Toluca-Atlacomulco, Toluca, Estado de México, Mexico.

[b]Facultad de Química, UAEM, Paseo Tollocan esq Paseo Colon C.P 50120, Toluca, Estado de México, Mexico.

[c]Universidad del Mar, Campus Puerto Ángel, Ciudad Universitaria S/N, C. P.70902, Puerto Ángel, Oaxaca, Mexico.

*Corresponding authors: rnatividadr@uaemex.mx (R. Natividad), groam@uaemex.mx (G. Roa)

Abstract

In the context of water remediation, advanced oxidation processes have been proven to be an effective solution. In most of the cases, however, the reaction systems are usually highly expensive, because of the addition of chemical substances or energy consumption. This usually constrains their application at an industrial scale. This has motivated several researchers to develop technologies able not only to intensify the processes but able also to increase the sustainability of the whole process. In this context, this work aimed to assess a relatively novel technology, a Downflow Bubble Column Electrochemical Reactor (DBCER), in the mineralization of a rather typical organic pollutant, phenol.

The studied variables were: current density (20-60 mA/cm^2), electrolyte concentration (0.025-0.1 M), liquid recirculation rate (4.7 and 6 L/min) and pH (3 and 7). The response variables were total organic carbon (TOC), phenol and by-products concentration, oxidant species concentration (O_2, H_2O_2 and O_3).

The highest mineralization degree was around 75 % under pH 3, 60 mA/cm^2, 4.7 L/min and an electrolyte concentration of 0.05 M. Under these conditions, it was figured out that the phenol oxidation occurs mainly by ozone attack and the main remaining compound was oxalic acid. Although at pH 7 the mineralization degree was lower than at pH 3, it was demonstrated by a biotoxicity study on *Cyprinus carpio* that the original toxicity was significantly decreased.

Thus, it was demonstrated that the DBCER with BDD electrodes allows not only the production of $^{\bullet}OH$, but also the *in situ* production of O_2, H_2O_2 and O_3 (without the addition of any gas) and more importantly their utilization to conduct an electro-peroxone process.

1. Introduction

Advanced Oxidation Processes (AOPs) have become of paramount importance in the context of water remediation [1]. Despite their proven efficiency, and in the context of sustainability mainly, research on this topic is still needed since there remain challenges to be addressed like energy consumption, scaling-up, process intensification to reduce the treatment time and minimization of operating costs, mainly. An important strategy in this sense is the improvement of existing processes by minimizing the addition of chemical reagents and the discharge of waste to the environment. In this sense, since five years ago, several researchers have focused on the improvement of the peroxone process [2] that mainly consists on the generation of strongly oxidant species by the reaction of hydrogen peroxide with ozone,

$$2H_2O_2 + 2O_3 \rightarrow H_2O + 3O_2 + HO_2^{\bullet} + OH^{\bullet} \quad (1)$$

Conventionally, the two reagents are added to the reaction system, the first with commercial H_2O_2 and the second one supplying oxygen to an ozone generator to produce it. Lately, however, H_2O_2 *in-situ* electrochemical production has been widely reported by using carbonaceous materials as electrodes [3,4]. This has been mainly applied to carry out electro-fenton and electro-peroxone processes that consist on conducting reaction 1 but with electrogenerated hydrogen peroxide by reduction of oxygen at the cathode,

$$O_{2(g)} + 2H^+ + 2e^- \rightarrow H_2O_2 \quad (2)$$

This reaction has also been reported to occur with boron doped diamond electrodes (BDD) [3,5].

The increase in the use of the electro-peroxone process has been motivated by the following advantages in the mineralization of pollutants [6–9],

- Accelerates the transformation of O_3 to $^{\bullet}OH$ [10].
- The addition of H_2O_2 and O_3 does not generate polluting by-products, only H_2O and O_2 [11–13].
- Reduced formation of bromates and bromide (compounds potentially carcinogenic) in effluents[14,15].
- The process efficiency is increased, and the energy demand is decreased, this is because the treatment time is shorter with respect to the separate processes. Also, it is a safer option with lower costs [9].
- Enhances the abatement kinetics of ozone resistant pollutants [16] .

Nevertheless, in a typical electro-peroxone process the external production and addition of O3 still is a common practice and represents an opportunity of improvement not only from the chemical point of view but also from an economical angle. In this sense, recently, the simultaneous generation of ozone and peroxide at neutral pH has been reported and this eliminates the implementation of an ozone generator, which saves the costs of the process. This reaction system was implemented using a carbon PTFE cathode and as anode a membrane electrode assembly (MEA) [17] and the following reactions were reported to be the via of reagents production,

$$Cathode \quad 1.5O_2 + 6H^+ + 6e^- \rightarrow 3H_2O \quad (3)$$

$$Anode \quad 3H_2O \rightarrow 6H^+ + 6e^- + O_3 \quad (4)$$

In the context of BDD electrodes application, however, since more than a decade ago is known that ozone is produced in the electro-oxidation process, in similar way to the abovementioned system [18]. The typical cells to achieve so, however, are not able to retain the produced gas within the system and therefore the generated O_3 is sub-utilized since it is only given a rather limited contact time with the reacting solution. Thus, it was the main

objective of this work to assess the performance of a Downflow Bubble Column Electrochemical Reactor (DBCER). This type of bubble column, albeit without electrodes, has been successfully applied to conduct photo-catalyzed processes and hydrogenation reactions [19–21]. Among its main documented advantages are the high mass transfer coefficients, absorption of gas in the liquid which prevents this phase from leaving the reactor, its design and scaling-up are relatively easy. A conventional operation of this bubble column implies the simultaneous injection on the top of the reactor of the two-phase, gas and liquid. In this proposal, however, no gas is fed into the reactor, but oxygen and ozone are electro-generated *in situ* as well as hydrogen peroxide. To test the efficiency of this electrochemical reactor, phenol was used as a model molecule, which is a highly persistent pollutant and is found as a raw material or typical by-product of degradation in the chemical and processing industries. A biotoxicity assay of the treated effluent is also presented.

2. Materials and methods

2.1 Chemicals

A phenol standard (99.5% purity) purchased from Merck was used to prepare solutions for experimentation and for HPLC analysis. Sodium sulfate (Na_2SO_4) provided by Reasol was used for the preparation of electrolyte solution. In some cases, the solutions were adjusted to a specific pH, employing solutions of NaOH or H_2SO_4 [1M], both reagents supplied by Fermont. With respect to chromatographic analysis, the mobile phases were prepared with methanol HPLC grade, purchased from Fermont. Potassium phosphate monobasic (K_2HPO_4) and ortho-phosphoric acid (H_3PO_4 85%) purchased from J.T Baker and Merck, respectively, were used to prepare the buffer solution. To quantify the hydrogen peroxide concentration evolution with time, a titanium sulfate solution was prepared by reacting between TiO_2 (Degussa) and H_2SO_4 [22]. To determine ozone concentration, a solution with phosphate monobasic, ortho-phosphoric acid and potassium indigotrisulfonate supplied by Sigma Aldrich, was prepared [23]. All solutions for calibration were prepared with deionized water.

2.2 Downflow Bubble Column Electrochemical Reactor (DBCER)

This reaction system is shown in Figure 1. The DBCER is a cylindrical undivided cell made of borosilicate, the volume is 2.0 L with an internal diameter of 5 cm and 100 cm of length, and a couple of electrodes of Boron Doped Diamond (BDD manufactured by CONDIAS) with 50 cm^2 of active area. At the top flange there is a small orifice (4 mm) that exerts a Venturi effect on the entering phases (electrolyte solution that is being recirculated). Because of the high energy at which the liquid enters the reactor, the generated gas at the electrodes is broken down and a matrix of small bubbles is generated thus increasing turbulence, contact area and mass transfer between gas-liquid-solid (electrodes). In addition, and unlike up-flow bubble columns, the arrangement proposed here offers the advantage of keeping the gas phase in contact with the liquid phase at all times. Also, because the cell is fully flooded with liquid, the length of electrodes is a plausible variable to be studied as well as the surrounding hydrodynamics (one or two-phase). This implies a near to 100% utilization of the either input or generated gas. The gap between electrodes used in this study was 8 mm at all experiments. Current density was controlled by a power supply EXTECH 1683. The oxygen generated *in situ* by BDD electrolysis was on-line monitored by an oxygen analyzer HACH 400. At the same time ozone was *in situ* generated with the oxygen produced by electrolysis. At the end of the process, the unconsumed ozone was sent to a device called ozone destroyer (manufactured by Pacific Ozone Technology).

The pipelining, valves, tank and cooler were fabricated of stainless steel. To recirculate the solution in the system a WEG centrifugal pump of 1 HP was employed. The pump used to recirculate the solution, transfers heat to the solution and this is an advantage if temperature was a variable to be assessed. Nevertheless, a cooling system was necessary to conduct an experiment at constant temperature. For this purpose, a Rotoplas^{RM} centrifugal pump of 0.5 HP, was coupled to a cooling tank to control temperature.

2.3 Phenol Oxidation

In order to establish the feasibility of conducting oxidation processes in the DBCER, phenol removal was studied.

First of all, the conductive-diamond electro-generation of O_2, H_2O_2 and O_3 was studied without the addition of phenol. For this purpose, only water (from the mains) was employed. This water had an initial TOC of 35 mg/L, initial O_2 concentration of 5.9-6.5 mg/L, pH_0 (7.4-8.1) and conductivity (950-983 µS). This study was conducted under a liquid recirculation rate of 4.7 L/min and the effect of current density (20, 40 and 60 mA/cm^2) and pH (3, 7 and without control) was established.

For the study of phenol removal, 100 mg/L phenol solutions were prepared and for that purpose mains water was used at all times. The studied variables were liquid recirculation flowrate (Q_L), electrolyte concentration and pH. Current density was kept constant at all times at 60 mA/cm^2. The effect of Q_L was investigated at two levels, the minimum and the highest given by the recirculating pump. These were 4.7 and 6 L/min. This was carried out only at acidic conditions (pH=3) and with an electrolyte concentration of 0.05 M. When studying the effect of electrolyte concentration, the acidic conditions were maintained, and, in this case, the lowest flowrate was employed. Finally, the effect of pH (3 and 7) was studied and for this purpose the other reaction conditions were elected according to the highest attained TOC removal, i.e. Q_L=4.7 L/min, [electrolyte]=0.05 M and j=60 mA/cm^2. At all cases the response variables were total organic carbon (TOC) removal and phenol concentration (when added). Phenol oxidation by-products concentration and conductive-diamond electrogenerated species concentration (O_2, H_2O_2 and O_3) were also established when studying the effect of pH. Temperature was 23°C ± 2 at all experiments. Although the reactor design allows to conduct the experiment at pressures in the range of 0 – 4 bar, all experiments were conducted at an absolute pressure of 0.74 bar.

2.4 Analytical procedures

The mineralization degree was established by the quantification of Total Organic Carbon (TOC) with a Shimadzu TOC-L analyzer by injecting aliquots of 50 µL per sample.

Regarding pH control, this variable was monitored by a Fischer Scientific TB-150 pH-meter.

An UHPLC Vanquish diode array detector (Thermo Scientific) was used to quantify the phenol and its oxidation by-products (Aromatic compounds and carboxylic acids). The used software was Chromeleon 7.2. In this procedure, the injection volume was 5 µL and

temperature was controlled at 25°C to conduct the chromatography in isocratically mode. Aromatic compounds were analyzed in a column Ascentis Express C-18 (Supelco) 3.0 cm in length and 4.6 mm in diameter. The mobile phase was Methanol/H_2O_2 (20:80 v/v and 5mM H_2SO_4) at 1.0 mL/min. Regarding wavelength, this was set at 246, 270 and 280 nm. The rest of by-products were separated by a ZORBAX Eclipse XDB C-18 (Agilent) column, 15.0 cm in length and 4.6 mm in diameter, employing a buffer solution as a mobile phase of Methanol/H_2O_2 (10:90 v/v) and 30 mM K_2HPO_4 adjusted at pH 2.5 with H_3PO_4. This solution was pumped at 0.5 mL/min and the wavelength was set at 210 nm.

To quantify the amount of hydrogen peroxide, an aliquot from reaction solution was treated with titanium sulfate and then analyzed at λ: 408nm [22]. At the same time, other sample was taken to determine ozone concentration employing Potassium indigotrisulfonate at λ: 600nm [23]. Both spectroscopic determinations were analyzed by a PerkinElmer Model Lambda 25 UV/Vis spectrophotometer using a quartz cell with 1 cm of optical path.

2.5 Biotoxicity study

In order to establish the biological efficiency of the treatment conducted at pH 7 in the DBCER, sub-lethal toxicity tests on fish were conducted. For this purpose, two biomarkers were employed, i.e. 1) single-cell gel electrophoresis (comet assay) and 2) Micronuclei assay. Both tests were conducted on erythrocites of the test specimens.

2.5.1 Acquisition and adaptation of test organisms

Cyprinus carpio was the bio-indicator organism employed to conduct the sub-lethal toxicity studies. This specie is largely used in ecotoxicological studies due to relatively easy maintenance and large sensitivity to different xenobiotic agents[24]. The test specimens were de 21.35 ± 0.42 cm in length and weighed 61.35 ± 4.23 g. Such organisms were from a special fish centre were carps are grown. This centre is located in Tiacaque, State of Mexico. Specimens were transported to the lab in polyethylene bags with previously oxygenated water. Once in the lab, carps were placed in 160 L fish containers (50 carps per fish container) and they were given a 20- day adaptation time. Water conditions were continuous aeration, room temperature with light and darkness periods (12:12). Carps were fed with Pedregal Silver™ food for fish.

2.5.2 Sub-lethal toxicity assays

In order to conduct these assays, 120 L fish containers were used with reconstituted water. This water was prepared with different salts as follows: $NaHCO_3$ (174 mg/L), $MgSO_4$ (120 mg/L), KCl (8 mg/L) and $CaSO_4.2H_2O$ (120 mg/L). All systems were kept under continuous aeration and under natural photo-periods of light/darkness and at room temperature (25 ± 2ºC). The systems were static, without medium renovation and during the experiment the test organisms were not fed. The experimental systems were prepared considering the following treatments: 1) Control (mains water), 2) Positive control (ciclofosfamide 20 mg/Kg fish weight for comet assay), 3) Phenol without electrolyte (C= 100 mg/L) and 4) Phenol (100 mg/L) added to an electrolyte solution (Na_2SO_4 0.05M). 10 specimens were placed in each system. The experiments were performed by triplicate and different exposure times were assessed (12, 24, 48, 72 and 96 h). After each exposure time, fish were moved into a new fish container with a xylocaine solution (0.02 mg/L) in order to anaesthetize the carps. Once this was achieved, a blood sample was taken from the tail vein of the C. *carpio* by using a hypodermic heparinized syringe. 100 microliters of sample were added to 600 microliters of PBS in Eppendorf tubes. Prior analysis, these vials were stored under ultra-freezing conditions (-70ºC). Samples were split into two in order to perform single-cell electrophoresis (comet essay) and smear tests to establish micronuclei presence.

2.5.3 Single-cell gel Electrophoresis (comet assay)

The DNA damage was measured by the comet assay proposed by Tice *et al.* (2000). Glass slides were prepared 1-hour prior sampling. The glass slides were coated with 200 µL of 1% agarose solution and they were left to dry at room temperature. Blood (10 µL) was mixed with 75 µL of agarose (0.7%) and 50 µL of this mixture were placed over the initial agarose, this was extended and solidified on ice. For DNA extraction, the glass slides were placed in a Coplin glass containing lysis buffer [NaCl 2.5 M, EDTA 100 mM, Tris 10 mM, 10% dimethylsulphoxide (DMSO), 1% Triton X-100], under a pH=10 for 1 h at 4 °C. After this time, the glass slides were placed inside an electrophoresis chamber with alkaline solution [NaOH 300 mM and EDTA 1 mM] at pH 13 during 20 min. The electrophoresis was conducted at 300 mA and 25 V (4 °C, 20 min, field intensity: 0.8 V/cm) and was stopped with a neutralization tampon [Trizma base 0.4 M pH 7.4]. Finally, the DNA was

dyed with 50 mL of ethidium bromide (10 mg/mL) and the glass slides were then examined under a Zeiss Axiophot-1 epifluorescence microscope equipped with a Zeiss AxioCam HRc digital camera.

2.5.6 Micronuclei assay

The blood samples were employed to prepare smear that was fixed with pure ethanol for 5 minutes and then dyed with 10% Giemsa (Hycel, DF, México) for further 9 minutes. The results were expressed in terms of total number of micronuclei cells per every 1000 carp blood cells [25].

3. Results and discussion

3.1 Conductive-diamond electro-generated O_2, H_2O_2 and O_3

As starting point, the concentration of *in situ* electro-generated oxidant species was established. Such species were hydrogen peroxide, oxygen and ozone at different reaction conditions. Figure 2 depicts the concentration profiles of each oxidant in the current density range of 20 – 60 mA/cm^2, recirculation flowrate at 4.7 L/min, electrolyte concentration of 0.05 M Na_2SO_4 and pH 3. In order to study the distribution of oxidant species, phenol was not added. Similar experiments are reported at pH 7 as supplementary material S1.

In all cases, the water used in these tests has an associated initial oxygen concentration (5.9-6.5 mg/L). Nevertheless, when a current density is applied, oxygen concentration tends to increase (see figures 2 and S1) and this can be ascribed to the side reaction of oxygen evolution that can be represented as follows [26],

$$2H_2O \rightarrow O_2 + 4H^+ + 4e^- \qquad (5)$$

In conventional electrochemical cells, the oxygen generated from reaction (5) is typically released to atmosphere. Advantageously enough, the DBCER not only allows to keep this gas inside the reactor but also to efficiently disperse it into the electrolyte to maximize its use and consumption. As can be seen from Figure 2, oxygen concentration increases with respect to the initial value up to 9 mg/L. Although oxygen evolution does not favor the

formation of hydroxyl radicals, this gas can be transformed to ozone and hydrogen peroxide. The latter is expected to be produced at the cathode by oxygen reduction according to reaction (2) and it is also formed by the addition of two hydroxyl radicals, as observed in reaction (6) [4],

$$OH^{\bullet} + OH^{\bullet} \rightarrow H_2O_2 \qquad (6)$$

On the other hand, ozone can be produced by water electrolysis according to the following reaction [27],

$$3H_2O \rightarrow O_3 + 6H^+ + 6e^- \qquad (7)$$

To obtain this reaction (7), specifically with BDD electrodes, several authors have documented and proposed a mechanism based on the following reactions [27],

$$H_2O \rightarrow OH^{\bullet} + H^+ + e^- \qquad (8)$$

$$OH^{\bullet} \rightarrow O^{\bullet} + H^+ + e^- \qquad (9)$$

$$2O^{\bullet} \rightarrow O_2 \qquad (10)$$

$$2OH^{\bullet} \rightarrow H_2O_2 \qquad (11)$$

$$H_2O_2 \rightarrow O_2 + 2H^+ + 2e^- \quad (12)$$

$$O_2 + O^{\bullet} \rightarrow O_3 \quad (13)$$

As can be observed in reaction 12, the hydrogen peroxide is decomposed to oxygen and protons. This may explain why oxygen concentration increases even when ozone is being produced and also why hydrogen peroxide is not appreciable. It is plausible too that hydrogen peroxide could be reacting with produced ozone as follows[11],

$$H_2O_2 + O_3 \rightarrow {}^{\bullet}OH + {}^{\bullet}O_2^- + O_2 \quad (14)$$

This reaction not only would explain the increase in oxygen concentration but also explains the minimum quantified amount of H_2O_2 when phenol is not added. This phenomenon has also been previously reported [11] .

Despite the O_3 consumption by reaction 14, it is worth noticing that ozone concentration was practically constant (5 ± 0.5 mg/L) during the whole experiment, excepting at pH 3 and 60 mA/cm^2, where ozone concentration decays down to 2.9 mg/L. This can be associated with the increase of hydroxyl radicals production and the presence of protons which facilitates to maintain the acidic media, that is represented by the following reaction [28],

$$\text{BDD} + H_2O \rightarrow BDD(\text{OH}^{\bullet}) + H^+ + e^- \quad (15)$$

It is worth clarifying that even when phenol was not added, the initial TOC of the electrolyte solution for this study was 35 mg/L. This is due to the electrolyte solution being prepared with mains water. Thus, TOC analyses were also conducted in this experiment at the beginning and at the end of experiments (6 h). The results show a reduction from 40% and 55% when current densities of 20 mA/cm^2 and 40 mA/cm^2 are applied, respectively. However, the highest value is obtained with 60 mA/cm^2 where the TOC removal is approximately 98 %. Therefore, the ozone concentration decreases (observed at the highest TOC removal, i.e. when a current density 60 mA/cm^2 of is applied). This is also a clear indicative that in acidic media and high current densities the concentration of the *in-situ*

produced oxidants is enough to eliminate the remove organic matter from water. It should also be kept on mind that at high current densities, the amount of hydroxyl radicals is also expected to increase by reaction (15) and thus the direct oxidation over the electrodes surface by means of reaction 16,

$$BDD(OH^{\bullet}) + R \rightarrow BDD + CO_2 + H_2O + H^+ + e^- \quad (16)$$

3.2 Phenol oxidation: Effect of Recirculation flow-rate and electrolyte concentration

In the previous section, the quantification of oxygen, hydrogen peroxide and ozone demonstrated that is possible to generate them simultaneously *in-situ* and to keep them inside the electrochemical reactor and use them to mineralize organic matter, thus showing the feasibility of conducting an electro-peroxone treatment without the external addition of ozone or hydrogen peroxide but generating them *in situ*. Nevertheless, it was decided to add phenol in order to fully demonstrate the capabilities of the assessed technology.

The effect of recirculation flowrate (Q_L) on TOC removal is shown in Figure 3. These results show a significant lower TOC removal rate when maximum recirculation flowrate is applied. Reynolds number (Re) and residence time (τ) were calculated for every liquid flowrate. At 4.7 L/min, Re was 1995 and τ was 25 s. These parameters were 2545 and 19.6 s for 6 L/min. Thus, in terms of TOC removal, it can be concluded that is more beneficial to increase residence time rather than turbulence, i.e. Re number.

Another important aspect of the process is the electrolyte concentration, since is directly related to the solution conductivity and the generation of oxidant species. Regarding to this variable, the preferable value in Electro-Fenton and Electro-Oxidation is 0.05 M of sodium sulfate [28–31], only in few investigations this value has been increased to 0.1 M [32]. In this work, the effect of this variable on TOC removal was assessed in the range of 0.025-0.1 M and the results are shown in Figure 4. It is well known that the solution conductivity is directly related to the concentration of supporting electrolyte, in this case with the value of 0.025 M is obtained 20% less than at 0.05M at the end of treatment. However, when this value is duplicated, the TOC removal decreases 3%. This indicates that a high sodium sulphate concentration does not aid mineralization, despite of the already reported

disinfecting effect of sulphates [26]. The addition of sulphuric acid to keep pH 3, promotes the generation of sulphate radicals and peroxodisulphate by the following reactions [26],

$$SO_4^{-2} + OH \rightarrow SO_4^{-} + OH^{-} \quad (17)$$

$$2HSO_4^{-} + OH \rightarrow S_2O_8^{2-} + 2H_2O \quad (18)$$

These species are reactive oxygen species (ROS), albeit their standard potential is lower than O_3, H_2O_2 and $OH^{\bullet}$. Therefore the excess of sulphate ions inhibits the action of OH radical by reacting like scavengers of others mediators [26]. Considering this, it is very important to establish an ideal concentration of supporting electrolyte to generate high amounts of ROS with high standard potential and minimize reagent consumption. In this case, it can be observed that the best concentration of electrolyte in terms of TOC removal rate is 0.05M. Therefore, this concentration was used for the remained experiments and is in concordance with previous investigations.

3.3 Phenol oxidation: pH effect on O_2/O_3/H_2O_2 accumulation, by-products and kinetics

Figure 5 shows the effect of pH on TOC removal percentage. It can be observed that after 6 hours of treatment the maximum attained TOC removal was 75% at pH 3 and 65% at pH 7. None of these values are at stationary state though, meaning that the longer the treatment the higher the attained TOC removal. It can be observed in figure 5 that, as expected, these profiles depend on both, pH and time. At acidic conditions, two main stages are distinguished. The first one lasts for about 30 minutes and only in this time about 35% of the total TOC content is removed. In the following 5.5 h of treatment, however, TOC removal dramatically slows down and only a further 40% is removed. In order to explain this phenomenon, the phenol and oxidation by-products concentration profiles with time were obtained and these are shown in figures 6 and 7. It can be observed in Figure 6, that in the first 30 minutes 25% of phenol was removed. During this time, however, the only appreciable by-product is maleic acid at pH 3 (see Figure 7 a). A longer time under acidic conditions leads to obtain aromatic compounds (catechol, hydroquinone, benzoquinone)

and acids (maleic, malonic, fumaric and oxalic). It can also be observed in Figure 7 that all by-products but oxalic acid are further degraded at some point of the treatment. Thus, it can be concluded that the first stage observed in the TOC removal profile at pH 3 is due to the phenol degradation following the sequence maleic acid (by cleavage of the aromatic ring by an electrophilic attack of molecular ozone), fumaric and malonic acids and then their oxidation towards CO_2 and water. In this sense, it has been reported [33] that double-bond acids readily react with ozone via Criege's mechanism. It is worth noticing that hydrogen peroxide has been reported [34] as one of the products when the aromatic ring is destroyed to produce maleic fumaric acids by molecular ozone attack. The electrophilic attack of ozone to the phenol molecule has also been reported [33,34] to lead to hydroxylation products, i.e. catechol and hydroquinone, which are further oxidized towards benzoquinone, oxalic acid and CO_2 and water. It can also be observed in Figure 7a that oxalic acid accumulates, and, unlike the aromatics, it is not further oxidized. This is something expected in an ozonation treatment since the nucleophilic reaction of ozone with a carboxyl group is rather slow[33]. Thus, it can be concluded that the slowing down of the TOC removal profile (after 30 min) can be ascribed to the prevalence of direct oxidation by molecular ozone and the appearance of hydroxylation products and compounds with carboxyl groups. This does not rule out the oxidation by hydroxyl radicals though.

According to Figure 5, phenol is also mineralized at pH 7 albeit with a rather different behavior than at pH 3. Unlike at pH 3, in this case the TOC profile exhibits three rate stages, the first one lasts for 60 minutes and no mineralization at all is observed ($-r_{TOC}=0$). The second stage lasts for further 180 minutes and its removal rate is rather similar to the second stage of TOC profile at pH 3. A third stage, with a clear higher removal rate, is observed after 240 minutes. All this and the products distribution (Figure 7) suggest a different oxidation mechanism prevailing at pH 7.

With the results shown in Figure 6, the kinetic parameters for phenol oxidation were estimated. At both pH, 3 and 7, the reaction was pseudo-first order and the specific rate constants are of the same order of magnitude ($k = 0.0187\ min^{-1}$ at pH 3 and $k= 0.0119\ min^{-1}$at pH 7). This result was unexpected since pH has been reported (although not in an electrochemical process) to positively affect phenol removal not only because of ozone decomposition but because of phenol dissociation leading to the appearance of phenolates [33]. In this case, despite the similarity in specific rate constants, the products distribution

at pH 7 (Figure 7 b) show that the main accumulated compounds are hydroxylation products that build up during the first 60 minutes. Phenol oxidation then might be occurring by oxidant radicals attack rather than by molecular ozone. Also, it should kept on mind that in this system O_3 is not being fed at anytime but *in situ* produced. This fact along with the contact time, might be limiting the oxidants species concentration, mainly the hydroxyl radicals concentration, which seems to be increasing with time and this is suggested, once again by the products distribution, since after 120 and 180 minutes, the hydroxylation products, i.e. hydroquinone, catechol and benzoquinone, readily decay. This decay is related to the presence of more hydroxyl radicals evidenced by a decrease in H_2O_2 concentration (Figure 8) and thus suggesting the prevailing phenol and by-products oxidation mechanism at pH 7 is via an electro-peroxone process (reaction 1). Thus, at this pH, O_3 is mainly being used to react with H_2O_2 and produce hydroxyl radicals that are able to oxidize carboxylic compounds, and this explains the less extent of accumulation of oxalic acid compared to pH 3 (see Figure 7). In neutral media carboxylic acids remain in deprotonated form and with this condition is easier to destroy this kind of molecules [11], this is not applied to all cases and also has been reported that some molecules are easier to be removed in acidic rather than in neutral media [35].

Figure 8 depicts the effect of pH on the concentration of $O_2/O_3/H_2O_2$ cumulative concentration. Unlike the results obtained without phenol addition (figure 2), in this case the production and accumulation of hydrogen peroxide with time is noticeable at both pH, 3 and 7. Also at pH 3, hydrogen peroxide concentration and accumulation rate are higher than at pH 7. This can be ascribed to less consumption of this compound at pH 3 because its dissociation is lower than at pH 7, and the oxidation mechanism is mainly via molecular attack of O_3. Besides, pH 2.8 – 3 has been reported as the best range to electro-generate this oxidant [36,37]. With respect to pH 7, hydrogen peroxide concentration tends to diminish after three hours of treatment. This can be ascribed to the e-peroxone process taking over and leading to a higher H_2O_2 consumption to produce hydroxyl radicals (reaction 1) and this is reflected on the oxidation of aromatic compounds and carboxylic acids (figure 7b) and on an increase on the TOC removal rate (figure 5). Thus, it can be concluded that this technology allows to conduct the electro-peroxone process with the simultaneous electro-generation of oxygen, ozone and hydrogen peroxide.

3.4 Biotoxicity study

Because the TOC removal was not 100% achieved in the assessed treatment time, it was decided to evaluate the toxicity of the treated water under pH 7.

3.4.1 Comet assay

Figure 9 shows the DNA damage, which is statistically significant in both, the positive control and the exposed to phenol group. In the case of the positive control, the increase is from 45.8 to 51% and in the case of the group exposed to phenol the increase goes from 45.7 to 52.9% with respect to the control group ($P<0.05$). It can be observed, however, that the DNA damage was significantly reduced in the treated phenol solution (EP) with respect to the positive control and the exposed to phenol group. The observed increase of 11.2-16% with respect to the control is not statistically significant ($P>0.05$). These results are in concordance to those observations made through the epifluorescence microscope and placed as insets in Figure 9.

3.4.2 Micronuclei test

The results of this test are shown in Figure 10. There are in the positive control group and in the exposed to phenol group, statistically significant increases with respect to the control group. In the case of the positive control group, these increases are in the range of 853-1277% and in the case of the exposed to phenol group they are in the range of 731-1233% ($P<0.05$). In the case of the treated phenol solution, a micronuclei decrease was observed with respect to the positive control group and to the exposed to phenol group. The increase respect the control group is in the range of 7.7-20%, and this was concluded not being statistically significant ($P>0.05$).

In this work it was decided to use single-cell electrophoresis (comet assay) as a biomarker of damage, which is a technique to assess genotoxic damage. This test detects DNA single-strand breaks (strand breaks and incomplete excision repair sites), alkali-labile sites and cross-linking, with the single-cell approach typical of cytogenetic assays [38]. In the test, it was decided to use cyclophosphamide (this is a drug from the family of alkylating agents used as an antineoplastic and immunosuppressant) as a positive control, because it has been

shown to be an agent that has high genotoxic effects, besides being carcinogenic in aquatic organisms[39,40].

The model molecule used in this work was phenol, it is well known that this compound and its derivatives induce toxic responses in various fish species, the alterations that have been reported are genotoxicity, carcinogenesis, immunotoxicity, hematological damage and physiological alterations[41–45]. The mechanism through which this compound induces its toxic effects is through oxidative stress[46–50].

In addition, the micronuclei test was performed as a complimentary study. This biomarker was selected because the micronuclei (MNi) are nuclear residues produced during mitosis (or meiosis) when a fragment of a chromosome or a complete chromosome can not migrate with one of the two daughter nuclei formed. MNi can occur at different times of the event of DNA damage, depending on the kinetics of the cell cycle and the mechanism of induction [51,52]. The results obtained in this study showed that phenol at the concentration of 100 mg/L was able to induce in an important way the presence of micronuclei in erythrocytes. These findings agree with that reported by [53] who demonstrated that phenol at different concentrations (0.7, 1.4 and 2.8 mg / L) is able to induce the production of micronuclei in *Oreochromis niloticus.*

Once the samples were treated by electroperoxone process a substantial decrease in DNA damage and MNi were observed, albeit the treatment was conducted at pH 7 and the mineralization degree was not maximum.

4. Conclusions

The Downflow Bubble Column Electrochemical Reactor allows conducting the electro-peroxone process with *in situ* production of hydrogen peroxide and ozone, without injecting air/oxygen from an external source. This reactor is able to maintain the produced gas (oxygen and/or ozone) dispersed as bubbles within the reaction system to maximize its absorption and utilization and to eliminate its waste.

The main variables affecting the overall process efficiency, in terms of TOC removal rate and/or extent, are liquid flowrate, electrolyte concentration and pH. TOC removal rate is favored at an electrolyte concentration of 0.05 M, when liquid flowrate and pH decreased. pH does exert a great effect on TOC removal rate, being higher at acidic pH. Phenolic

compounds, however, can be mineralized in this system at either pH 3 or 7 with similar TOC removal extent, 75 with the former and 65 with the latter. In both cases, after 360 mins of treatment, the prevailing compounds are carboxylic acids in low concentrations.

Unlike TOC removal, phenol oxidation readily occurs at either pH, 3 or 7, and this variable determines the mechanism by which phenol is mineralized. At acidic conditions molecular ozonation attack prevails while at pH 7 the electro-peroxone process is presumed to be the main responsible of phenol mineralization. In this sense, it can also be concluded that electro-peroxone process of phenol favours hydroxylation products.

pH also affects H_2O_2, O_3 and O_2 cumulative concentrations. At pH 7 H_2O_2 consumption is higher than at pH 3 and therefore its cumulative concentration at the end of treatment is only 4 mg/L, while at pH 3 is 15 mg/L. The opposite effect was found for O_3 and O_2, although in less extent than for H_2O_2.

Although the mineralization degree is lower at pH 7 than at pH 3, conducting the electro-peroxone treatment at this condition eliminates the biotoxicity of by-products of the phenolic solution therefore water after treatment can be used for other applications.

The results at pH 7 suggest that this technology might also be applied to conduct selective oxidations and not only for water remediation.

Acknowledgements

Authors are grateful to CONACYT (Projects 168305 and 269093) for financial support. In the same way for the scholarship (CONACYT) 295553, to conduct postgraduate studies of Germán Santana-Martínez. Technical support of Citlalit Martínez Soto is also acknowledged.

References

[1] R. Natividad-Rangel, M.A.R. Rodrigo, J.J.M. Mesa, R.M.G. Espinosa, Water Remediation, J. Chem. 2017 (2017).

[2] J. Staehelin, J. Hoigne, Decomposition of ozone in water: rate of initiation by

hydroxide ions and hydrogen peroxide, Environ. Sci. Technol. 16 (1982) 676–681.

[3] E. Peralta, R. Natividad, G. Roa, R. Marín, R. Romero, T. Pavon, A comparative study on the electrochemical production of H2O2 between BDD and graphite cathodes, Sustain. Environ. Res. (2013) 259–266.

[4] S.-M. Germán, R.-M. Gabriela, S.-C. Dora, R. Rubí, N. Reyna, Advanced Oxidation Processes: Ozonation and Fenton Processes Applied to the Removal of Pharmaceuticals, in: Springer Berlin Heidelberg, Berlin, Heidelberg (2019) 1–24..

[5] E. Isarain-Chávez, C.A. Martínez-Huitle, J.M. Peralta-Hernández, C. De la Rosa, On-site Hydrogen Peroxide Production at Pilot Flow Plant: Application to Electro-Fenton Process, 8 (2013) 3084–3094.

[6] W. Guo, Q.-L. Wu, X.-J. Zhou, H.-O. Cao, J.-S. Du, R.-L. Yin, N.-Q. Ren, Enhanced amoxicillin treatment using the electro-peroxone process: key factors and degradation mechanism, Rsc Adv. 5 (2015) 52695–52702.

[7] B. Bakheet, C. Qiu, S. Yuan, Y. Wang, G. Yu, S. Deng, J. Huang, B. Wang, Inhibition of polymer formation in electrochemical degradation of p-nitrophenol by combining electrolysis with ozonation, Chem. Eng. J. 252 (2014) 17–21.

[8] X. Li, Y. Wang, S. Yuan, Z. Li, B. Wang, J. Huang, S. Deng, G. Yu, Degradation of the anti-inflammatory drug ibuprofen by electro-peroxone process, Water Res. 63 (2014) 81–93.

[9] Y. Wang, G. Yu, S. Deng, J. Huang, B. Wang, The electro-peroxone process for the abatement of emerging contaminants: Mechanisms, recent advances, and prospects, Chemosphere. 208 (2018) 640–654.

[10] A. Fischbacher, J. von Sonntag, C. von Sonntag, T.C. Schmidt, The •OH Radical Yield in the $H_2O_2 + O_3$ (Peroxone) Reaction, Environ. Sci. Technol. 47 (2013) 9959–9964.

[11] B. Bakheet, S. Yuan, Z. Li, H. Wang, J. Zuo, S. Komarneni, Y. Wang, Electro-peroxone treatment of Orange II dye wastewater, Water Res. 47 (2013) 6234–6243.

[12] C.A. Martínez-Huitle, E. Brillas, Decontamination of wastewaters containing

synthetic organic dyes by electrochemical methods: A general review, Appl. Catal. B Environ. 87 (2009) 105–145.

[13] C.A. Martínez-Huitle, M.A. Rodrigo, I. Sirés, O. Scialdone, Single and Coupled Electrochemical Processes and Reactors for the Abatement of Organic Water Pollutants: A Critical Review, Chem. Rev. 115 (2015) 13362–13407.

[14] Y. Li, W. Shen, S. Fu, H. Yang, G. Yu, Y. Wang, Inhibition of bromate formation during drinking water treatment by adapting ozonation to electro-peroxone process, Chem. Eng. J. 264 (2015) 322–328.

[15] X. Li, Y. Wang, J. Zhao, H. Wang, B. Wang, J. Huang, S. Deng, G. Yu, Electro-peroxone treatment of the antidepressant venlafaxine: Operational parameters and mechanism, J. Hazard. Mater. 300 (2015) 298–306.

[16] B. Wang, Y. Zhang, H. Ren, C. Yue, Mechanism of Mn3O4-catalyzed ozonation of drilling wastewater, Chinese J. Environ. Eng. 9 (2015) 4811–4816.

[17] B. Yang, J. Deng, G. Yu, S. Deng, J. Li, C. Zhu, Q. Zhuo, H. Duan, T. Guo, Effective degradation of carbamazepine using a novel electro-peroxone process involving simultaneous electrochemical generation of ozone and hydrogen peroxide, Electrochem. Commun. 86 (2018) 26–29.

[18] B. Marselli, J. Garcia-Gomez, P.-A. Michaud, M.A. Rodrigo, C. Comninellis, Electrogeneration of Hydroxyl Radicals on Boron-Doped Diamond Electrodes, J. Electrochem. Soc. 150 (2003) D79–D83.

[19] I.J. Ochuma, R.P. Fishwick, J. Wood, J.M. Winterbottom, Photocatalytic oxidation of 2,4,6-trichlorophenol in water using a cocurrent downflow contactor reactor (CDCR)., J. Hazard. Mater. 144 (2007) 627–633.

[20] I.J. Ochuma, R.P. Fishwick, J. Wood, J.M. Winterbottom, Optimisation of degradation conditions of 1,8-diazabicyclo 5.4.0 undec-7-ene in water and reaction kinetics analysis using a cocurrent downflow contactor photocatalytic reactor., Appl. Catal. B-Environmental. 73 (3-4) (2007) 259–268.

[21] E. Martín del Campo, J.S. Valente, T. Pavón, R. Romero, Á. Mantilla, R. Natividad, 4-Chlorophenol Oxidation Photocatalyzed by a Calcined Mg–Al–Zn Layered Double

Hydroxide in a Co-current Downflow Bubble Column, Ind. Eng. Chem. Res. 50 (2011) 11544–11552.

[22] G. Eisenberg, Colorimetric determination of hydrogen peroxide, Ind. Eng. Chem. Anal. Ed. 15 (1943) 327–328.

[23] H. Bader, J. Hoigné, Determination of ozone in water by the indigo method, Water Res. 15 (1981) 449–456.

[24] N. SanJuan-Reyes, L.M. Gómez-Oliván, M. Galar-Martínez, S. García-Medina, H. Islas-Flores, E.D. González-González, J.D. Cardoso-Vera, J.M. Jiménez-Vargas, NSAID-manufacturing plant effluent induces geno- and cytotoxicity in common carp (Cyprinus carpio), Sci. Total Environ. 530–531 (2015) 1–10.

[25] T. Çavaş, S. Ergene-Gözükara, Induction of micronuclei and nuclear abnormalities in Oreochromis niloticus following exposure to petroleum refinery and chromium processing plant effluents, Aquat. Toxicol. 74 (2005) 264–271. doi:https://doi.org/10.1016/j.aquatox.2005.06.001.

[26] C. Comninellis, G. Chen, Electrochemistry for the Environment, Springer New York, New York, NY, (2010). .

[27] P.A. Michaud, M. Panizza, L. Ouattara, T. Diaco, G. Foti, C. Comninellis, Electrochemical oxidation of water on synthetic boron-doped diamond thin film anodes, J. Appl. Electrochem. 33 (2003) 151–154.

[28] A. Thiam, R. Salazar, E. Brillas, I. Sirés, Electrochemical advanced oxidation of carbofuran in aqueous sulfate and/or chloride media using a flow cell with a RuO_2-based anode and an air-diffusion cathode at pre-pilot scale, Chem. Eng. J. 335 (2018) 133–144.

[29] G. Santana-Martínez, G. Roa-Morales, E.M. Del Campo, R. Romero, B.A. Frontana-Uribe, R. Natividad, Electro-Fenton and Electro-Fenton-like with in situ electrogeneration of H_2O_2 and catalyst applied to 4-chlorophenol mineralization, Electrochim. Acta. 195 (2016).

[30] S. Garcia-Segura, E. Brillas, Combustion of textile monoazo, diazo and triazo dyes by solar photoelectro-Fenton: Decolorization, kinetics and degradation routes, Appl.

Catal. B Environ. 181 (2016) 681–691.

[31] H. Olvera-Vargas, N. Oturan, M.A. Oturan, E. Brillas, Electro-Fenton and solar photoelectro-Fenton treatments of the pharmaceutical ranitidine in pre-pilot flow plant scale, Sep. Purif. Technol. 146 (2015) 127–135.

[32] D. Amado-Piña, G. Roa-Morales, C. Barrera-Díaz, P. Balderas-Hernandez, R. Romero, E. Martín del Campo, R. Natividad, Synergic effect of ozonation and electrochemical methods on oxidation and toxicity reduction: Phenol degradation, Int. Mex. Congr. Chem. React. Eng. (IMCCRE 2016). 198 (2017) 82–90.

[33] I. Chairez, P. Tatyana, R. Tapia, J. Vivero, Effect of pH to the Decomposition of Aqueous Phenols Mixture by Ozone, 2006.

[34] F. Beltrán, Ozone Reaction Kinetics for Water and Wastewater Systems, 1a ed., New York, Estados Unidos, 2004.

[35] O. Turkay, Z.G. Ersoy, S. Barışçı, Review—the application of an electro-peroxone process in water and wastewater treatment, J. Electrochem. Soc. 164 (2017) E94--E102.

[36] S. Garcia-Segura, Á.S. Lima, E.B. Cavalcanti, E. Brillas, Anodic oxidation, electro-Fenton and photoelectro-Fenton degradations of pyridinium- and imidazolium-based ionic liquids in waters using a BDD/air-diffusion cell, Electrochim. Acta. 198 (2016) 268–279.

[37] R.C. Burgos-Castillo, I. Sirés, M. Sillanpää, E. Brillas, Application of electrochemical advanced oxidation to bisphenol A degradation in water. Effect of sulfate and chloride ions, Chemosphere. 194 (2018) 812–820.

[38] L.D. Knopper, J.P. McNamee, Use of the comet assay in environmental toxicology, in: Environ. Genomics, Springer, 2008: pp. 171–184.

[39] M. Novak, B. Žegura, B. Modic, E. Heath, M. Filipič, Cytotoxicity and genotoxicity of anticancer drug residues and their mixtures in experimental model with zebrafish liver cells, Sci. Total Environ. 601–602 (2017) 293–300.

[40] T.G. Fonseca, M. Auguste, F. Ribeiro, C. Cardoso, N.C. Mestre, D.M.S. Abessa,

M.J. Bebianno, Environmental relevant levels of the cytotoxic drug cyclophosphamide produce harmful effects in the polychaete Nereis diversicolor, Sci. Total Environ. 636 (2018) 798–809.

[41] L. Taysse, D. Troutaud, N.A. Khan, P. Deschaux, Structure-activity relationship of phenolic compounds (phenol, pyrocatechol and hydroquinone) on natural lymphocytotoxicity of carp (Cyprinus carpio), Toxicology. 98 (1995) 207–214.

[42] T. Tsutsui, N. Hayashi, H. Maizumi, J. Huff, J.C. Barrett, Benzene-, catechol-, hydroquinone- and phenol-induced cell transformation, gene mutations, chromosome aberrations, aneuploidy, sister chromatid exchanges and unscheduled DNA synthesis in Syrian hamster embryo cells, Mutat. Res. Mol. Mech. Mutagen. 373 (1997) 113–123. .

[43] M.C.L. Erbe, W.A. Ramsdorf, T. Vicari, M.M. Cestari, Toxicity evaluation of water samples collected near a hospital waste landfill through bioassays of genotoxicity piscine micronucleus test and comet assay in fish Astyanax and ecotoxicity Vibrio fischeri and Daphnia magna, Ecotoxicology. 20 (2011) 320–328.

[44] H.S.H.S. Remya Varadarajan, J. Jose, B. Philip, Sublethal effects of phenolic compounds on biochemical, histological and ionoregulatory parameters in a tropical teleost fish Oreochromis mossambicus (Peters), (n.d.).

[45] W. Duan, F. Meng, H. Cui, Y. Lin, G. Wang, J. Wu, Ecotoxicity of phenol and cresols to aquatic organisms: A review, Ecotoxicol. Environ. Saf. 157 (2018) 441–456.

[46] H. Roche, G. Bogé, In vivo effects of phenolic compounds on blood parameters of a marine fish (Dicentrarchus labrax), Comp. Biochem. Physiol. Part C Pharmacol. Toxicol. Endocrinol. 125 (2000) 345–353.

[47] I.M. Avilez, T.S.F. Hori, L.C. de Almeida, A. Hackbarth, J. da C.B. Neto, V.L.F. da C. Bastos, G. Moraes, Effects of phenol in antioxidant metabolism in matrinxã, Brycon amazonicus (Teleostei; Characidae), Comp. Biochem. Physiol. Part C Toxicol. Pharmacol. 148 (2008) 136–142.

[48] T.S.F. Hori, I.M. Avilez, L.K. Inoue, G. Moraes, Metabolical changes induced by

chronic phenol exposure in matrinxã Brycon cephalus (teleostei: characidae) juveniles, Comp. Biochem. Physiol. Part C Toxicol. Pharmacol. 143 (2006) 67–72.

[49] A.A. Charan, A.I. Charan, O.M.P. Verma, S.S. Naushad, others, Profiling of antioxidant enzymes in cat fish (Clarias batrachus) exposed to phenolic compounds., Asian J. Bio Sci. 10 (2015) 6–14.

[50] K. Cho, C.-H. Lee, K. Ko, Y.-J. Lee, K.-N. Kim, M.-K. Kim, Y.-H. Chung, D. Kim, I.-K. Yeo, T. Oda, Use of phenol-induced oxidative stress acclimation to stimulate cell growth and biodiesel production by the oceanic microalga Dunaliella salina, Algal Res. 17 (2016) 61–66.

[51] V. V Arkhipchuk, N.N. Garanko, Using the nucleolar biomarker and the micronucleus test on in vivo fish fin cells, Ecotoxicol. Environ. Saf. 62 (2005) 42–52. .

[52] M. Hayashi, The micronucleus test—most widely used in vivo genotoxicity test—, Genes Environ. 38 (2016) 18.

[53] N.S. Gad, A.S. Saad, Effect of environmental pollution by phenol on some physiological parameters of Oreochromis niloticus, Glob. Vet. 2 (2008) 312–319.

Figure Captions

Figure 1. Downflow Bubble Column Electrochemical Reactor (DBCER).

Figure 2. Effect of current density on conductive-diamond electro-generation of O_2, O_3, H_2O_2. Operating conditions: pH=3, 0.05 M [Na_2SO_4], T: 23°C ±2, $[Ph]_o$=0 mg/L, Q_L= 4.7 L/min.

Figure 3. Effect of recirculation flow-rate on TOC removal. Reaction conditions: $[Phenol]_0$= 100mg/L, $[TOC]_0$= 118 mg/L, pH=3, j=60 mA/cm^2, 0.05 M [Na_2SO_4], V= 3.5 L and T= 23°C ±2.

Figure 4. Effect of electrolyte concentration [Na_2SO_4]. Reaction conditions: $[Phenol]_0$:100mg/L, pH=3, j=60 mA/cm^2, Q_L: 4.7 L/min, $[TOC]_0$: 118 mg/L, V: 3.5L and T: 23°C ±2.

Figure 5. Effect of pH on TOC removal percentage. Reaction conditions: $[Phenol]_0$:100 mg/L, 0.05 M [Na_2SO_4], *j*=60 mA/cm^2, Q_L= 4.7 L/min, $[TOC]_0$: 118 mg/L, V=3.5L and T= 23°C ±2.

Figure 6. Comparison of phenol degradation and kinetics order. Reaction conditions: j=60 mA /cm^2, $[Phenol]_0$: 100mg/L, 0.05 M [Na_2SO_4], R: 4.7 L/min, V:3.5L, $[TOC]_0$: 118 mg/L and T: 23°C ±2

Figure 7. Comparison of by-products in a) acidic and b) neutral media. Reaction conditions: j: 60 mA /cm^2, $[Phenol]_0$: 100mg/L, 0.05 M [Na_2SO_4], Q_L= 4.7 L/min, V: 3.5L. $[TOC]_0$: 118 mg/L and T= 23°C ±2.

Figure 8. Effect of pH on conductive-diamond electro-generation of O_2, O_3 and H_2O_2. Reaction conditions: j=60 mA/cm^2, 0.05 M [Na_2SO_4], $[TOC]_0$=118 mg/L, Q_L= 4.7 L/min, V=3.5L and T= 23°C ±2.

Figure 8. DNA Damage

Figure 9. Micronuclei test.

Figure 1

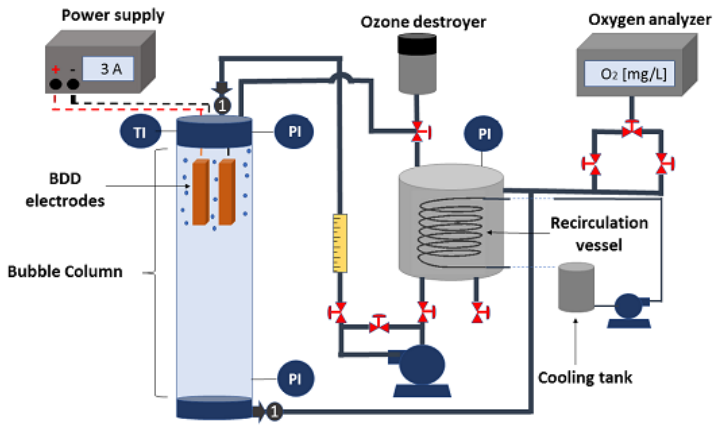
Power supply
3 A
Ozone destroyer
Oxygen analyzer
O2 [mg/L]
TI
PI
PI
BDD
electrodes
Bubble Column
Recirculation
vessel
PI
Cooling tank

Figure 2

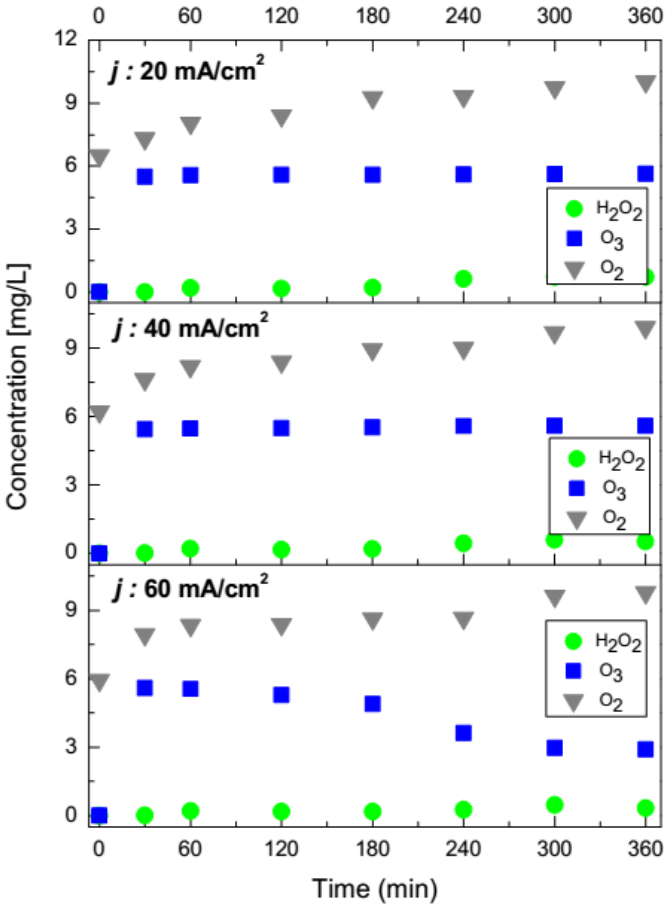
j : 20 mA/cm²
j : 40 mA/cm²
j : 60 mA/cm²
H2O2
O3
O2
Concentration [mg/L]
Time (min)
0
60
120
180
240
300
360
0
3
6
9
12

Figure 3

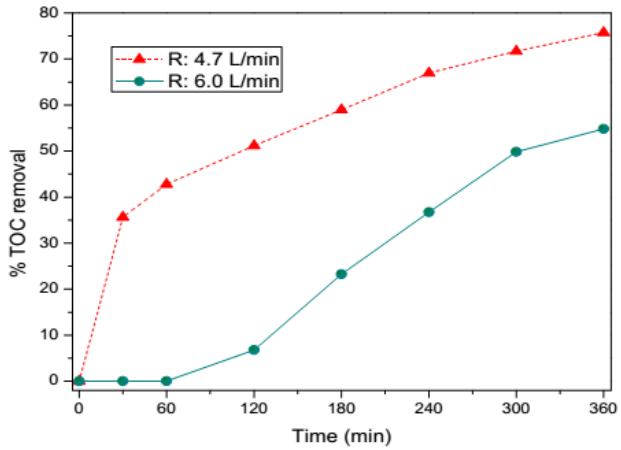
R: 4.7 L/min
R: 6.0 L/min
% TOC removal
Time (min)
0
10
20
30
40
50
60
70
80
0
60
120
180
240
300
360

Figure 4

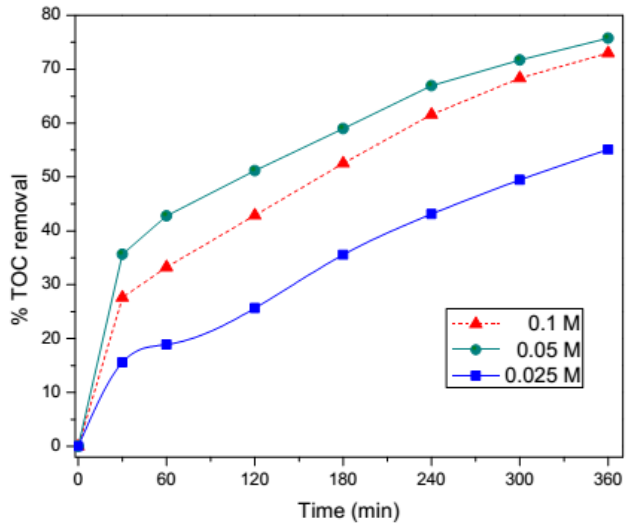
% TOC removal
Time (min)
0.1 M
0.05 M
0.025 M
0
10
20
30
40
50
60
70
80
0
60
120
180
240
300
360

Figure 5

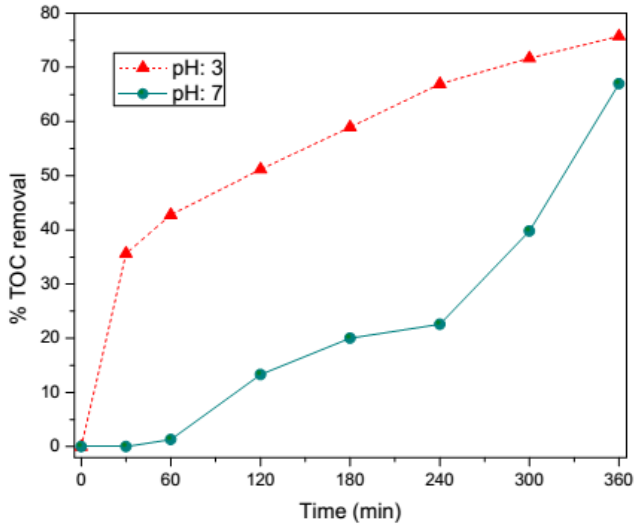
pH: 3
pH: 7
% TOC removal
Time (min)
0
10
20
30
40
50
60
70
80
0
60
120
180
240
300
360

Figure 6

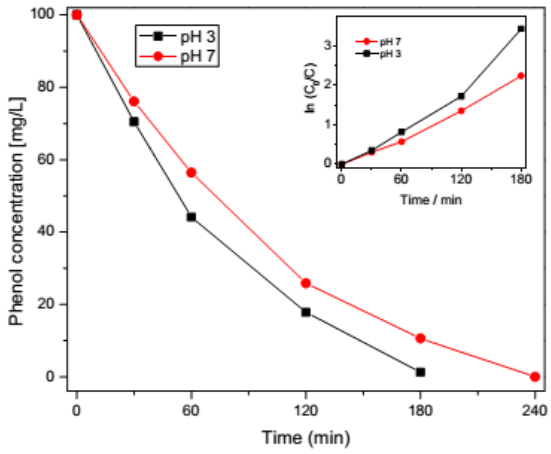

Figure 7

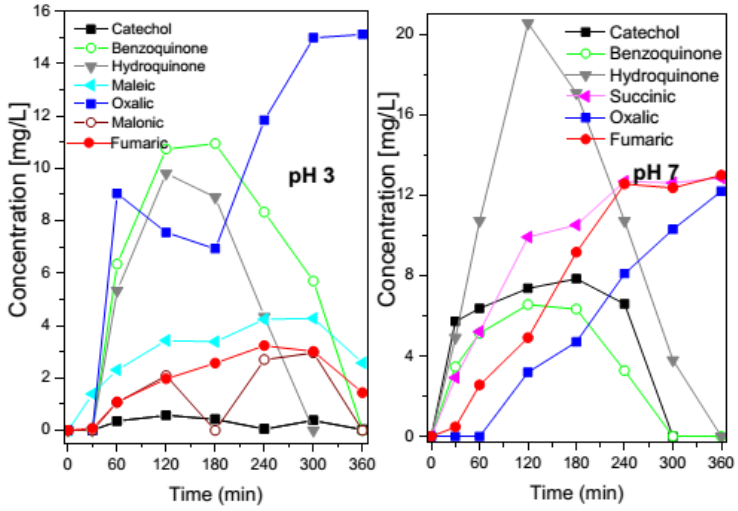
Catechol
Benzoquinone
Hydroquinone
Maleic
Oxalic
Malonic
Fumaric
pH 3
Concentration [mg/L]
Time (min)
Catechol
Benzoquinone
Hydroquinone
Succinic
Oxalic
Fumaric
pH 7
Concentration [mg/L]
Time (min)

(a) (b)

Figure 8

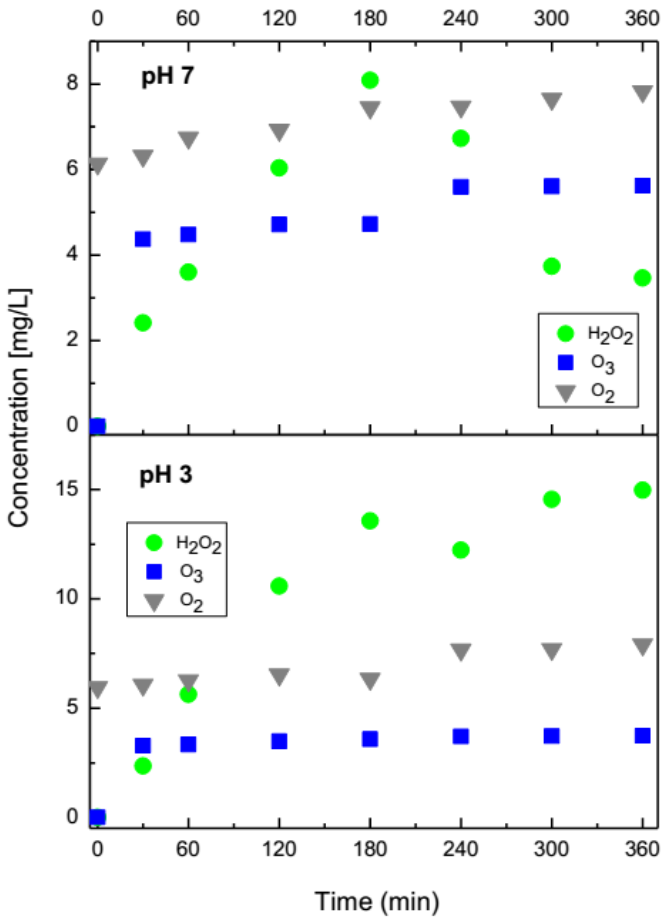
pH 7
pH 3
H_2O_2
O_3
O_2
Concentration [mg/L]
Time (min)
0
60
120
180
240
300
360
2
4
6
8
5
10
15

Figure 9

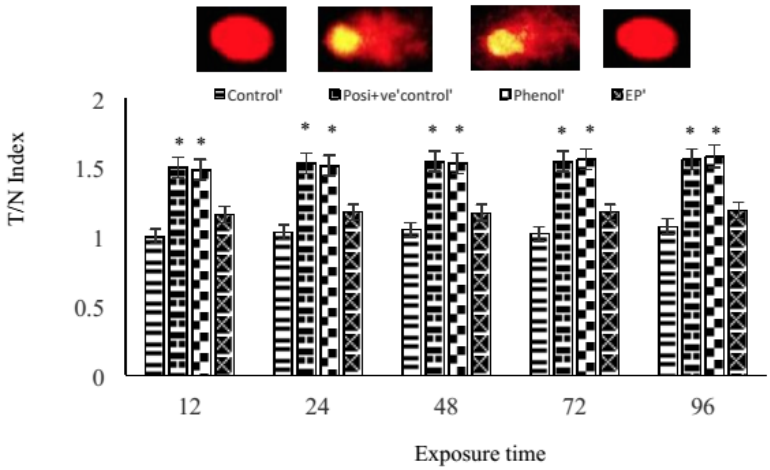
Control'
Posi+ve'control'
Phenol'
EP'
T/N Index
2
1.5
1
0.5
0
12
24
48
72
96
Exposure time

Figure 10

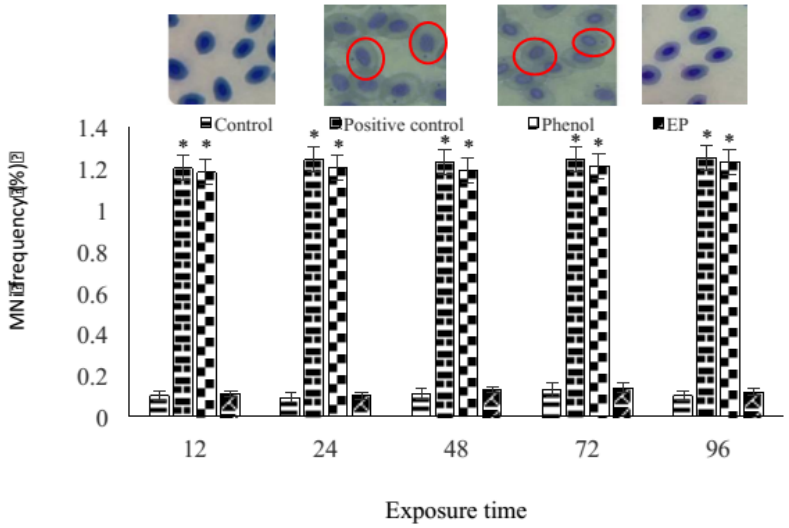
Control
Positive control
Phenol
EP
1.4
1.2
1
0.8
0.6
0.4
0.2
0
12
24
48
72
96
Exposure time

Supplementary material S1

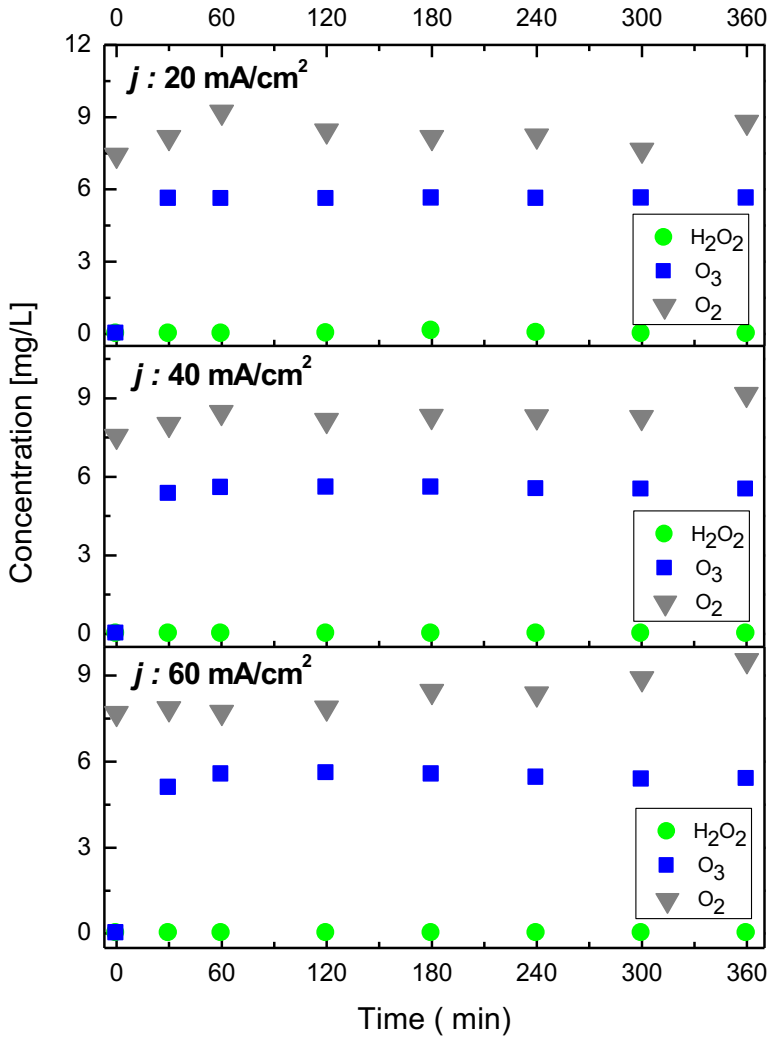

Figure S1.1. Electro-generation of oxidant species at pH 7. Reaction conditions 0.05 M Na_2SO_4 , Q_L: 4.7 L/min and T: 23°C ±2.

6. Discusión general

La primera etapa del proyecto consistió en determinar las concentraciones de las especies oxidantes (O_3, O_2 y H_2O_2) generadas *in situ* a partir del proceso de Electro-Oxidación empleando electrodos de DDB. Los experimentos fueron sin realizar la adición de contaminante, empleando agua del suministro municipal con un COT_0: 35 mg/L en un volumen de 3.5 L. El O_2 es un gas que se genera en todos los procesos electrolíticos y es comúnmente liberado a la atmósfera en la mayoría de los sistemas de reacción, sin embargo, en una columna de burbujeo de flujo paralelo descendente (CBFPD) es absorbido en el volumen de la solución tratada y por medio de una reducción de catódica es transformado a H_2O_2. Otra reacción en competencia es la formación del O_3, obtenido a partir de la electrólisis del agua. Con respecto a los experimentos, se evaluaron las siguientes condiciones de reacción: 0.05 M Na_2SO_4, j: 20, 40 y 60 mA/cm^2, empleando valores de pH 3 y 7. Las mejores condiciones de reacción se encontraron a 0.05 M Na_2SO_4, pH 3 y *j:* 60 mA/cm^2, obteniendo una remoción del 98% con respecto al COT inicial.

De la sección anterior se comprobó la eliminación de la materia orgánica disuelta en el agua del suministro municipal, por lo cual en la segunda etapa se procedió a adicionar el contaminante (fenol) a una concentración de 100mg/L para evaluar los efectos del flujo de recirculación, concentración de electrolito y pH.

En la CBFPD, se tiene un flujo mínimo y máximo de recirculación, los cuales son 4.7 y 6 L/min, respectivamente. Comparando los porcentajes de remoción de COT en ambos casos, se obtiene 75% y 55% de remoción, lo cual indica que a mayor flujo de recirculación la remoción disminuye en un 20%. Para explicar esto se procedió a calcular el número de Re y el tiempo de residencia (τ) de la solución en el volumen ocupado por los electrodos. En el primer caso se tiene un Re de 1995 y τ: 25 s, para el caso del flujo máximo se presenta un Re 2545 y τ: 19.6 s. Estos datos indican que a mayores tiempos de residencia se obtiene mayor remoción a pesar de que la turbulencia del fluido disminuye.

En cuanto a la concentración de electrolito, la bibliografía reporta que 0.05 M de sulfato de sodio es el valor más empleado. La evaluación del efecto de esta variable, sin embargo, también se realizó modificando el valor a 0.025 y 0.1 M, obteniendo una disminución del 20% y 3% de COT, con respecto al porcentaje obtenido con 0.05 M de sulfato de sodio.

Deleted: y por consecuencia disminuye

Deleted: se tiene reportado de la bibliografía

Deleted: a

Esto implica que al disminuir a 0.025 la concentración de electrolito, la cantidad de iones sulfato no es suficiente para tener una alta conductividad en la solución y adicionalmente su efecto desinfectante disminuye. Cuando se duplica la concentración de electrolito, el sistema se satura de iones sulfato los cuales actúan como secuestrantes de radicales hidroxilo, por ello no se ve reflejado en un aumento en la taza de remoción del COT inicial, contrariamente existe una disminución del porcentaje de mineralización.

Tomando en cuenta las variables anteriormente presentadas, se procedió a comparar el efecto del pH en valores de 3 y 7, nuevamente tomando en cuenta 0.05 M Na_2SO_4, pH 3 y *j:* 60 mA/cm^2. En este caso se removió un 65% de la concentración inicial a pH 7, siendo un 10% menor que a pH 3. Hasta este punto, la mineralización es parcial, por ello se procedió a cuantificar las concentraciones de los sub-productos del fenol, mediante cromatografía de líquidos de alta resolución. Efectuando este análisis, se comprueba que la concentración de fenol se disminuye en un 100% en ambos casos (pH 3 y pH 7), quedando únicamente la presencia de ácidos carboxílicos en concentraciones bajas. En la Figura 16, se presentan los mecanismos propuestos mediante los cuales se obtienen los ácidos carboxílicos como subproductos a partir de la molécula de fenol. Con respecto a pH 3 se establece que el mecanismo de degradación de fenol es por medio de la ozonación directa y para pH 7 se presenta el mecanismo de Electro-peroxonación. En ambos mecanismos se obtienen prácticamente los mismos subproductos de degradación, sin embargo a pH 7 se ven favorecidos los productos de hidroxilación, ya que se presenta una acumulación de estos al final del tratamiento, mientras que en pH 3 no existe una acumulación de compuestos, únicamente hay acumulación de ácido oxálico.

Deleted: las rutas mediante las cuales

Deleted: una concentración

La mineralización parcial del contaminante y las concentraciones de ácidos carboxílicos en el volumen de agua tratado, motivó a realizar algunas pruebas de bio-toxicidad empleando como bio-indicador a la carpa común. Se realizaron dos pruebas: micronúcleos y ensayo cometa. En ambas pruebas se examinó una muestra de agua obtenida después del tratamiento electroquímico, obteniendo como resultado la eliminación de la bio-toxicidad.

Finalmente se realizó la determinación de algunos parámetros hidrodinámicos, obtenidos a partir de la dispersión de burbujas en el interior de la columna de burbujeo, realizando las mediciones de 30 burbujas para cada caso. Los datos correspondientes a los diámetros y fórmulas matemáticas se encuentran en el Anexo 5. El diámetro de burbuja (d_B) obtenido

fue 3.6mm y la fracción volumétrica de gas (ε_G) fue 0.303 para las condiciones de reacción de pH 3, j: 60mA/cm^2 y 4.7 L/min. En tanto para pH 7, j: 60mA/cm^2 y 4.7 L/min fueron de d_B 3.5mm y ε_G 0.282**.** Con los valores obtenidos en este apartado a diferentes densidades de corriente, se comprueba que el diámetro de burbuja no es afectado por el incremento de la densidad de corriente ni por el valor de pH, únicamente la fracción volumétrica tiende a incrementar al elevar la densidad de corriente, ya que la producción de la fase gas tiene un incremento.

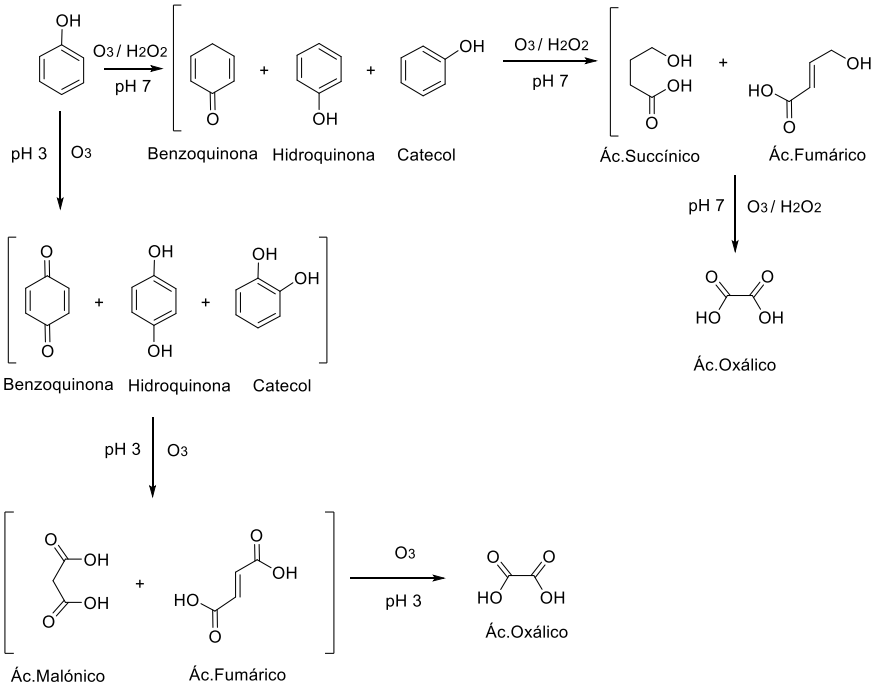

Figura 16. Mecanismos de degradación del fenol

7.Conclusiones.

La columna de burbujeo de flujo paralelo descendente permite llevar a cabo la remoción total de fenol mediante electro-oxidación y evita el desperdicio de la fase gas en porcentajes cercanos al 100%.

Las variables que principalmente afectan la velocidad y grado remoción de carbón orgánico total son tiempo de residencia, pH y concentración de electrolito. La remoción de TOC es favorecida a una concentración de electrolito de 0.05 M, a un tiempo de residencia alto y pH ácido. La mineralización del contaminante se observa a pH ácido y neutro, siendo del 75% y 65%, respectivamente, en ambos casos en un tiempo de 360 minutos. Después del tiempo de tratamiento, únicamente se encuentran presentes ácidos carboxílicos a bajas concentraciones.

En este proceso el valor de pH determina el mecanismo mediante el cual se mineraliza el fenol. A valores de pH ácido prevalece el mecanismo de ozonación directa, con respecto al pH neutro el mecanismo que se favorece es el de electro-peroxonación. Este último mecanismo favorece la generación de productos de hidroxilación.

Deleted: ,

Esta tecnología permite llevar a cabo el proceso de electro-peroxonación con generación in situ de peróxido de hidrógeno y ozono, y elimina la adición de gases, como aire u ozono, y de reactivos como peróxido de hidrógeno. En el interior de la columna es posible mantener la fase gas (oxígeno y ozono) en una dispersión de burbujas, lo cual incrementa la absorción y elimina el desperdicio de los gases producidos.

El pH también afecta la acumulación de H_2O_2, O_3 y O_2. A pH 7 la acumulación de H_2O_2 es mayor que a pH 3 y al final del tratamiento es de solo 4 mg/L, mientras que a pH 3 es de 15 mg/L. El efecto contrario se encuentra para O_3 y O_2.

Aunque el porcentaje de mineralización es menor a pH 7 que a pH 3, el proceso de electro-peroxonación en pH 7 elimina la bio-toxicidad de los subproductos de degradación, los cuales pueden ser utilizados para otras aplicaciones.

Los resultados a pH 7 sugieren que esta tecnología también puede ser aplicada para oxidaciones selectivas y no solo en la remediación de aguas.

En la evaluación de parámetros hidrodinámicos, el diámetro de las burbujas no es afectado por el cambio de pH de la solución y la densidad de corriente, puesto que la diferencia

obtenida en las mediciones realizadas en el diámetro de Sauter es de 0.1mm. Por otra parte, la fracción volumétrica de gas, tiende a incrementar con la aplicación de una densidad de corriente mayor, la cual está directamente relacionada con la generación de gas por medio de las reacciones de electrólisis secundarias.

Referencias

8.Referencias

Amado-Piña, D. *et al.* (2017) 'Synergic effect of ozonation and electrochemical methods on oxidation and toxicity reduction: Phenol degradation', *International Mexican Congress on Chemical Reaction Engineering (IMCCRE 2016)*, 198(Supplement C), pp. 82–90. doi: 10.1016/j.fuel.2016.10.117.

Armijos-Alcocer, K. G. *et al.* (2017) 'Electrochemical {Degradation} of {Nonylphenol} {Ethoxylate}-7 ({NP}7EO) {Using} a {DiaClean}® {Cell} {Equipped} with {Boron}-{Doped} {Diamond} {Electrodes} ({BDD})', *Water, Air, & Soil Pollution*, 228(8), p. 289. doi: 10.1007/s11270-017-3471-9.

Assumpção, M. H. M. T. *et al.* (2013) 'Low tungsten content of nanostructured material supported on carbon for the degradation of phenol', *Applied Catalysis B: Environmental*, 142–143, pp. 479–486. doi: 10.1016/j.apcatb.2013.05.024.

ATSDR (2008) *A. for T.S and D. R. Public health statement*.

Babuponnusami, A. and Muthukumar, K. (2012) 'Advanced oxidation of phenol: A comparison between Fenton, electro-Fenton, sono-electro-Fenton and photo-electro-Fenton processes', *Chemical Engineering Journal*, 183, pp. 1–9. doi: 10.1016/j.cej.2011.12.010.

Bader, H. and Hoigné, J. (1981) 'Determination of ozone in water by the indigo method', *Water research*, 15(4), pp. 449–456.

Bakheet, B. *et al.* (2013) 'Electro-peroxone treatment of Orange II dye wastewater', *Water Research*, 47(16), pp. 6234–6243. doi: 10.1016/j.watres.2013.07.042.

Barrera-Díaz, C. *et al.* (2014) 'Electrochemical advanced oxidation processes: an overview of the current applications to actual industrial effluents', *Journal of the Mexican Chemical Society*, 58(3), pp. 256–275.

Beltrán, F. (2004) *Ozone Reaction Kinetics for Water and Wastewater Systems*. 1a edn. New York, Estados Unidos.

Beltrán, F. J. *et al.* (2012) 'Kinetic studies on black light photocatalytic ozonation of diclofenac and sulfamethoxazole in water', *Industrial & Engineering Chemistry Research*, 51(12), pp. 4533–4544.

Brillas, E. and Huitle, C. A. M. (2011) *Synthetic diamond films: preparation, electrochemistry, characterization and applications*. John Wiley & Sons.

Brillas, E. and Martínez-Huitle, C. A. (2015a) 'Decontamination of wastewaters containing synthetic organic dyes by electrochemical methods. An updated review', *Applied Catalysis B: Environmental*, 166–167, pp. 603–643. doi: 10.1016/j.apcatb.2014.11.016.

Brillas, E. and Martínez-Huitle, C. A. (2015b) 'Decontamination of wastewaters containing synthetic organic dyes by electrochemical methods. An updated review', *Applied Catalysis B: Environmental*, 166–167, pp. 603–643. doi: 10.1016/j.apcatb.2014.11.016.

Busca, G. *et al.* (2008) 'Technologies for the removal of phenol from fluid streams: A short review of recent developments', *Journal of Hazardous Materials*, 160(2–3), pp. 265–288. doi: 10.1016/j.jhazmat.2008.03.045.

del Campo, E. *et al.* (2011) '4-{Chlorophenol} {Oxidation} {Photocatalyzed} by a {Calcined} {Mg}–{Al}–{Zn} {Layered} {Double} {Hydroxide} in a {Co}-current {Downflow} {Bubble} {Column}', *Industrial & Engineering Chemistry Research*, 50(20), pp. 11544–11552. doi: 10.1021/ie200412p.

Carrera, J. (2008) *Aguas continentales, Gestión de recursos hídricos, tratamiento y calidad del agua.* nformes CSIC, D. Barceló (coord.).

Christensen, P. A., Yonar, T. and Zakaria, K. (2013) 'The electrochemical generation of ozone: a review', *Ozone: Science & Engineering*, 35(3), pp. 149–167.

Comninellis, C. (1994) 'Electrocatalysis in the electrochemical conversion/combustion of organic pollutants for waste water treatment', *Electrochimica Acta*, 39(11–12), pp. 1857–1862. doi: 10.1016/0013-4686(94)85175-1.

Comninellis, C. and Chen, G. (2010) *Electrochemistry for the Environment*. New York, NY: Springer New York. Available at: http://www.scopus.com/inward/record.url?eid=2-s2.0-84887920143&partnerID=tZOtx3y1.

Crousier, C. *et al.* (2016) 'Urban Wastewater Treatment by Catalytic Ozonation', *Ozone: Science & Engineering*, 38(1), pp. 3–13. doi: 10.1080/01919512.2015.1113119.

Duan, X. *et al.* (2013) 'Electrochemical degradation of phenol in aqueous solution using PbO2 anode', *Journal of the Taiwan Institute of Chemical Engineers*, 44(1), pp. 95–102. doi: 10.1016/j.jtice.2012.08.009.

Eisenberg, G. (1943) 'Colorimetric determination of hydrogen peroxide', *Industrial & Engineering Chemistry Analytical Edition*. ACS Publications, 15(5), pp. 327–328.

Fischbacher, A. *et al.* (2013) 'The •OH Radical Yield in the H2O2 + O3 (Peroxone) Reaction', *Environmental Science & Technology*. American Chemical Society, 47(17), pp. 9959–9964. doi: 10.1021/es402305r.

Garcia-Segura, S. *et al.* (2016) 'Anodic oxidation, electro-{Fenton} and photoelectro-{Fenton} degradations of pyridinium- and imidazolium-based ionic liquids in waters using a {BDD}/air-diffusion cell', *Electrochimica Acta*, 198, pp. 268–279. doi: 10.1016/j.electacta.2016.03.057.

Garcia-Segura, S. and Brillas, E. (2014) 'Advances in solar photoelectro-Fenton: decolorization and mineralization of the Direct Yellow 4 diazo dye using an autonomous solar pre-pilot plant', *Electrochimica Acta*. Elsevier, 140, pp. 384–395.

Garcia-Segura, S. and Brillas, E. (2016) 'Combustion of textile monoazo, diazo and triazo dyes by solar photoelectro-Fenton: Decolorization, kinetics and degradation routes', *Applied Catalysis B: Environmental*, 181, pp. 681–691. doi: 10.1016/j.apcatb.2015.08.042.

Gomes, D. S. *et al.* (2017) 'Removal of Sulfamethoxazole and Diclofenac from water: Strategies involving O3 and H2O2', *Environmental Technology*, (just-accepted), pp. 1–42.

Gottschalk, C., Libra, J. A. and Saupe, A. (2009) *Ozonation of water and waste water: A practical guide to understanding ozone and its applications*. John Wiley & Sons.

Hoigné, J. (1998) 'Chemistry of Aqueous Ozone and Transformation of Pollutants by Ozonation and Advanced Oxidation Processes', in Hrubec, J. (ed.) *Quality and Treatment*

of Drinking Water II. Berlin, Heidelberg: Springer Berlin Heidelberg, pp. 83–141. Available at: http://dx.doi.org/10.1007/978-3-540-68089-5_5.

Hurwitz, G. *et al.* (2014) 'Degradation of phenol by synergistic chlorine-enhanced photo-assisted electrochemical oxidation', *Chemical Engineering Journal*, 240, pp. 235–243. doi: 10.1016/j.cej.2013.11.087.

Isarain-Chávez, E. *et al.* (2013) 'On-site Hydrogen Peroxide Production at Pilot Flow Plant: Application to Electro-Fenton Process', 8, pp. 3084–3094.

Johnson, P. N. and Davis, R. A. (1996) 'Diffusivity of Ozone in Water', *Journal of Chemical & Engineering Data*. American Chemical Society, 41(6), pp. 1485–1487. doi: 10.1021/je9602125.

Li, X. *et al.* (2015) 'Electro-peroxone treatment of the antidepressant venlafaxine: {Operational} parameters and mechanism', *Journal of Hazardous Materials*, 300, pp. 298–306. doi: 10.1016/j.jhazmat.2015.07.004.

Li, Y. *et al.* (2015) 'Inhibition of bromate formation during drinking water treatment by adapting ozonation to electro-peroxone process', *Chemical Engineering Journal*, 264, pp. 322–328. doi: 10.1016/j.cej.2014.11.120.

Lu, X.-X., Boyes, A. P. and Winterbottom, J. M. (1994) 'Operating and hydrodynamic characteristics of a cocurrent downflow bubble column reactor', *Chemical Engineering Science*, 49(24), pp. 5719–5733. doi: 10.1016/0009-2509(94)00264-9.

Lucas, M. S. *et al.* (2009) 'Ozonation kinetics of winery wastewater in a pilot-scale bubble column reactor', *Water research*, 43(6), pp. 1523–1532.

Marselli, B. *et al.* (2003) 'Electrogeneration of Hydroxyl Radicals on Boron-Doped Diamond Electrodes', *Journal of The Electrochemical Society*, 150(3). doi: 10.1149/1.1553790.

Mart'\inez-Huitle, C. A. *et al.* (2015) 'Single and coupled electrochemical processes and reactors for the abatement of organic water pollutants: a critical review', *Chemical reviews*. ACS Publications, 115(24), pp. 13362–13407.

Martínez-Huitle, C. A. *et al.* (2015) 'Single and Coupled Electrochemical Processes and Reactors for the Abatement of Organic Water Pollutants: A Critical Review', *Chemical Reviews*, 115(24), pp. 13362–13407. doi: 10.1021/acs.chemrev.5b00361.

Martínez-Huitle, C. A. and Brillas, E. (2009) 'Decontamination of wastewaters containing synthetic organic dyes by electrochemical methods: A general review', *Applied Catalysis B: Environmental*, 87(3–4), pp. 105–145. doi: 10.1016/j.apcatb.2008.09.017.

Michaud, P. A. *et al.* (2003) 'Electrochemical oxidation of water on synthetic boron-doped diamond thin film anodes', *Journal of Applied Electrochemistry*, 33(2), pp. 151–154. doi: 10.1023/A:1024084924058.

Mohammadi, S. *et al.* (2014) 'Phenol removal from industrial wastewaters: a short review', *Desalination and Water Treatment*, 53(8), pp. 2215–2234. doi: 10.1080/19443994.2014.883327.

Montiel, E. (2013) *Preparación y caracterización de materiales mesoporosos de óxido de*

silicio con óxidos de metal para la degradación fotocatalítica de compuestos aromáticos halogenados. UNAM.

Moreira, F. C. *et al.* (2017) 'Electrochemical advanced oxidation processes: A review on their application to synthetic and real wastewaters', *Applied Catalysis B: Environmental*, 202, pp. 217–261. doi: 10.1016/j.apcatb.2016.08.037.

Moussavi, G., khavanin, A. and Alizadeh, R. (2010) 'The integration of ozonation catalyzed with MgO nanocrystals and the biodegradation for the removal of phenol from saline wastewater', *Applied Catalysis B: Environmental*, 97(1–2), pp. 160–167. doi: 10.1016/j.apcatb.2010.03.036.

Mousset, E. *et al.* (2014) 'Treatment of synthetic soil washing solutions containing phenanthrene and cyclodextrin by electro-oxidation. Influence of anode materials on toxicity removal and biodegradability enhancement', *Applied Catalysis B: Environmental*, 160–161, pp. 666–675. doi: 10.1016/j.apcatb.2014.06.018.

Natividad, R. (2004) 'A kinetic,selectivity and hydrodynamic study of liquid-phase alkyne hydrogenation in a monolith cocurrent downflow contactor (CDC) reactor.'

Ochuma, I. J. *et al.* (2007) 'Photocatalytic oxidation of 2,4,6-trichlorophenol in water using a cocurrent downflow contactor reactor (CDCR).', *Journal of hazardous materials*, 144(3), pp. 627–633. doi: 10.1016/j.jhazmat.2007.01.086.

Olvera-Vargas, H. *et al.* (2015) 'Electro-{Oxidation} of the {Pharmaceutical} {Furosemide}: {Kinetics}, {Mechanism}, and {By}-{Products}', *Clean - Soil, Air, Water*, 43(11), pp. 1455–1463. doi: 10.1002/clen.201400656.

Özcan, A. *et al.* (2008) 'Carbon sponge as a new cathode material for the electro-Fenton process. Comparison with carbon felt cathode and application to degradation of synthetic dye Basic Blue 3 in aqueous medium.', *J. Electroanal. Chem.*, 616(1), pp. 71–78. Available at: https://hal-upec-upem.archives-ouvertes.fr/hal-00730647.

Peralta, E. *et al.* (2013) 'A comparative study on the electrochemical production of H2O2 between BDD and graphite cathodes', *Sustainable Environment Research*, (23), pp. 259–266. Available at: http://www.researchgate.net/publication/257873807_A_comparative_study_on_the_electrochemical_production_of_H2O2_between_BDD_and_graphite_cathodes.

Peralta, E. (2013) *Electrosíntesis de H2O2 en una Columna de Burbujeo de Flujo Paralelo Descendente.* Tesis Doctoral. Universidad Autónoma del Estado de México, México.

Pérez, J. F. *et al.* (2017) 'The jet aerator as oxygen supplier for the electrochemical generation of {H}2O2', *Electrochimica Acta*, 246, pp. 466–474. doi: 10.1016/j.electacta.2017.06.085.

Pérez, J. F. *et al.* (2018) 'The pressurized jet aerator: {A} new aeration system for high-performance {H}2O2 electrolyzers', *Electrochemistry Communications*, 89, pp. 19–22. doi: 10.1016/j.elecom.2018.02.012.

Pérez, T. *et al.* (2015) 'Solar photoelectro-Fenton degradation of the antibiotic metronidazole using a flow plant with a Pt/air-diffusion cell and a CPC photoreactor', *Electrochimica Acta*, 165, pp. 173–181. doi: 10.1016/j.electacta.2015.02.243.

Pimentel, M. *et al.* (2008) 'Phenol degradation by advanced electrochemical oxidation process electro-Fenton using a carbon felt cathode', *Applied Catalysis B: Environmental*, 83(1–2), pp. 140–149. doi: 10.1016/j.apcatb.2008.02.011.

Prince, J. *et al.* (2015) 'Photocatalytic degradation of phenol by semiconducting mixed oxides derived from Zn(Ga)Al layered double hydroxides', *Applied Catalysis B: Environmental*, 163(0), pp. 352–360. doi: 10.1016/j.apcatb.2014.08.019.

Quiñones, D. H. *et al.* (2015) 'Boron doped TiO2 catalysts for photocatalytic ozonation of aqueous mixtures of common pesticides: Diuron, o-phenylphenol, MCPA and terbuthylazine', *Photocatalysis: Science and Applications*, 178, pp. 74–81. doi: 10.1016/j.apcatb.2014.10.036.

Sanchez-Dominguez, M. *et al.* (no date) 'Synthesis of Zn-doped TiO2 nanoparticles by the novel oil-in-water (O/W) microemulsion method and their use for the photocatalytic degradation of phenol', *Journal of Environmental Chemical Engineering*, (0). doi: 10.1016/j.jece.2015.03.010.

Santana-Martínez, G. *et al.* (2016) 'Electro-Fenton and Electro-Fenton-like with in situ electrogeneration of H2O2 and catalyst applied to 4-chlorophenol mineralization', *Electrochimica Acta*, 195, pp. 246–256. doi: 10.1016/j.electacta.2016.02.093.

dos Santos, A. J. *et al.* (2018) 'Electrochemical advanced oxidation processes as decentralized water treatment technologies to remediate domestic washing machine effluents', *Environmental Science and Pollution Research*, 25(7), pp. 7002–7011. doi: 10.1007/s11356-017-1039-2.

Sun, H. *et al.* (2011) 'Combination of adsorption, photochemical and photocatalytic degradation of phenol solution over supported zinc oxide: Effects of support and sulphate oxidant', *Chemical Engineering Journal*, 170(1), pp. 270–277. doi: 10.1016/j.cej.2011.03.059.

Sun, S. *et al.* (2011) 'Highly efficient photocatalytic oxidation of phenol over ordered mesoporous Bi2WO6', *Applied Catalysis B: Environmental*, 106(3–4), pp. 559–564. doi: 10.1016/j.apcatb.2011.06.016.

Turkay, O., Ersoy, Z. G. and Barışçı, S. (2017) 'Review—the application of an electro-peroxone process in water and wastewater treatment', *Journal of the Electrochemical Society*, 164(6), pp. E94--E102. doi: 10.1149/2.0321706jes.

USEPA (2002) *USEPA Toxicological review Phenol 635*.

Wade Jr, L. G. (2012) 'Qu{'\i}mica Orgánica, Vol. 1, 7ªedición, 6-10 y 40-56'. Pearson Educación de México, SA de CV, México.

Wang, B. *et al.* (2015) 'Mechanism of Mn3O4-catalyzed ozonation of drilling wastewater', *Chinese Journal of Environmental Engineering*, 9(10), pp. 4811–4816. Available at: https://www.scopus.com/inward/record.uri?eid=2-s2.0-84945333245&partnerID=40&md5=1a60870677fe78e959e7bf521a28619f.

Wang, Y. *et al.* (2018) 'The electro-peroxone process for the abatement of emerging contaminants: Mechanisms, recent advances, and prospects', *Chemosphere*, 208, pp. 640–654. doi: https://doi.org/10.1016/j.chemosphere.2018.05.095.

Yang, B. *et al.* (2018) 'Effective degradation of carbamazepine using a novel electro-peroxone process involving simultaneous electrochemical generation of ozone and hydrogen peroxide', *Electrochemistry Communications*, 86, pp. 26–29. doi: 10.1016/j.elecom.2017.11.003.

Zhang, F. *et al.* (2015) 'Zinc ferrite catalysts for ozonation of aqueous organic contaminants: Phenol and bio-treated coking wastewater', *Separation and Purification Technology*, 156, pp. 625–635. doi: 10.1016/j.seppur.2015.10.058.

Anexos

9. ANEXOS

Anexo 1. Curva de calibración para la determinación del H_2O_2.

Para realizar la cuantificación del peróxido de hidrógeno electro-generado *in-situ* se procedió a elaborar una curva de calibración en un intervalo de 0 - 30 mg/L, de H_2O_2 grado estándar a 30% de pureza. Al preparar la solución a concentración conocida de 30 mg/L, se procedió a realizar diluciones a 20, 15, 10 y 5 mg/L, estas disoluciones se mezclaron con sulfato de titanio, con ello se obtuvo ácido per-titánico y se cuantificó espectrofotométricamente a λ: 408nm. A continuación, se presentan los resultados por triplicado, de la curva de calibración. Se eligió la curva con el mejor coeficiente de correlación, para calcular la concentración de H_2O_2, electro-generado.

Tabla 9. Curvas de calibración de H_2O_2

Concentración [mg/L]	Curva 1 (u.a)	Curva 2 (u.a)	Curva 3 (u.a)
0	0	0	0
5	0.075	0.085	0.09
10	0.158	0.149	0.17
15	0.248	0.225	0.25
20	0.366	0.396	0.38
30	0.51	0.534	0.54
R^2	0.9954	0.9809	0.9956

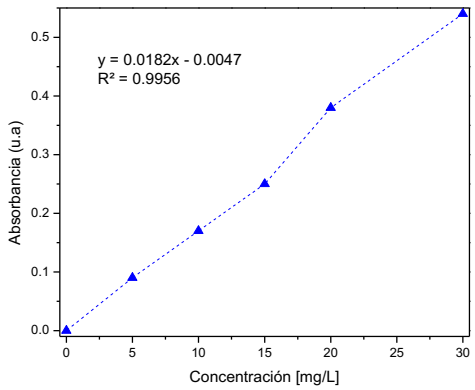

Figura 17. Regresión lineal de curva de calibración de H_2O_2

Anexo 2. Preparación de la solución de trisulfonato potásico de índigo para la determinación del O_3.

a) Preparación de la solución madre de trisulfonato potásico de índigo:
En un matraz aforado de 1 litro, agregar 500 mL de agua, agregar 1 mL de ácido fosfórico concentrado y añadir, con agitación, 770 mg de trisulfonato potásico de índigo, aforar con agua destilada. Una dilución de 1:100 exhibe una absorbancia de 0.02 cm a 600 nm. **La solución madre es estable por cuatro meses almacenada en frasco ámbar.**

b) Reactivo I. En un matraz aforado de 1 L, añadir 20 mL de solución madre, 10 g de fosfato monobásico de sodio y 7 mL de ácido fosfórico concentrado. Diluir hasta el aforo (almacenar en frasco ámbar).
Reactivo II. Proceder como el reactivo índigo, añadiendo 100 mL de solución madre en lugar de 20 mL. **Es estable por una semana almacenada en frasco ámbar.**

Procedimiento espectrofotométrico:

1)Para un intervalo de concentración de ozono de 0.01 a 0.1 mg L^{-1}. Añadir 10 mL de reactivo de índigo a 2 matraces aforados de 100 mL. Llenar uno de ellos hasta al aforo con agua efluente del tratamiento primario (blanco) y el segundo con la muestra a analizar. Medir la absorbancia de las 2 soluciones a 600 nm lo antes posible, y siempre dentro de las cuatro horas siguientes. Utilizar celdas con un tamaño de paso 1 cm de ancho.

2)Para un intervalo de concentración de ozono de 0.05 a 0.5 mg L^{-1}. Proceder como en 1), pero utilizar 10 mL de reactivo índigo II en lugar del reactivo I. Medir preferentemente la absorbancia en celdas con un tamaño de paso 1 cm de ancho.

3)Para concentraciones superiores a 0.3 mg L^{-1} se procede a utilizar el reactivo índigo II, pero utilizando un volumen menor de muestra. Diluir la mezcla resultante a un factor de disolución 1/10 con agua destilada.

Anexo 3. Curvas de calibración empleadas en las técnicas cromatográficas de UHPLC, para el fenol y subproductos.

En las secciones 4.8.1 y 4.8.2, se presentaron las condiciones de la separación cromatográfica del fenol y sus subproductos de degradación. Para esta molécula, aplican dos métodos distintos, los cuales difieren por la naturaleza de los contaminantes, entre estos tenemos dos clasificaciones: los compuestos aromáticos y los alifáticos. Para los primeros, se identificaron tres compuestos, los cuales son fenol, catecol y benzoquinona. El máximo valor de concentración se presentó a diferente longitud de onda, siendo 270, 280 y 246 nm, respectivamente.

Por otra parte, en los compuestos alifáticos se identificó la presencia de algunos ácidos carboxílicos, entre ellos el acético, fumárico, succínico, maleico, malónico, fumárico y oxálico. En estos ácidos, se presentan un pico máximo a una longitud de onda de 210 nm. Adicionalmente, se obtiene la separación de la molécula de hidroquinona a las mismas condiciones de los ácidos carboxílicos, debido a que el área de los picos es muy baja en las condiciones de separación de los compuestos aromáticos. En la siguiente tabla se presentan las condiciones de separación cromatográfica de ambos compuestos (aromáticos y alifáticos). Posteriormente se muestran las curvas de calibración obtenidas para cada subproducto de degradación, cada una se realizó por triplicado y se eligió la curva con el coeficiente de correlación más alto, para cuantificar la concentración de los subproductos de degradación obtenidos para cada una de las condiciones de reacción del proceso electroquímico de electro-oxidación.

Fenol (λ: 270 nm).

Tabla 10. Condiciones de separación cromatográfica por UHPLC.

Parámetro	Aromáticos	Alifáticos
Fase móvil	MeOH/H_2O/H_2SO_4 80 / 20 / 5mM (v/v)	H_2O/ MeOH 30mMK_2HPO_4 90 / 10 pH 2.5
Flujo de fase móvil	1 mL/min	0.5 mL/min
Columna	Ascentis® Express C-18 Supelco	Eclipse ZORBAX XDB C-18
λ	246, 270 y 280 nm	210 nm

Tabla 11. Curvas de calibración de fenol

Concentración [mg/L]	Curva 1 Área (mAU*min)	Curva 2 Área (mAU*min)	Curva 3 Área (mAU*min)
0	0	0	0
40	16.78	18.28	14.53
80	32.68	34.18	30.43
120	50.69	49.44	51.26
160	69.24	59.39	62.51
200	87.35	86.10	87.92
R^2	0.9992	0.9871	9915

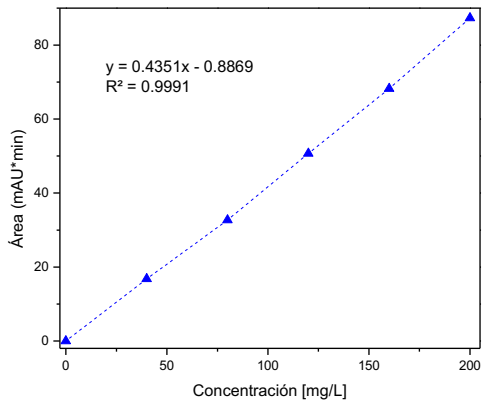

Figura 18. Regresión lineal de curva de calibración de fenol

Catecol (λ: 280 nm).

Tabla 12. Curvas de calibración de catecol

Concentración [mg/L]	Curva 1 Área (mAU*min)	Curva 2 Área (mAU*min)	Curva 3 Área (mAU*min)
0	0	0	0
40	17.14	18.25	18.80
80	32.45	33.70	34.17
120	58.43	59.68	55.96
160	81.29	78.64	78.86
200	103.98	101.33	101.56
R^2	0.9928	0.9956	0.9952

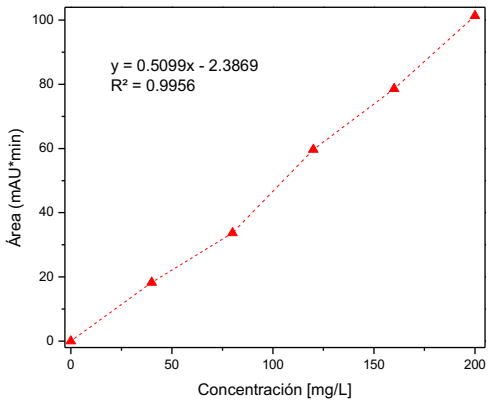

Figura 19. Regresión lineal de curva de catecol.

Benzoquinona (λ: 246 nm).

Tabla 13. Curvas de calibración de benzoquinona.

Concentración [mg/L]	Curva 1 Área (mAU*min)	Curva 2 Área (mAU*min)	Curva 3 Área (mAU*min)
0	0.00	0.00	0.00
40	48.72	53.12	50.92
80	116.87	105.67	111.27
120	164.17	168.12	166.14
160	207.12	206.85	206.99
200	236.83	245.84	241.34
R^2	0.986	0.9935	0.991

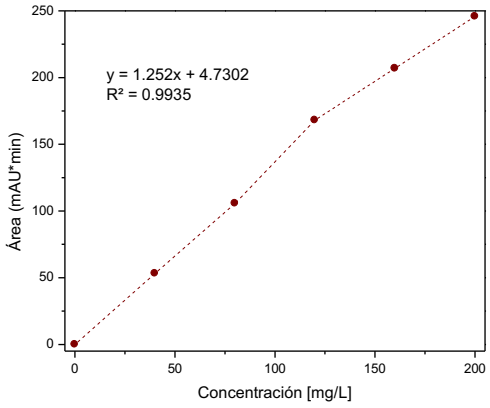

Figura 20. Regresión lineal de curva de calibración de benzoquinona.

Hidroquinona (λ: 210 nm).

Tabla 14. Curvas de calibración de hidroquinona.

Concentración [mg/L]	Curva 1 Área (mAU*min)	Curva 2 Área (mAU*min)	Curva 3 Área (mAU*min)
0	0.00	0.00	0.00
40	15.05	16.11	25.11
80	27.45	28.51	39.00
120	46.11	44.50	42.15
160	64.16	59.65	50.18
200	84.58	80.07	68.36
R^2	0.9934	0.9791	0.94

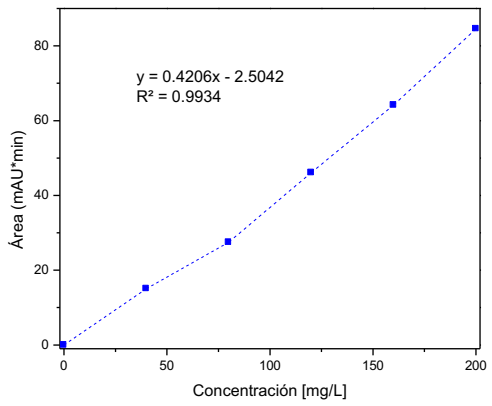

Figura 21. Regresión lineal de curva de calibración de hidroquinona.

´Ácido acético (λ: 210 nm).

Tabla 15. Curvas de calibración de ácido acético

Concentración [mg/L]	Curva 1 Área (mAU*min)	Curva 2 Área (mAU*min)	Curva 3 Área (mAU*min)
0	0.00	0.00	0.00
40	0.94	1.23	1.37
80	1.72	2.01	2.25
120	2.73	3.01	2.68
160	3.86	3.57	3.18
200	5.14	4.86	4.32
R^2	0.9928	0.912	0.9656

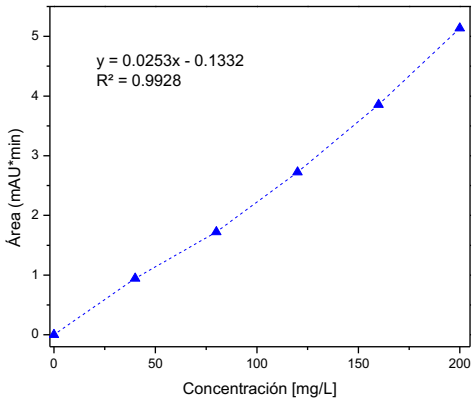

Figura 22. Regresión lineal de curva de calibración de ácido acético.

Ácido maleico (λ: 210 nm).

Tabla 16. Curvas de calibración de ácido maleico.

Concentración [mg/L]	Curva 1 Área (mAU*min)	Curva 2 Área (mAU*min)	Curva 3 Área (mAU*min)
0	0.00	0.00	0.00
40	1.53	1.78	2.12
80	4.45	5.89	4.47
120	6.54	6.43	6.66
160	7.64	9.98	9.31
200	11.49	11.43	11.55
R^2	0.9804	0.9743	0.991

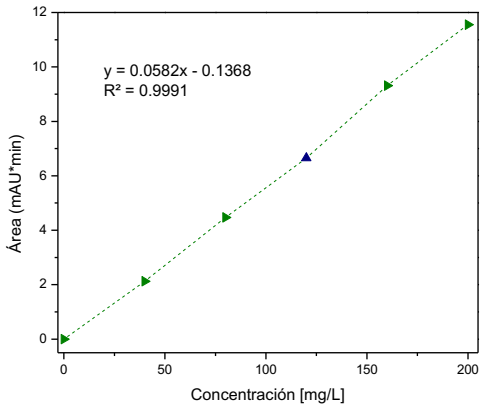

Figura 23. Regresión lineal de curva de calibración de ácido maleico

Ácido succínico (λ: 210 nm).

Tabla 17. Curvas de calibración de ácido succínico.

Concentración [mg/L]	Curva 1 Área (mAU*min)	Curva 2 Área (mAU*min)	Curva 3 Área (mAU*min)
0	0.00	0.00	0.00
40	247.86	246.71	250.28
80	455.63	395.84	428.74
120	568.10	518.03	546.06
160	662.02	652.24	660.13
200	723.13	752.78	730.96
R^2	0.9373	0.9764	0.9556

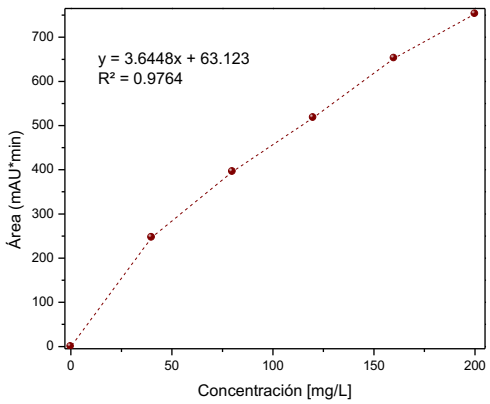

Figura 24. Regresión lineal de curva de calibración de ácido succínico.

Ácido fumárico (λ: 210 nm).

Tabla 18. Curvas de calibración de ácido fumárico.

Concentración [mg/L]	Curva 1 Área (mAU*min)	Curva 2 Área (mAU*min)	Curva 3 Área (mAU*min)
0	0.00	0.00	0.00
40	224.88	227.26	222.39
80	461.20	463.59	419.72
120	631.87	634.26	607.39
160	751.87	754.25	749.38
200	845.60	877.99	889.99
r	0.9706	0.978	0.9913

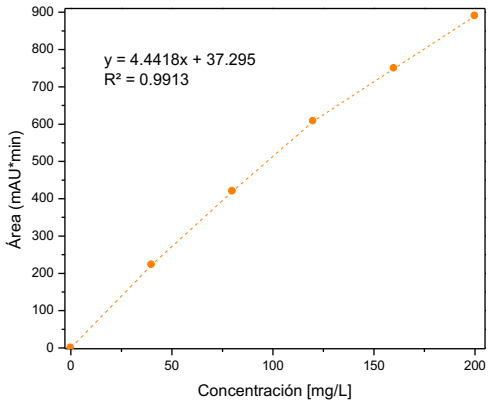

Figura 25. Regresión lineal de curva de calibración de ácido fumárico.

Anexo 4.Cálculo de los tiempos de residencia a 4.7 L/min y 6 L/min de recirculación

Volumen ocupado por los electrodos en el interior de la columna de burbujeo:

$$V = \pi r^2 L = \pi(2.5cm)^2(22.5cm) = 441.7864cm^3\left(\frac{1m^3}{(100cm)^3}\right) = 4.4178x10^{-4}m^3$$

Determinación del tiempo de residencia considerando el volumen utilizado por los electrodos a 4.7 L/min.

$$\tau = \frac{V}{Q} = \frac{4.4178x10^{-4}m^3}{\left(4.7\frac{L}{min}\right)\left(\frac{1m^3}{1000L}\right)} = 0.09399min$$

Volumen ocupado por los electrodos en el interior de la columna de burbujeo

$$V = \pi r^2 L = \pi(2.5cm)^2(100cm) = 1963.4954cm^3\left(\frac{1m^3}{(100cm)^3}\right) = 1.9634x10^{-3}m^3$$

Determinación del tiempo de residencia considerando el volumen utilizado por los electrodos a 4.7 L/min.

$$\tau = \frac{V}{Q} = \frac{1.9634x10^{-3}m^3}{\left(4.7\frac{L}{min}\right)\left(\frac{1m^3}{1000L}\right)} = 0.4177min$$

Volumen ocupado por los electrodos en el interior de la columna de burbujeo

$$V = \pi r^2 L = \pi(2.5cm)^2(22.5cm) = 441.7864cm^3\left(\frac{1m^3}{(100cm)^3}\right) = 4.4178x10^{-4}m^3$$

Determinación del tiempo de residencia considerando el volumen utilizado por los electrodos a 6 L/min.

$$\tau = \frac{V}{Q} = \frac{4.4178x10^{-4}m^3}{\left(6\frac{L}{min}\right)\left(\frac{1m^3}{1000L}\right)} = 0.07363min$$

Volumen ocupado por los electrodos en el interior de la columna de burbujeo:

$$V = \pi r^2 L = \pi(2.5cm)^2(100cm) = 1963.4954cm^3\left(\frac{1m^3}{(100cm)^3}\right) = 1.9634x10^{-3}m^3$$

Determinación del tiempo de residencia considerando el volumen utilizado por los electrodos a 6 L/min.

$$\tau = \frac{V}{Q} = \frac{1.9634x10^{-3}m^3}{\left(6\frac{L}{min}\right)\left(\frac{1m^3}{1000L}\right)} = 0.3272min$$

Anexo 5. Caracterización Hidrodinámica del reactor.

La primera parte del estudio hidrodinámico, consistió en determinar el diámetro de burbuja, en la zona de transición (de laminar a turbulento), la cual está ubicada en el volumen donde se encuentran los electrodos. Para ello se procedió a colocar una escala milimétrica en la columna de burbujeo, esto para establecer un factor de conversión, entre la imagen tomada con el apoyo de una cámara fotográfica y la medición real del diámetro de burbuja. A continuación, se presenta el factor de conversión realizado para cada una de las mediciones:

$$d = (unidades\ de\ diámetro\ digital)\left(\frac{50mm\ diámetro\ real}{312\ unidades\ de\ diámetro\ digital}\right)$$

El factor de conversión es aplicado para cada una de las mediciones digitales, realizadas mediante la cámara fotográfica Fuji 300. Esta técnica tiene un porcentaje de error, por ello se contempló realizar 30 mediciones al lecho de burbujas generado por los electrodos, para cada condición de reacción. Para minimizar el error del diámetro de burbuja medido, se utilizó el diámetro medio de Sauter, el cual se presenta en la siguiente expresión matemática:

$$\boldsymbol{d_{ms} = \frac{\sum_{i=1}^{N} d_i^3}{\sum_{i=1}^{N} d_i^2}}$$

La evaluación realizada con esta expresión contempla los 30 diámetros de burbuja medidos, con lo cual nos da una medida más exacta. Desarrollando los cálculos para la densidad de corriente de 60 mA/cm^2, pH 3 y 4.7 L/min de recirculación, se obtiene un diámetro medio de Sauter de d_{ms}=3.6 mm..

Así como en el ejemplo anterior el cálculo se repite para cada condición de reacción, de las siguientes dos tablas.

No	60 mA/cm²			40 mA/cm²			20 mA/cm²		
	pH3	pH7	sc	pH3	pH7	sc	pH3	pH7	sc
	4.7 L/min			4.7 L/min			4.7 L/min		
	Diámetro (mm)			Diámetro (mm)			Diámetro (mm)		
1	3.2	3	2.9	3.0	2.9	3.0	2.9	2.7	2.7
2	3.9	3.8	3.7	3.7	3.6	3.8	3.6	3.5	3.5
3	3.2	3.4	3.1	3.0	2.9	3.2	2.9	2.9	2.9
4	2.6	2.8	2.5	2.4	2.3	2.6	2.3	2.3	2.3
5	3.8	4	3.7	3.6	3.5	3.8	3.5	3.5	3.5
6	2.8	3	2.7	2.6	2.5	2.8	2.5	2.5	2.5
7	3.7	3.9	3.6	3.9	3.7	3.7	3.6	3.6	3.4
8	2.8	3	2.7	3.0	2.8	2.8	2.7	2.7	2.5
9	3.3	3.5	3.2	3.5	3.3	3.3	3.2	3.2	3.0
10	3.5	3.7	3.4	3.7	3.5	3.5	3.4	3.4	3.2
11	4.1	4.3	4.0	4.3	4.1	4.1	4.0	4.0	3.8
12	3.4	2.9	3.0	3.6	3.7	3.1	3.3	3.1	2.8
13	3.6	3.8	3.5	3.8	3.9	3.6	3.5	3.6	3.3
14	4.8	4.5	4.5	5.0	5.1	4.3	4.7	4.6	4.2
15	4.1	3.8	3.8	4.3	4.4	3.6	4.0	3.9	3.5
16	3.1	2.8	2.8	3.3	3.4	2.6	3.0	2.9	2.5
17	2.8	1.8	2.1	3.0	3.1	2.0	2.7	2.2	1.8
18	4.1	3.5	3.6	4.3	4.4	3.5	4.0	3.7	3.3
19	2.5	2.5	2.3	2.7	2.8	2.2	2.4	2.4	2.0
20	2.9	2.1	2.3	3.1	3.2	2.2	2.8	2.4	2.0
21	2.2	1.9	1.9	2.4	2.5	1.7	2.1	2.0	1.6
22	3.8	3.5	3.5	4.0	4.1	3.3	3.7	3.6	3.2
23	3.7	2.4	2.9	3.9	4.0	2.7	3.6	3.0	2.6
24	3.2	1.9	2.4	3.4	3.5	2.2	3.1	2.5	2.1
25	2.7	2.4	2.4	2.9	3.0	2.2	2.6	2.5	2.1
26	3.9	3.6	3.6	4.1	4.2	3.4	3.8	3.7	3.3
27	4.1	3.4	3.6	4.3	4.4	3.4	4.0	3.7	3.3
28	2.1	1.5	1.6	2.3	2.4	1.5	2.0	1.7	1.3
29	3.6	4.3	3.8	3.8	3.9	3.6	3.5	3.9	3.5
30	3.7	3.4	3.4	3.9	4.0	3.2	3.6	3.5	3.1
dms	**3.6**	**3.5**	**3.5**	**3.7**	**3.8**	**3.3**	**3.4**	**3.3**	**3.1**

Figura 25. Determinación de diámetro medio de Sauter a recirculación de 4.7 L/min

No	60 mA/cm²			40 mA/cm²			20 mA/cm²		
	pH3	pH7	sc	pH3	pH7	sc	pH3	pH7	sc
	6 L/min			6 L/min			6 L/min		
	Diámetro (mm)			Diámetro (mm)			Diámetro (mm)		
1	2.7	2.6	2.5	2.6	2.5	2.7	2.7	2.5	2.5
2	3.4	3.4	3.3	3.3	3.2	3.4	3.4	3.3	3.3
3	2.8	2.8	2.7	2.6	2.7	2.9	2.7	2.7	2.7
4	2.2	2.2	2.1	2.0	2.1	2.3	2.1	2.1	2.1
5	3.4	3.4	3.3	3.2	3.3	3.5	3.3	3.3	3.3
6	2.4	2.4	2.3	2.2	2.3	2.5	2.3	2.3	2.3
7	3.5	3.3	3.3	3.3	3.2	3.4	3.4	3.4	3.2
8	2.6	2.4	2.4	2.4	2.3	2.5	2.5	2.5	2.3
9	3.1	2.9	2.9	2.9	2.8	3.0	3.0	3.0	2.8
10	3.3	3.1	3.1	3.1	3.0	3.2	3.2	3.2	3.0
11	3.9	3.7	3.7	3.7	3.6	3.8	3.8	3.8	3.6
12	3.1	2.7	2.7	3.0	2.5	2.7	3.1	2.9	2.6
13	3.5	3.2	3.3	3.2	3.1	3.3	3.3	3.4	3.1
14	4.5	4.1	4.2	4.4	3.9	4.1	4.5	4.4	4.0
15	3.8	3.4	3.5	3.7	3.2	3.4	3.8	3.7	3.3
16	2.8	2.4	2.5	2.7	2.2	2.4	2.8	2.7	2.3
17	2.4	1.7	1.8	2.4	1.6	1.7	2.5	2.0	1.6
18	3.8	3.2	3.3	3.7	3.1	3.2	3.8	3.5	3.1
19	2.3	1.9	2.0	2.1	1.8	1.9	2.2	2.2	1.8
20	2.5	1.9	2.0	2.5	1.8	1.9	2.6	2.2	1.8
21	1.9	1.5	1.6	1.8	1.3	1.5	1.9	1.8	1.4
22	3.5	3.1	3.2	3.4	2.9	3.1	3.5	3.4	3.0
23	3.2	2.5	2.6	3.3	2.3	2.5	3.4	2.8	2.4
24	2.7	2.0	2.1	2.8	1.8	2.0	2.9	2.3	1.9
25	2.4	2.0	2.1	2.3	1.8	2.0	2.4	2.3	1.9
26	3.6	3.2	3.3	3.5	3.0	3.2	3.6	3.5	3.1
27	3.7	3.2	3.3	3.7	3.0	3.2	3.8	3.5	3.1
28	1.8	1.2	1.3	1.7	1.1	1.2	1.8	1.5	1.1
29	3.6	3.4	3.5	3.2	3.2	3.4	3.3	3.7	3.3
30	3.4	3.0	3.1	3.3	2.8	3.2	3.4	3.3	2.9
dms	3.4	3.2	3.2	3.3	3.1	3.2	3.2	3.1	2.9

Figura 26. . Determinación de diámetro medio de Sauter a recirculación de 6 L/min

pH	d_{bms} (mm)	j (mA/cm^2)	ε_G
3	3.6 ± 2	20	0.123
		40	0.245
		60	0.303
7	3.5 ± 3	20	0.16
		40	0.26
		60	0.282

Tabla 19. Parámetros hidrodinámicos

Anexo 6. Determinación del coeficiente de transferencia de masa a pH 7 y 60mA/cm^2

Para realizar la determinación del coeficiente de transferencia de masa, se efectuó con base a la teoría de película, la cual aplica para los fenómenos de transferencia de masa entre líquidos y gases. La expresión resultante del balance de materia realizado en sistemas de tipo no estacionario, se presenta a continuación (Beltrán, 2004):

$$\frac{dC_{O_3}}{dt} = k_L a\left(C^* - C_{O_3}\right)$$

Integrando

$$In\left|\frac{C^*}{C^* - C_{O_3}}\right| = k_L at$$

Graficando los datos de generación de ozono a pH7, se obtiene el siguiente coeficiente:

$k_La = 0.0029 min^{-1}$

Modelo, considerando la transferencia de masa y reactividad del ozono (Beltran, 2004):

$$\frac{dC_{O_3}}{dt} = k_L a\left(C^* - C_{O_3}\right) - k_1 C_{O_3}$$

Asumiendo estado estacionario y el valor de $k_La=0.0029min^{-1}$

$$\frac{dC_{O_3}}{dt} = k_L a\left(C^* - C_{O_3}\right) - k_1 C_{O_3} \approx 0 \qquad k_L a\left(C^* - C_{O_3}\right) = k_1 C_{O_3}$$

Si C_{O3} =4.7127 mg/L y C^*=6 mg/L

$$k_1 = \frac{k_L a\left(C^* - C_{O_3}\right)}{C_{O_3}} = \frac{0.0029/min\left(6\frac{mg}{L} - 4.7127\frac{mg}{L}\right)}{4.7127\frac{mg}{L}} = 7.9215x10^{-4} min^{-1}$$

Cálculo de área interfacial gas-líquido por unidad de volumen

$$a = \frac{6\varepsilon_g}{d_{ms}} = \frac{6(0.2828)}{3.5x10^{-3}m} = 484.8m^{-1}$$

Cálculo de coeficiente de transferencia de masa k_L

$$k_L = \frac{k_L a}{a} = \frac{0.0029 min^{-1}}{484.8 m^{-1}} = 5.9818x10^{-6}\frac{m}{min}$$

Cálculo del número de Hatta

$$Ha_1 = \frac{\sqrt{k_1 D_{O_3}}}{k_L}$$

Do_3=1.8x10^{-9} m^2/s (Johnson and Davis, 1996)

$$Ha_1 = \frac{\sqrt{(7.9215x10^{-4} min^{-1})\left(1.8x10^{-9}\frac{m^2}{s}\right)\left(\frac{60s}{1min}\right)}}{5.9818x10^{-6}\frac{m}{min}} = 1.54$$

Segunda etapa de ozonación

Si C_{O3} =5.62196 mg/L y C^*=6 mg/L

$$k_1 = \frac{k_L a(C^* - C_{O_3})}{C_{O_3}} = \frac{0.0029/min\left(6\frac{mg}{L} - 5.62196\frac{mg}{L}\right)}{5.62196\frac{mg}{L}} = 1.95x10^{-4} min^{-1}$$

Cálculo de área interfacial gas-líquido por unidad de volumen

$$a = \frac{6\varepsilon_g}{d_{ms}} = \frac{6(0.2828)}{3.5x10^{-3}m} = 484.8m^{-1}$$

Cálculo de coeficiente de transferencia de masa k_L

$$k_L = \frac{k_L a}{a} = \frac{0.0029 min^{-1}}{484.8 m^{-1}} = 5.9818x10^{-6}\frac{m}{min}$$

Cálculo del número de Hatta

$$Ha_1 = \frac{\sqrt{k_1 D_{O_3}}}{k_L}$$

Do_3=1.8x10^{-9} m^2/s (Johnson and Davis, 1996)

$$Ha_1 = \frac{\sqrt{(1.95x10^{-4} min^{-1})\left(1.8x10^{-9}\frac{m^2}{s}\right)\left(\frac{60s}{1min}\right)}}{5.9818x10^{-6}\frac{m}{min}} = 0.767$$

Disociación del fenol

$$\propto = \frac{1}{1+10^{pk-pH}} = \frac{1}{1+10^{10-7}} = 9.99x10^{-4}$$

Cálculo de número de Re a flujo de recirculación de 4.7 L/min

$$Q_L = vA \qquad v = \frac{Q_L}{A} = \frac{(4.7L/min)\left(\frac{1m^3}{1000L}\right)\left(\frac{1min}{60s}\right)}{\pi(2.5cm)^2} = 0.039896\frac{m}{s}$$

$$Re = \frac{\rho v D}{\eta} = \frac{\left(1090\frac{kg}{m.s}\right)\left(0.039896\frac{m}{s}\right)(5x10^{-2}m)}{1015\frac{kg}{m.s}} = 1995$$

Cálculo de número de Re a flujo de recirculación de 6.0 L/min

$$Q_L = vA \qquad v = \frac{Q_L}{A} = \frac{(6\ \mathrm{L/min})\left(\frac{1\mathrm{m}^3}{1000\mathrm{L}}\right)\left(\frac{1\mathrm{min}}{60\mathrm{s}}\right)}{\pi(2.5\mathrm{cm})^2} = 5.09x10^{-5}\frac{m}{s}$$

$$Re = \frac{\rho v D}{\eta} = \frac{\left(1090\frac{kg}{m.s}\right)\left(5.09x10^{-5}\frac{m}{s}\right)(5x10^{-2}m)}{1015\frac{kg}{m.s}} = 2545$$

**Datos de densidad, viscosidad y temperatura, tomados con respecto a una temperatura de 23°C. (Geankoplis, 2013)

Anexo 7. Eficiencia de corriente, consumo energético y remoción de COT

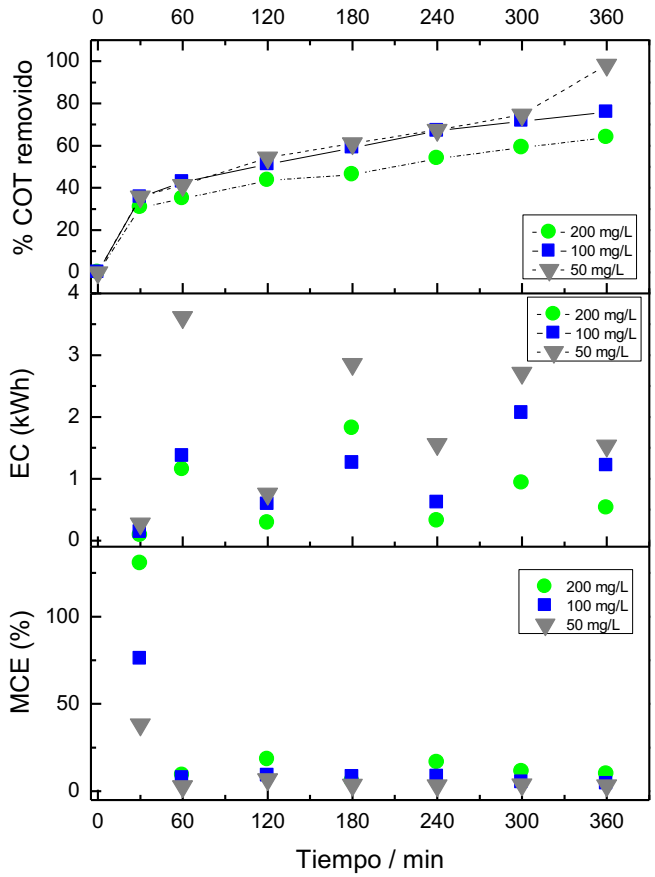

Figura 27. Consumo energético, eficiencia y remoción de COT. Condiciones de reacción J:60 mA/cm^2, 0.05 M [Na_2SO_4], pH 3, R: 4.7 L/min and T: 23°C ±2.

Anexo 8. Artículo publicado

Electrochimica Acta 195 (2016) 246–256

Contents lists available at ScienceDirect

Electrochimica Acta

journal homepage: www.elsevier.com/locate/electacta

Electro-Fenton and Electro-Fenton-like with *in situ* electrogeneration of H_2O_2 and catalyst applied to 4-chlorophenol mineralization

Germán Santana-Martínez[a], Gabriela Roa-Morales[a,*], Eduardo Martin del Campo[b], Rubí Romero[a], Bernardo A. Frontana-Uribe[a,c], Reyna Natividad[a,*]

[a] Centro Conjunto de Investigación en Química Sustentable, UAEM-UNAM. km 14.5 carretera Toluca-Atlacomulco, 50200 Toluca, Estado de México, Mexico
[b] Facultad de Química, Universidad Autónoma del Estado de México, Paseo Colon esquina Paseo Tollocan, Toluca, Estado de México, Mexico[c] Permanent Position at Instituto de Química UNAM, Mexico
[c] Permanent Position at Instituto de Química UNAM, Mexico

ARTICLE INFO

Article history:
Received 28 December 2015
Received in revised form 5 February 2016
Accepted 15 February 2016
Available online 24 February 2016

Keywords:
electro-oxidation
electrochemical reactor
copper
iron
graphite electrodes

ABSTRACT

The in situ generation of H_2O_2 and its dissociation catalyst were conducted in an undivided electrochemical cell with two set of electrodes (graphite for the former and Fe or Cu for the latter) energized by two different power sources. This arrangement allowed to conduct Electro-Fenton and Electro-Fenton like processes with less addition of chemicals than the conventional chemical process. 4-Chlorophenol was elected as model molecule. The studied variables were catalyst type (iron or copper), current density, oxygen flowrate, number and length of current pulses. It was concluded that Cu is a better catalyst for H_2O_2 dissociation. Within the studied conditions, a maximum of 70% removal of TOC was attained by the Electro-Fenton-Like process. At the same conditions, only a 45% of TOC removal was achieved by Electro-Fenton. It was also concluded that unlike Cu, Fe should be added only at the beginning of the process since its later addition is rather detrimental due mainly to an accelerated $^{\bullet}OH$ consumption by excess of metallic ions.

1. Introduction

To remove persistent organic pollutants, the application of advanced oxidation processes (AOPs) has emerged as one excellent alternative. When the AOPs are combined with electrochemistry, these processes are called Electrochemical Advanced Oxidation Processes (EAOPs). These technologies are based on the electro-generation of hydroxyl radicals ($E°$ ($^{\bullet}OH/H_2O$) = 2.8 V/SHE) and the main advantage over other AOPs is the use of a clean reagent, i.e. electron. EAOPs can be efficiently applied to contaminants solutions with a chemical oxygen demand in the range of 0.1–100 g/L [1]. Electro-Fenton (EF) is an EAOP and unlike the typical Fenton process where the hydrogen peroxide is added, in the EF process the hydrogen peroxide is electrogenerated *in situ* by the reduction of oxygen at the cathode (reaction (1)). Then the oxidant species (hydroxyl radicals) are produced by the well known Fenton reaction where the H_2O_2 decomposition is catalyzed by Fe^{2+} ions (reaction (2)). In the EF process, the regeneration of the catalytic species (Fe^{2+} ions) is expected to occur via reaction (3). This process has been successfully applied to mineralize persistent organic pollutants [2].

$$O_2 + 2H^+ + 2e^- \rightarrow H_2O_2 \quad (1)$$

$$Fe^{2+} + H_2O_2 \rightarrow Fe^{3+} + {}^{\bullet}OH + OH^- \quad (2)$$

$$Fe^{3+} + e^- \rightarrow Fe^{2+} \quad (3)$$

The H_2O_2 decomposition via reaction (2) can also be catalyzed by other transition metals rather than with only the redox couple Fe^{3+}/Fe^{2+} ($E° = 0.77$ V/SHE) [3]. If a transition metal other than Fe is used to catalyze reaction (2), this is called Fenton-like reaction and can be represented as follows,

$$M^{n+} + H_2O_2 \rightarrow M^{(n+1)+} + {}^{\bullet}OH + OH^- \quad (4)$$

In a similar manner, if the H_2O_2 is electrogenerated *in situ* the process is known as Electro-Fenton-Like. In this sense, different metals have been tested: Ag^+, Co^{2+}, Fe^{3+} and Cu^{2+} and the last two are the most investigated in Fenton-Like reaction systems due to their removal efficiency [3–6].

* Corresponding authors.
E-mail addresses: groam@uaemex.mx (G. Roa-Morales), reynanr@gmail.com (R. Natividad).

http://dx.doi.org/10.1016/j.electacta.2016.02.093
0013-4686/

Due to their high efficiency in the *in situ* electrogeneration of H_2O_2, the carbonaceous materials have been most widely used for it, some examples are carbon sponge [7], graphite [8], oxygen diffuser cathode [9], carbon PTFE [10] and carbon felt [11]. With respect to the anode material, the Boron-Doped Diamond (BDD) is the preferred one [9–13]. In the last decade, however, some works using graphite electrodes as anode and cathode have also been reported [8,14–17]. Unlike electrochemical cells with BDD electrodes, using both graphite electrodes (anode and cathode) reduces the cost of the electrochemical system, on one side by the price of the electrodes and on the other side by the relative low applied current density [18].

Generally, in the Electro-Fenton process, the catalyst (Fe^{2+} ions) of the H_2O_2 dissociation is obtained from an iron salt, the most common one is $FeSO_4{\cdot}7H_2O$ [3,6,8,10,12,17,19–23]. In this work, however, not only the hydrogen peroxide is being generated *in situ* with graphite electrodes but also the catalyst is being electrogenerated by adding another pair of electrodes, metallic though. This is expected to exert a better control on the $[H_2O_2]/M^{n+}$ ratio, to a cleaner addition of catalyst, to make metal ions more available and to reduce the amount of added reagents. Hence, the aim of this work was to assess this proposal and to do so, the mineralization of 4-chlorophenol was elected. This study also aimed to compare the efficiency on 4-chlorophenol oxidation by Electro-Fenton and Electro-Fenton-Like. For this purpose, the catalyst was dosed to the system by current pulses at iron or copper electrodes, accordingly. In this context, it is noteworthy that the addition of Fe^{2+} ions from a Fe sacrificial anode by continuously applying direct current and not by pulses, has been previously reported [24]. Such an arrangement, however, does not allow to polarize electrodes with different current densities nor during different periods of time and therefore peroxicoagulation is favored. It is not of the authors knowledge that neither the use of two pairs of electrodes polarized at different conditions nor the efficiency of adding M^{n+} ions by this procedure has been assessed.

4-Chlorophenol was elected as model molecule to assess the efficiency of the proposed cell since chlorophenols have been classified as persistent organic pollutants (POPs) due to their high toxicity and low biodegradability [25]. Some environmental organizations like the US EPA and European Directive 2013/39/UE have been included them in their list of priority toxic compounds. These pollutants are the most common synthetic phenols and they are widely used as intermediate substances in the synthesis of herbicides, disinfectant dyes, pharmaceuticals and phenolic resins [26]. In addition, they are also generated in wood pulp and paper bleaching, incineration of solid residues and in the drinking water disinfection are formed as by-products. Due to the risks to human health, the limiting permissible concentration of chlorophenols in drinking water should not excess 10 μg/L.

2. Materials and Methods

2.1. Chemicals

The standard of 4-Chlorophenol (purity 99%) was reagent grade supplied by Sigma-Aldrich. Sodium sulphate (Na_2SO_4) reagent grade was purchased from Reasol and used to prepare the electrolyte solution. For pH adjustment, NaOH and H_2SO_4 [1M] solutions were employed. These reagents were supplied by Fermont and Sigma–Aldrich, respectively. The solvents (methanol and acetonitrile) for chromatographic analysis to prepare the mobile phase were HPLC grade and purchased from Sigma–Aldrich. All reagents were used without further purification.

2.2. 4-Chlorophenol degradation experiments

The experimentation was performed in one undivided cylindrical electrochemical cell with a volume of 1 L. The experimental set-up is depicted in Fig. 1. In this electrochemical cell two sets of electrodes were placed at each experiment. One set of electrodes (graphite) was used to in-situ electro-generate the H_2O_2 [18] and the other set (Fe or Cu) to dose the catalyst. Therefore, one power supply was used for each set of electrodes. This arrangement allowed to apply different current densities to each set of electrodes and to control the electrolysis time with each set of electrodes. Two processes were assessed, Electro-Fenton and Electro-Fenton-Like. For the Electro-Fenton process, the electrochemical cell was constituted by one pair of electrodes of graphite and the other one was of iron. Both of them had a 50 cm^2 area. To perform the Electro-Fenton-Like process, copper electrodes (50 cm^2) were used instead of iron electrodes. For controlling the current density in the graphite electrodes at 4 mA/cm^2, a power supply EXTECH 1683 was used. In a similar manner for the iron electrodes (or copper electrodes in the case of Electro-Fenton-Like process) an EPSCO power supply was used. It is worth noticing that current was applied continuously only to the graphite electrodes while current was applied only during 5 minutes to the metallic electrodes (Fe or Cu) at the beginning of each experiment. Therefore and as aforementioned, having two power supplies allows not only to apply different current densities to each pair of

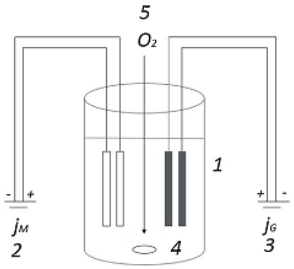

Fig. 1. Graphical set up. (1) Undivided electrochemical cell (2) Power supply number one connected to metallic electrodes (3) Power supply number two connected to graphite electrodes (4) Stirrer (5) Oxygen feed.

electrodes but also to control the period of time during which current is applied to them. The experiments were carried out by triplicate and the results show the average and the standard deviation of the determinations.

Oxygen was fed through a diffuser placed at the bottom part of the electrochemical reactor (see Fig. 1). This variable was controlled by a flow-meter in the range of 0–200 mL/min. To promote convection a stirrer was placed in the cell at a constant speed of 600 rpm.

At all experiments, the reaction volume was 0.850 L of 0.05 M Na_2SO_4 and 100 mg/L 4-Chlorophenol solution. The reaction temperature was kept constant (18 °C ± 2). In order to improve the production of hydroxyl radicals, prior treatment the initial pH of the solution was adjusted to 3.0 by adding H_2SO_4 [1M]. This pH value has been reported in other publications as optimal value to produce H_2O_2 *in situ* [3,18,27–30].

The studied variables were catalyst type for hydrogen peroxide dissociation, current density, oxygen flowrate, current pulse length and number of current pulses applied to the metallic electrodes. The response variable was mainly the Total Organic Carbon (TOC). Concentration of 4-chlorophenol was determined by HPLC only at the best conditions with each catalyst. Two divalent ions, iron and copper, were assessed as hydrogen peroxide dissociation catalysts. These ions were in situ generated by applying current pulses to a pair of electrodes of the corresponding metal. Current density and oxygen flow were only studied when using iron electrodes. The former was evaluated in the range of 10–40 mA/cm^2 and the latter between 0 and 180 mL/min. To study the effect of pulse length, during treatment current density was kept constant at 4 mA/cm^2 at graphite electrodes. The other power supply that controlled current density at iron and copper electrodes was used only at the process beginning when one pulse was applied during 0, 2.5, 5, 7 and 10 minutes and then this power supply was turned off. Once the best current pulse length was established, this was employed to study the effect of number of current pulses per experiment. To do so, 1, 2 or 4 pulses of 5 minutes length each were applied during an experiment. At all experiments, one current pulse with a length of 5 minutes was applied to the Fe or Cu electrodes at the beginning of reaction. When 2 or 4 current pulses were applied, these were spaced 30 minutes.

2.3. Analytical procedures

The pH was monitored by a Fischer Scientific TB-150 pH-meter. Total Organic Carbon (TOC) values at different reaction times were established with a Shimadzu TOC-L analyzer. From the mineralization data the Mineralization Current Efficiency (*MCE*) percentage was estimated by the following equation [28],

$$MCE(\%) = \frac{nFV_s\Delta(TOC)_{EXP}}{4.32x10^7 mIt}100 \quad (5)$$

Where $\boldsymbol{F}$ is the Faraday constant (96487C*mol^{-1}), $\boldsymbol{V_S}$ is the solution volume in liters (L), $\boldsymbol{\Delta\ (TOC)_{EXP}}$ is the experimental TOC decay, 4.32×10^7 is a conversion factor to homogenize units (=3600s h^{-1} × 12,000 mg carbon mol^{-1}), $\boldsymbol{m}$ is the number of carbon atoms in the 4-Chlorophenol molecule (6 atoms), $\boldsymbol{I}$ is the applied current (Amperes) and $\boldsymbol{t}$ is treatment time (h). Finally, $\boldsymbol{n}$ is the number of consumed electrons if assuming total 4-chlorophenol mineralization according to the following reaction,

$$C_6H_5OCl + 11H_2O \rightarrow 6CO_2 + Cl^- + 27H^+ + 26e^- \quad (6)$$

The Energy Consumption per unit of TOC was estimated by equation (7), where E_{cell} is the voltage applied to cell and I is the constant current intensity in Amperes [28],

$$EC\left(kWh(gTOC)^{-1}\right) = \frac{E_{cell}It}{V_s\Delta(TOC)_{EXP}} \quad (7)$$

At the best mineralization conditions (EFL with 4 pulses), the 4-Chlorophenol and the intermediates concentration was established by high performance liquid chromatography (HPLC). This was conducted in a chromatograph equipped with a UV–vis detector series Waters 2487 Dual λ, using Waters 1515 Isocratic Pump. Data analysis was performed using Breeze 2 software. Separation was isocratically achieved at 25 °C. The injection volume was 20 μL. To separate and identify the aromatic compounds by HPLC, the mobile phase consisted of methanol-water (80:20 v/v and 5 mM of H_2SO_4) and was pumped at a flow rate of 1.0 mL/min. The quantification wavelength was set at 280 nm. The employed column was Ascentis® Express C-18 (Supelco), 3.0 cm in length and 4.6 mm in diameter. For the identification of carboxylic acids and hydroquinone by HPLC, the mobile phase consisted of water: acetonitrile: phosphoric acid (89.9:10:0.1 v/v) and was pumped at a flow rate of 0.6 mL·min^{-1}.

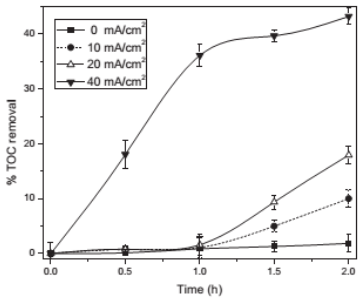

Fig. 2. Effect of current density at iron electrodes on TOC removal. Reaction conditions: 1 current pulse during 5 minutes at iron electrodes at t = 0. Current density at graphite electrodes *j*: 4 mA/cm^2. Oxygen flowrate = 100 mL/min, stirring speed 600 rpm, [Na_2SO_4] = 0.05 M and pH = 3.

The injection volume was 20 μL. The identification wavelength was set at 210 nm. A reverse phase column was employed (Eclipse XDB C-18, 15.0 cm in length and 4.6 mm in diameter, Agilent).

Chlorine ions concentration was determined by Mohr method during the experiment conducted by EFL with 4 pulses [31].

3. Results and discussion

3.1. Effect of current density

The effect of this variable on 4-chlorophenol (4-CP) mineralization was only studied under Electro-Fenton conditions. This variable was studied in the range of 10–40 mA/cm^2 and only when using iron electrodes. On the other hand, current density in the graphite electrodes was kept constant at 4 mA/cm^2, so that the electro-generated H_2O_2 was presumably the same at all experiments. This value was taken from previous studies [18]. The other reaction conditions were kept constant. The results are shown in Fig. 2. It can be observed that at low current densities the TOC removal is minimal (only 9%) at 10 mA/cm^2. When current density was increased to 20 mA/cm^2 and 40 mA/cm^2, TOC removal values of 17% and 44% were obtained, respectively.

The increase of TOC removal with current density can be related to the chemical dissolution of Fe (reaction (8)) which was calculated by Faraday's law and the cell volume obtaining the following concentrations: 0.91, 1.83 and 3.66 mM, at current densities of 10, 20 and 40 mA/cm^2, accordingly.

$$Fe \rightarrow Fe^{2+} + 2e^- \quad (8)$$

In Fenton's reaction (2), the Fe^{2+} ions promote H_2O_2 decomposition and this increases the production of hydroxyl radicals. However, during the first hour of treatment, it can be observed in Fig. 2 that with current densities equal or lower than 20 mA/cm^2, there is not mineralization of 4-chlorophenol. This suggests that the amount of hydroxyl and hydroperoxyl radicals produced is not enough to fully oxidize the 4-chlorophenol molecule. Also, it should be bear on mind that the produced oxidant species are not selective and are involved in other reactions rather than only in the organic molecules oxidation. These reactions involve the conversion of oxidant radicals again to H_2O_2 (reactions (9) and (12)), the conversion of a strong radical oxidant into a radical will less oxidant power (reaction (11)). In addition, hydrogen peroxide may also be converted to hydroperoxyl radical instead of hydroxyl radical (reaction (10)) [32,33],

$$^{\bullet}OH + {}^{\bullet}OH \rightarrow H_2O_2 \quad (9)$$

$$H_2O_2 \rightarrow HO_2^{\bullet} + H^+ + 1e^- \quad (10)$$

$$H_2O_2 + {}^{\bullet}OH \rightarrow H_2O + HO_2^{\bullet} \quad (11)$$

$$HO_2^{\bullet} + HO_2^{\bullet} \rightarrow H_2O_2 + O_2 \quad (12)$$

Reactions (10) and (11) are expected to reduce the treatment efficiency not only because a less oxidant radical is produced but also because to do so a highly oxidant radical is consumed via reaction (11). This kind of reactions have been reported in boron doped diamond and platinum anodes [10]. At this stage the possibility that these reactions may also occur in graphite anodes cannot be ruled out.

In addition, hydroxyl radicals may not only be consumed in the aforesaid reactions but also by reaction (13). Besides the hydroxyl radicals consumption, this reaction is also detrimental because reduces the amount of available Fe^{2+} ion to catalyze hydrogen peroxide dissociation [32,33]. Thus, from the results in Fig. 2, it can be inferred that at current densities <20 mA/cm^2 applied at the iron electrodes, the amount of catalyst (Fe^{2+}) is not adequate to catalyze enough the H_2O_2 decomposition and produce the necessary amount of hydroxyl radicals.

$$Fe^{2+} + {}^{\bullet}OH \rightarrow Fe^{3+} + OH^- \quad (13)$$

When current density applied to iron electrodes is increased to 40 mA/cm^2, the catalyst concentration is adequate to promote H_2O_2 decomposition and consequently there is a greater amount of hydroxyl radicals to attack the organic compounds, either aromatic or saturated, and this can be represented by reactions (14) and (15), respectively [32,33],

$$ArH + {}^{\bullet}OH \rightarrow ArHOH^{\bullet} \quad (14)$$

$$RH + {}^{\bullet}OH \rightarrow R^{\bullet} + H_2O \quad (15)$$

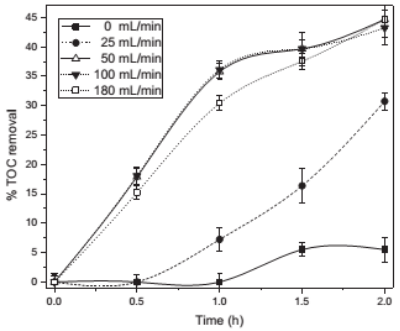

Fig. 3. Effect of oxygen flowrate on TOC removal. Reaction conditions: H_2O_2 dissociation catalyst: iron, number of current pulses at iron electrodes = 1 (applied at the experiment beginning, pulse length = 5 minutes, current density at graphite electrodes *j*: 4 mA/cm^2, at iron electrodes *j*: 40 mA/cm^2, stirring speed = 600 rpm, [Na_2SO_4] = 0.05 M and pH = 3.

Therefore, it was concluded that among the studied values and in terms of Fe^{2+} generation, $j = 40\ mA/cm^2$ was the best current density and therefore was selected to conduct the rest of experiments. It was observed that higher current densities (more than $40\ mA/cm^2$) generate excessive gas (O_2) at counter electrode and provoke strong change in solution pH.

3.2. Oxygen flow-rate

Oxygen flow is required to electro-generate H_2O_2 *in situ* and this variable was also studied only under Electro-Fenton conditions. This is mainly due to the fact that the dissolved oxygen in water is rather low. For this purpose, the following volumetric oxygen flowrates were assessed: 0, 25, 50, 100 and 180 mL/min. The effect of this variable on TOC removal profiles is shown in Fig. 3. It can be observed that after 2 hours of treatment, the results of TOC removal were 5, 30, 45, 44 and 45%, for oxygen flowrates of 0, 25, 50, 100 and 180 mL/min, respectively. As expected, TOC removal increases with oxygen flowrate since H_2O_2 production is also expected to increase and so hydroxyl radicals. However, flowrates higher than 50 mL/min do not seem to significantly affect neither rate nor maximum TOC removal. From this, it can be inferred that accumulated H_2O_2 after 2 hours is practically the same. This can be ascribed to the cathodic reduction reaction of oxygen (see reaction (1)) being the controlling step in the production of H_2O_2. Because of the aforesaid, 50 mL/min was elected to conduct the rest of the experimental work.

3.3. Effect of current pulse length applied to metallic electrodes

Taking into account the reaction conditions previously set and the best values of the variables evaluated in sections 3.1 and 3.2 (current density and oxygen flow rate), the following variable to evaluate was the length of current pulse applied to metallic electrodes, which had remained constant in previous experiments. The effect of this variable on TOC removal was assessed during two processes, Electro-Fenton and Electro-Fenton-Like, using as a second pair of electrodes iron and copper, respectively. Regarding H_2O_2 electrogeneration, a current density of $4\ mA/cm^2$ was kept constant at the graphite electrodes during the whole experiment. The second power supply, connected to the metallic electrodes, however, was turned on only during a certain period of time (0.5, 2.5, 5, 7.5 or 10 minutes) at the beginning of every experiment. This period of time being the current pulse length. This variable was used to modify the initial concentration of H_2O_2 dissociation catalyst (Fe or Cu). To calculate the concentration of electro-generated catalyst (iron or copper) at different times, once more the Faraday's law and the cell volume were employed. Table 1 summarizes the concentration of catalyst electrochemically generated at different current pulse lengths applied to the metallic electrodes. It is evident that the amount of catalyst increases when the time of electrolysis is greater, for this reason it is important to determine the optimal amount of catalyst in both processes.

Table 1
Concentration of electro-generated catalyst.

Pulse length (min)	Fe or Cu Concentration (mM)
0.5	0.37
2.5	1.83
5	3.66
7.5	5.49
10	7.32

3.3.1. Effect of current pulse length on 4-chlorophenol mineralization by Electro-fenton

As in previous experiments, the effect of this variable on TOC removal was tested by electrolyzing a 0.85 L 100 mg/L 4-Chlorophenol solution. In order to establish the optimal catalyst concentrations, 5 current pulse lengths were evaluated (see Table 1). The effect of this variable on TOC removal profiles is shown in Fig. 4. It can be observed that after 2 hours of treatment, 32, 38, 45, 34 y 34% of TOC removal is achieved for pulses lengths of 0.5, 2.5, 5, 7.5 and 10 minutes, respectively. By a statistical analysis, it can be concluded that the values obtained with 2.5 and 5 minutes pulse lengths are the only ones that lead to values with significant differences with respect to the others. From Fig. 4, it is evident that with a pulse length of 0.5 minutes, the initial mineralization rate is the lowest. To improve the TOC removal the current pulse length should be increased in order to produce more hydroxyl radicals. For that reason the length of the applied current pulse was increased to 2.5 and 5 minutes to electro-generate more catalyst and in consequence the TOC removal was increased. Conversely, when applying a current pulse during 7.5 or 10 minutes, the mineralization percentage decreased. Thus, it can be concluded that an excess of Fe^{2+} ions in the electrochemical cell is counter-productive. This can be explained by the scavenging reaction (13) where the hydroxyl radicals are consumed by Fe^{2+} ions [28,34]. Albeit these ions are regenerated by means of reaction (16), this may be slower than reaction (3) and therefore mineralization efficiency decays. Furthermore, there is a competition of reactions in the cathode, the electro-generation of H_2O_2 and the reduction of Fe^{3+} to Fe^{2+}. So, it can also be concluded that the best catalyst concentration under the studied conditions is 3.66 mM attained with a pulse length of 5 minutes to electro-generate Fe^{2+}.

$$Fe^{3+} + HO^{\bullet}{}_2 \rightarrow Fe^{2+} + O_2 + H^+ \quad (16)$$

3.3.2. Effect of current pulse length on 4-chlorophenol mineralization by Electro-Fenton-Like

The same reactions conditions tested in Electro-Fenton were used to evaluate the copper catalytic activity. This metal was obtained by the reduction reaction in the cathode (17) of the second set of electrodes,

$$Cu^{2+} + e^- \rightarrow Cu^+ \quad (17)$$

In this case the ion Cu^+ increased the production of hydroxyl radicals by catalyzing the H_2O_2 dissociation and this can be explained by the following Fenton-like reaction (18),

$$Cu^+ + H_2O_2 \rightarrow Cu^{2+} + OH^- + {}^{\bullet}OH \quad (18)$$

TOC removal results are shown in Fig. 5. It can be observed that the results trend is similar to that obtained by Electro-Fenton. Firstly, a current pulse length of 0.5 minutes only removed a 25% of TOC after two hours of reaction. However, when increasing the current pulse length to 2.5 and 5 minutes the percentage of TOC removal increased to 34% and 60%, respectively. A further increase on current pulse length, i.e. increasing the copper concentration to 5.49 and 7.32 mM, was found to diminish mineralization. Therefore, it can be concluded that the current pulse length of 5 minutes is the best to produce more hydroxyl radicals. In this process the regeneration of Cu^+ ion has been reported to be rather fast ($k = 5 \times 10^7\ M^{-1}s^{-1}$) [4] and this is explained by the following reactions,

$$Cu^{2+} + HO^{\bullet}{}_2 \rightarrow Cu^+ + H^+ + O_2 \quad (19)$$

$$Cu^{2+} + H_2O_2 \rightarrow HO_2{}^{\bullet} + H^+ + Cu^+ \quad (20)$$

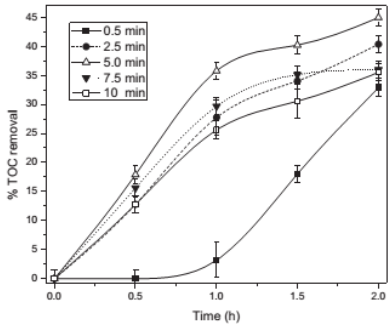

Fig. 4. Electro-Fenton process: effect of pulse length. Current density at graphite electrodes *j*: 4 mA/cm², at iron electrodes *j*: 40 mA/cm², number of pulses applied at iron elecrodes: one (applied at the experiment beginning), stirring speed 600 rpm, Na_2SO_4 (0.05 M), oxygen flowrate: 50 mL/min and pH = 3.

When Cu^+ is regenerated by reactions (19) and (20), the amount of oxidant species (hydroxyl and perhydroxyl radicals) increases by means of reactions (18) and (20). In addition, Cu^{2+} can form complexes with some intermediates (short organic diacids for example) or can be reduced by an organic radical $R^\bullet$ [4],

$$Cu^{2+} + R^\bullet \rightarrow Cu^+ + R^+ \quad (21)$$

It is likely that the fast conversion of Cu^{2+}/Cu^+ and the competitive reactions of Cu^{2+} prevent the formation of cathodic precipitate of $Cu(OH)_2$ [35]. Higher concentrations of Cu^{2+} do not increase the TOC removal. This can be ascribed to a thin layer of metal deposited on the cathode (graphite electrode). This was visually observed and this decreases the H_2O_2 electrogeneration efficiency.

3.3.3. Comparison

To better contrast the Electro-Fenton and Electro-Fenton-Like results, the initial removal rates were obtained from the TOC profiles shown in Figs. 3 and 4. These initial removal rates are plotted in Fig. 6a and 6b as a function of current pulse length at the metallic electrodes. These values were obtained through the adjustment of each experiment presented in Figs. 3 and 4 to a polynomial. The first derivative of each polynomial was obtained and then evaluated at zero time. This result indicates the initial oxidation rate and is specific to 4-Chlorophenol since the presence of intermediate products is expected to be minimum.

Fig. 6a and 6b not only show the comparison of initial mineralization rates ($-r_0$) of both processes but also shows the mineralization current efficiency (M.C.E.) as calculated by equation (5). At all experiments, it can be observed that both values, initial 4-Chlorophenol oxidation rate and M.C.E., are greater with the Electro-Fenton-Like process. In both processes, the mineralization rate increases when increasing current pulse length, reaches a maximum at a length of 5 minutes and then decreases with longer current pulses. The TOC removal behaves alike and after 1 hour of treatment, a maximum value of 58% is achieved with copper electrodes (Fig. 7). On the basis of Fig. 6a and 6b, it can be concluded that by using copper ions as catalyst of the hydrogen peroxide dissociation the mineralization current efficiency and the initial 4-chlorophenol oxidation rate are about twice than those

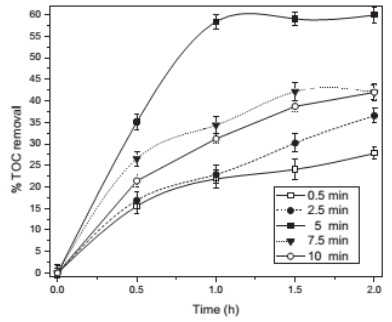

Fig. 5. Electro-Fenton-Like process: effect of pulse length on TOC removal. Reaction conditions: electrodes material = copper, number of pulses = 1, current density at graphite electrodes *j*: 4 mA/cm², at copper electrodes *j*: 40 mA/cm², stirring speed = 600 rpm, [Na_2SO_4] = 0.05 M and pH = 3, oxygen flowrate = 50 mL/min.

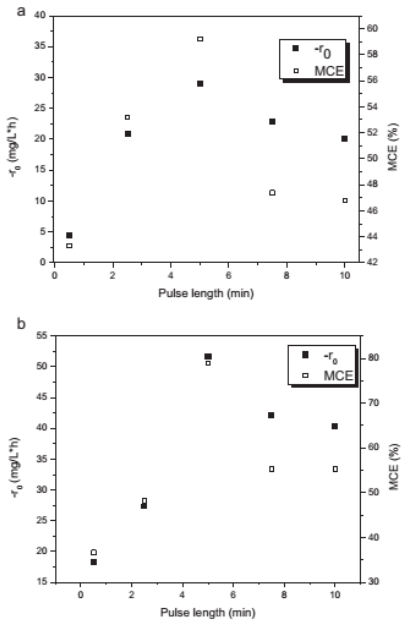

Fig. 6. (a) Comparison of 4-Chlorophenol initial mineralization rate (r_0) and Mineralization Current Efficiency (MCE) in Electro-Fenton Process. Current density in graphite electrodes *j:* 4 mA/cm². Iron electrodes *j:* 40 mA/cm², stirring = speed 600 rpm, $[Na_2SO_4]$ = 0.05 M, oxygen flow = 50 mL/min and pH = 3. (b) Comparison of 4-Chlorophenol initial mineralization rate (r_0) and Mineralization Current Efficiency (MCE) in Electro-Fenton-Like Process. Current density in graphite electrodes *j:* 4 mA/cm². Copper electrodes *j:* 40 mA/cm², stirring = speed 600 rpm, $[Na_2SO_4]$ = 0.05 M, oxygen flow = 50 mL/min and pH = 3.

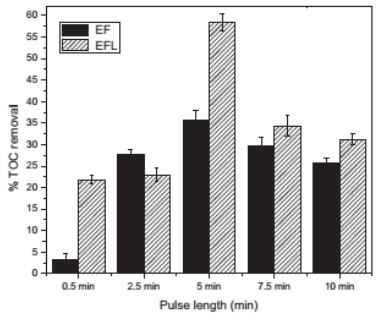

Fig. 7. Comparison of 4-Chlorophenol mineralization by Electro-Fenton and Electro-Fenton-Like after 1 hour of treatment. Current density in graphite electrodes *j:* 4 mA/cm². Copper electrodes and iron *j:* 40 mA/cm², stirring speed 600 rpm, $[Na_2SO_4]$ = 0.05 M, oxygen flow: 50 mL/min and pH = 3.

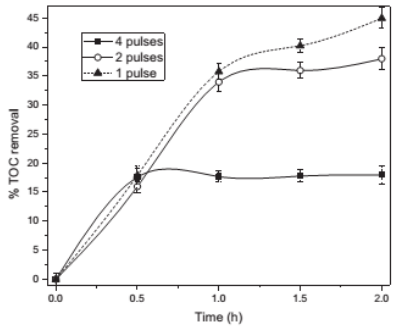

Fig. 8. Electro-Fenton: Effect of number of pulses per experiment applied to iron electrodes. Current density in graphite electrodes *j*:4 mA/cm². Iron electrodes *j*: 40 mA/cm², stirring speed 600 rpm, $[Na_2SO_4]$ = 0.05 M, oxygen flow = 50 mL/min and pH = 3.

obtained when using iron. In consequence, after 1 hour of treatment the degree of mineralization is about 1.7 times higher with copper than with iron. In both processes, when the current pulse lengths are greater than 5 minutes the initial mineralization rate and TOC removal decreases. This can be ascribed to the electro-generation of H_2O_2 and consequently the production of hydroxyl radicals is diminished by an excess of Fe or Cu ions, which promotes •OH scavenging by reactions (13) and (22). This also points out the need of controlling the catalyst amount since there is not a linear relationship between such a variable and the mineralization efficiency.

3.4. Effect of number of current pulses applied to the metallic electrodes for catalyst dosage

Previously in section 3.3, the effect on mineralization of applying only one current pulse to the Fe or Cu electrodes was assessed. It was observed that albeit Cu^+ and Fe^{2+} ions are constantly being regenerated, this process is slow compared to their consumption and this leads to a change on TOC removal after 1 hour during both treatments, EF and EFL. So, it was decided to study the effect of number of current pulses applied per experiment to the metallic electrodes. This was carried out according to what is described at the end of section 2.2. In the Electro-Fenton (EF) process, it was found (see Fig. 8) that the TOC removal after two hours of treatment decreases from 45% down to 37% (2 pulses) and 18% (4 pulses). This keeps suggesting that an excess of iron is rather detrimental because of the consumption of hydroxyl radicals (see reaction (13)) and because promotes sludge formation and electrodes passivation.

On the other hand, when evaluating the effect of number of pulses in the Electro-Fenton-Like (EFL) process (Fig. 9), it was found that there is an increase in the mineralization of 4-Chlorophenol and this is mainly due to an increase in the amount of copper and also to the regeneration of the pair Cu^+/Cu^{2+}. Furthermore, in EF and EFL the formation of M(II)-carboxylate complexes is expected and their destruction by •OH is slower in the former than in the latter. In addition, other complexes can be

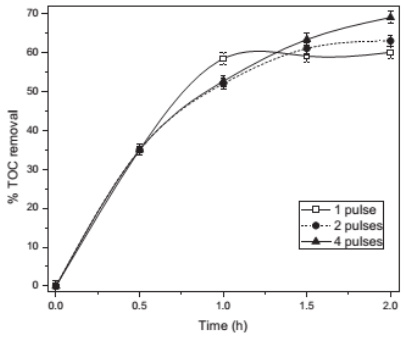

Fig. 9. Electro-Fenton-Like process: effect of number of pulses. Current density at graphite electrodes *j*: 4 mA/cm². Copper electrodes *j*: 40 mA/cm², stirring speed 600 rpm, $[Na_2SO_4]$ = 0.05 M, oxygen flow = 50 mL/min and pH = 3.

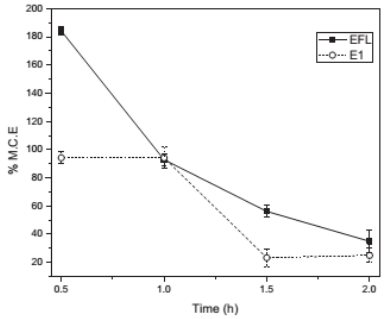

Fig. 10. Comparison of mineralization current efficiency (M.C.E). Current density in graphite electrodes 4 mA/cm². Current density in EF (Fe electrodes) and EFL (Cu electrodes) *j*: 40 mA/cm², stirring speed 600 rpm, [Na_2SO_4] = 0.05 M, oxygen flow = 50 mL/min and pH = 3.

formed by carboxylic acids, in this case oxamate and oxalate complexes, which can be produced by M (Fe or Cu) [5]. This partially explains the decrease of the mineralization rate after one hour in both processes (Figs. 8 and 9). Regarding EF, an excess of Fe^{3+} ions increases the quantity of $Fe(OH)_3$ and this promotes the pollutant removal by peroxicoagulation [24] rather than by oxidation. For this reason, an excess concentration of Fe^{3+} produces a competition between Electro-Fenton and peroxicoagulation, as consequence the ions of Fe^{2+} are not enough to catalyze the H_2O_2 dissociation and this leads to a mineralization rate decrease. It is worth noting that sludge formation was only observed during EF when four pulses were applied and not with EFL. Nevertheless, in both cases the formation of a thin layer of metal (Fe or Cu) at graphite cathode was observed. This definitely contributes to the mineralization plateau observed with both catalysts since hydrogen peroxide production is expected to be diminished.

3.5. Current Efficiency and energy consumption

Previously in section 3.4, it was established that the best catalyst concentration was obtained when applying 1 current pulse during 5 minutes at the beginning of reaction to the Fe electrodes for Electro-Fenton and 4 current pulses (during 5 minutes each and spaced 30 minutes) to the Cu electrodes for the Electro-Fenton-Like process (Fig. 9). At these experimental conditions and by applying equations (5) and (7), the mineralization current efficiency (M.C.E) and the energy consumption were established and they are presented in Figs. 10 and 11, respectively. Both calculations are based on TOC removal. For this purpose, only the parameters of graphite electrodes were employed since is the only power supply that continuously works (along treatment). Therefore the power supply of the metallic electrodes was not considered.

The highest efficiency is presented in Electro-Fenton-Like, which in the first 30 minutes of treatment is greater than 100%. This is associated to the low current density applied to graphite electrodes. In the same way, in Fig. 11 the Energy Consumption per

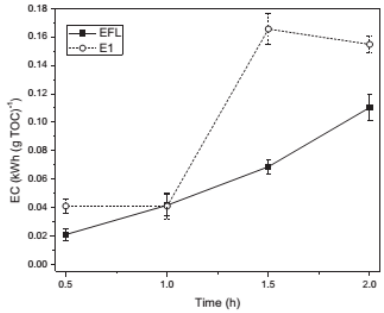

Fig. 11. Comparison of Energy Consumption (E.C) for EF and EFL. Current density in graphite electrodes 4 mA/cm². Current density in EF (1 current pulse on Fe electrodes) and EFL (4 pulses on Cu electrodes) *j*: 40 mA/cm², stirring speed 600 rpm, [Na_2SO_4] = 0.05 M, oxygen flowrate = 50 mL/min and pH = 3.

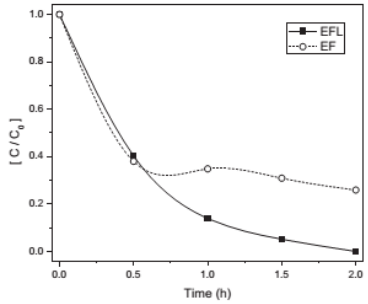

Fig. 12. Effect of type of process (EF or EFL) on 4-Chlorophenol degradation. Current density at graphite electrodes 4 mA/cm^2. Current density in EF (1 current pulse at Fe electrodes) and EFL (4 pulses at Cu electrodes) *j*: 40 mA/cm^2, stirring speed 600 rpm, [Na_2SO_4] = 0.05 M, oxygen flowrate = 50 mL/min and pH = 3.

unit of TOC as a function of time is plotted. It can be observed that Electro-Fenton-Like is better than Electro-Fenton, because the energy consumption is lower. Furthermore, the calculated energy consumption values suggest that the proposed process might be sustained, from an energy point of view, with solar panels.

Finally, the 4-Chlorophenol and degradation intermediates concentration was monitored by HPLC at the best experimentation conditions in terms of mineralization current efficiency (M.C.E) (4 current pulses with EFL and 1 current pulse with EF, see Figs. 8 and 9). At such conditions, 4-chlorophenol concentration profiles were obtained for both processes (EF and EFL) and they are shown in Fig. 12. It can be observed that at the first 30 minutes of treatment the pollutant removal is almost the same, with more than 50% of the initial concentration. However, only in the EFL process the removal is complete while in EF process the removal is only partial (Aprox. 70%), in both cases after two hours. Fig. 13 shows the intermediates profiles concentration obtained at the best oxidation conditions: 4 pulses with EFL. It can be observed that oxalic acid is formed from the very beginning of reaction and the only remained aromatic compound at the end of treatment is hydroquinone. Various carboxylic acids are also observed. It can be said that these carboxylic acids, mainly oxalic and maleic, are not further oxidized under the studied conditions and therefore limit mineralization. The prevalence of chlorinated compounds can be discarded not only because of HPLC results but also because of the chlorine ions concentration that was determined by Mohr method [31] (see supplementary material). In this sense, it is worth pointing out that the calculated theoretical chlorine ions concentration was 28 ppm while the maximum experimentally determined was 22 ppm. This suggests that most of the chlorine is not in an oxidized form.

4. Conclusions

An undivided electrochemical cell with two sets of electrodes powered with two different energy sources was tested and proved to be a feasible arrangement to conduct electro-fenton or electro-fenton like processes with *in situ* electrogeneration of both, H_2O_2 and its dissociation catalyst (metal ion). The proposed arrangement allows to separately control the current to electrogenerate

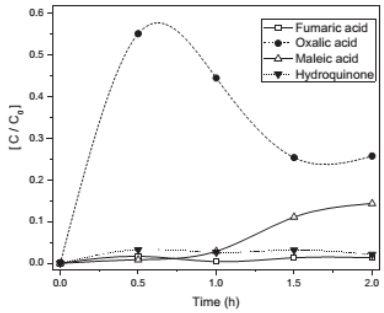

Fig. 13. Intermediates concentration profiles. Current density at graphite electrodes 4 mA/cm^2. Current density in EFL (4 pulses at Cu electrodes) *j*: 40 mA/cm^2, stirring speed 600 rpm, [Na_2SO_4] = 0.05 M, oxygen flowrate = 50 mL/min and pH = 3.

H_2O_2 and the current to control the electrochemical addition of the metal ion (catalyst) to the reacting solution. The *in situ* electro-generation of H_2O_2 and catalyst allowed to achieve the partial 4-chlorophenol mineralization by electro-fenton and electro-fenton-like processes. Compared to iron, copper is not only the most active towards H_2O_2 decomposition but also the one that regenerates faster. The studied variables, oxygen flowrate, catalyst concentration, length of current pulse and number of applied current pulses to the metallic electrodes, do not keep a linear relationship with mineralization rate and TOC removal. Thus, such variables must be limited to certain values since their further increase may lead to a decrease on mineralization efficiency. Among the studied conditions, the maximum mineralization degree (70% of TOC removal) was attained when using copper to catalyze H_2O_2 decomposition, 2 hours of reaction and 4 current pulses of 5 minutes length each. The energy consumption is also lower when copper rather than iron is employed as catalyst of H_2O_2 dissociation.

Acknowledgments

Authors are grateful to CONACYT (Projects 168305 and 179356) and PRODEP (project 103.5/13/5257) for financial support. Germán Santana-Martínez acknowledges CONACYT for scholarship number 553687 to conduct postgraduate studies. Technical support from Citlalit Martínez is also acknowledged.

Appendix A. Supplementary data

Supplementary data associated with this article can be found, in the online version, at http://dx.doi.org/10.1016/j.electacta.2016.02.093.

References

[1] I. Sirés, E. Brillas, M.A. Oturan, M.A. Rodrigo, M. Panizza, Electrochemical advanced oxidation processes: today and tomorrow. A review, Environ. Sci. Pollut. Res. Int. 21 (14) (2014) 8336–8367.
[2] M.A. Oturan, J.-J. Aaron, Advanced Oxidation Processes in Water/Wastewater Treatment: Principles and Applications. A Review, Crit. Rev. Environ. Sci. Technol. 44 (23) (2014) 2577–2641.
[3] N. Oturan, M. Zhou, M.A. Oturan, Metomyl degradation by electro-Fenton and electro-Fenton-like processes: a kinetics study of the effect of the nature and concentration of some transition metal ions as catalyst, J. Phys. Chem. A 114 (39) (2010) 10605–10611.
[4] H. Gallard, J. De Laat, B. Legube, Comparative study of the rate of descomposition of H2O2 and of atrazine by Fe(III)/H2O2, Cu(II)/H2O2, Fe(III)/Cu(II)/H2O2, Rev Sci Eau 12 (4) (1999) 713–728.
[5] I. Sirés, J.A. Garrido, R.M. Rodríguez, P.L. Luís Cabot, F. Centellas, C. Arias, E. Brillas, Electrochemical Degradation of Paracetamol from Water by Catalytic Action of Fe^{2+}, Cu^{2+}, and UVA Light on Electrogenerated Hydrogen Peroxide, J. Electrochem. Soc. 153 (1) (2006).
[6] M. Pimentel, N. Oturan, M. Dezotti, M.A. Oturan, Phenol degradation by advanced electrochemical oxidation process electro-Fenton using a carbon felt cathode, Appl. Catal. B Environ. 83 (September (1–2)) (2008) 140–149.
[7] A. Özcan, Y. Şahin, A.S. Koparal, M.A. Oturan, Carbon sponge as a new cathode material for the electro-Fenton process. Comparison with carbon felt cathode and application to degradation of synthetic dye Basic Blue 3 in aqueous medium, J Electroanal Chem 616 (1) (2008) 71–78.
[8] E. Rosales, M. Pazos, M. Longo, M. San Román, Influence of operational parameters on Electro-Fenton degradation of organic pollutants from soil, J. Environ. Sci. Health Part A 44 (2009) 1104–1110.
[9] N. Borràs, C. Arias, R. Oliver, E. Brillas, Anodic oxidation, electro-Fenton and photoelectro-Fenton degradation of cyanazine using a boron-doped diamond anode and an oxygen-diffusion cathode, J. Electroanal. Chem. 689 (2013) 158–167.
[10] F.C. Moreira, S. Garcia-Segura, R.A.R. Boaventura, E. Brillas, V.J.P. Vilar, Degradation of the antibiotic trimethoprim by electrochemical advanced oxidation processes using a carbon-PTFE air-diffusion cathode and a boron-doped diamond or platinum anode, Appl. Catal. B Environ. 160–161 (2014) 492–505.
[11] E. Mousset, N. Oturan, E.D. van Hullebusch, G. Guibaud, G. Esposito, M.A. Oturan, Treatment of synthetic soil washing solutions containing phenanthrene and cyclodextrin by electro-oxidation. Influence of anode materials on toxicity removal and biodegradability enhancement, Appl. Catal. B Environ. 160–161 (2014) 666–675.
[12] A.R.F. Pipi, A.R. De Andrade, E. Brillas, I. Sirés, Total removal of alachlor from water by electrochemical processes, Sep. Purif. Technol. 132 (2014) 674–683.
[13] S. Garcia-Segura, E.B. Cavalcanti, E. Brillas, Mineralization of the antibiotic chloramphenicol by solar photoelectro-Fenton, Appl. Catal. B Environ. 144 (2014) 588–598.
[14] K. Rajkumar, M. Muthukumar, Optimization of electro-oxidation process for the treatment of Reactive Orange 107 using response surface methodology, Environ. Sci. Pollut. Res. Int. 19 (1) (2012) 148–160.
[15] P. Kariyajjanavar, N. Jogttappa, Y.A. Nayaka, Studies on degradation of reactive textile dyes solution by electrochemical method, J. Hazard. Mater. 190 (1–3) (2011) 952–961.
[16] P.V. Nidheesh, R. Gandhimathi, Trends in electro-Fenton process for water and wastewater treatment: An overview, Desalination 299 (2012) 1–15.
[17] E. Rosales, M.A. Sanromán, M. Pazos, Application of central composite face-centered design and response surface methodology for the optimization of electro-Fenton decolorization of Azure B dye, Environ. Sci. Pollut. Res. Int. 19 (5) (2012) 1738–1746.
[18] A. El-Ghenymy, R.M. Rodríguez, E. Brillas, N. Oturan, M.A. Oturan, Electro-Fenton degradation of the antibiotic sulfanilamide with Pt/carbon-felt and BDD/carbon-felt cells. Kinetics, reaction intermediates, and toxicity assessment, Environ. Sci. Pollut. Res. Int. 21 (14) (2014) 8368–8378.
[19] I. Sirés, N. Oturan, M.A. Oturan, R.M. Rodríguez, J.A. Garrido, E. Brillas, Electro-Fenton degradation of antimicrobials triclosan and triclocarban, Electrochimica Acta 52 (2007) 5493–5503.
[20] H. Olvera-Vargas, N. Oturan, M.A. Oturan, E. Brillas, Electro-Fenton and solar photoelectro-Fenton treatments of the pharmaceutical ranitidine in pre-pilot flow plant scale, Sep. Purif. Technol. 146 (2015) 127–135.
[21] S.C. Elaoud, M. Panizza, G. Cerisola, T. Mhiri, Coumaric acid degradation by electro-Fenton process, J. Electroanal. Chem. 667 (2012) 19–23.
[22] E. Isarain-Chávez, C. Arias, P.L. Cabot, F. Centellas, R.M. Rodríguez, J.A. Garrido, E. Brillas, Mineralization of the drug β-blocker atenolol by electro-Fenton and photoelectro-Fenton using an air-diffusion cathode for H2O2 electrogeneration combined with a carbon-felt cathode for Fe2+ regeneration, Appl. Catal. B Environ. 96 (2010) 361–369.
[23] X. Florenza, A.M.S. Solano, F. Centellas, C.A. Martínez-Huitle, E. Brillas, S. Garcia-Segura, Degradation of the azo dye Acid Red 1 by anodic oxidation and indirect electrochemical processes based on Fenton's reaction chemistry. Relationship between decolorization, mineralization and products, Electrochimica Acta 142 (2014) 276–288.
[24] E. Brillas, J. Casado, Degradation of 4-Chlorophenol by Anodic Oxidation, Electro-Fenton, Photoelectro-Fenton, and Peroxi-Coagulation Processes, J. Electrochem. Soc. 145 (1998) 759–765.
[25] M. Kurian, D.S. Nair, Heterogeneous Fenton behavior of nano nickel zinc ferrite catalysts in the degradation of 4-chlorophenol from water under neutral conditions, J. Water Process Eng. (2014).
[26] L.F.G. Martins, M.C.B. Parreira, J.P.P. Ramalho, P. Morgado, E.J.M. Filipe, Prediction of diffusion coefficients of chlorophenols in water by computer simulation, Fluid Phase Equilibria 396 (2015) 9–19.
[27] E. Peralta, R. Natividad, G. Roa, R. Marín, R. Romero, T. Pavon, A comparative study on the electrochemical production of H2O2 between BDD and graphite cathodes, Sustain. Environ. Res. 23 (2013) 259–266.
[28] E. Brillas, I. Sirés, M.A. Oturan, Electro-Fenton Process and Related Electrochemical Technologies Based on Fenton's Reaction Chemistry, Chem. Rev. 109 (2009) 6570–6631.
[29] M.S. Yahya, N. Oturan, K. El Kacemi, M. El Karbane, C.T. Aravindakumar, M.A. Oturan, Oxidative degradation study on antimicrobial agent ciprofloxacin by electro-fenton process: Kinetics and oxidation products, Chemosphere 117 (2014) 447–454.
[30] M. Panizza, M.A. Oturan, Degradation of Alizarin Red by electro-Fenton process using a graphite-felt cathode, Electrochimica Acta 56 (20) (2011) 7084–7087.
[31] C.H. Harris, Quantitative chemical analysis, 8th ed, W.H Freeman and Co., New York, 2010.
[32] M.A. Oturan, N. Oturan, J.J. Aaron, Traitement des micropolluants organiques dans l'eau par des procédés d'oxydation avancée, Actual. Chim. 277–278 (2004) 57–64.
[33] E. Brillas, A review on the degradation of organic pollutants in waters by UV photoelectro-fenton and solar photoelectro-fenton, J. Braz. Chem. Soc. 25 (3) (2014) 393–417.
[34] E. Brillas, B. Boye, I. Sirés, J.A. Garrido, R.M. Rodrı'guez, C. Arias, P.-L. Cabot, C. Comninellis, Electrochemical destruction of chlorophenoxy herbicides by anodic oxidation and electro-Fenton using a boron-doped diamond electrode, Electrochimica Acta 49 (2004) 4487–4496.
[35] E. Brillas, M.A. Banos, S. Camps, C. Arias, P.-L. Cabot, J.A. Garrido, R.M. Rodriguez, Catalytic effect of Fe2+, Cu2+ and UVA light on the electrochemical degradation of nitrobenzene using an oxygen-diffusion cathode, New J. Chem. 28 (2) (2004) 314–322.